We thank the reviewer and editor for their comments. As well, we thank the reviewer for their intimate knowledge of the SP-AMS technique and their insightful questions.
The lead author, who did all of the new data analysis and plot-making for this manuscript, has a new position, so we addressed all of the comments posted here as best as we can given our constraints, but time for new analysis is limited. We have addressed all minor comments, and we have addressed the more substantive comments to the best of our current ability.

To aid the review process, we are placing reviewer and editor comments in black text, our responses in blue text, any changes to the text in red, and, in some instances, reproduce text from the previously submitted manuscript (*italic magenta*). We have numbered the reviewer (R) and editor (E) comments to assist the conversation. We note that the line numbers were unfortunately cut off in our submission, leading to difficulty for both the reviewer and the editor in identifying correct line numbers to cite. Fortunately, the reviewer often quoted sections they were referencing, allowing us to find and make corrections. There are unfortunately a small number of technical comments we were not able to address due to line number confusion and we have noted those throughout. The track-changes main text and supplement are included at the end of this document, with the main text starting on page 47 and the supplement starting on page 80.

Editor comments

E1) R1.25: Referee #1 had pointed out that changes in the Krevelen diagram may be also caused by mixing of different air masses. While you added the suggested references to Chen et al. (2015) to the method section, this information should be also added on p. 10.

After further consideration, we have decided that the Van Krevelen diagram (Figure S27) and discussion do not add any substantial information to the paper. We have removed the figure and associated text.

E2) R1.19: Referee #1 referred to your previous paper (Hodshire et al., 2019) where 'a variety of reasons' are discussed that may affect deltaOA/deltaCO evolution with ageing. I suggest that you include a bit more discussion on these reasons, i.e. similar to the information as included in the SI of your previous paper.

We have modified the text as follows:

"In general, both the cores and edges do not show any positive or negative trend in ΔOA/ΔCO with physical aging, with $R_{\Delta OA,initial}$ and R_{age} showing very weak correlations of 0.02 and +0.03 (with $R_{\Delta OA,initial}$ and R_{age} ranging between -0.25 to +0.17 and 0 to 0.07, respectively, when individual flights are left out sequentially; Table S2). The absolute variability is dominated by

differences between plumes. Many previous field campaigns similarly show little change in ΔOA/ΔCO with aging (Hodshire et al., 2019a and references therein). This may be due to a balance between evaporation and condensation over the period of time that the plume is observed (Hodshire et al., 2019a). This hypothesis is supported by the observed Δf_{60} and Δf_{44}: Δf_{60} and Δf_{44} show clear signs of changes with aging, consistent with previous studies (Cubison et al., 2011; Garofalo et al., 2019; May et al., 2015)."

E3) R1.39: Referee #1 asked for a detailed discussion to justify the assumption of the initial conditions. Your response is rather vague. I understand that you may not be able to do a quantitative estimate but some more discussion on how this assumption may be qualitatively affect your results should be added.

We copy comment R1.39 for reference (in black italics):
L308: Again, how can the authors rule out differences in the initial conditions that are independent of physical or chemical aging? This seems to be an underlying assumption throughout this entire study, but I do not find that the authors have really justified this assumption. Given how central it is to everything, I strongly suggest that an explicit discussion must be included wherein the authors review the evidence for and against their assumption.

We also copy our original response for reference (also in italics):

We have added more text and qualifiers to section 3 addressing this issue, following comments R1.24 and R2.47. We add the following text to this discussion:

"We were unable to quantify the impact on potential interfire variability in the emission values of the metrics studied here (such as variable f_{60} and f_{44}). We anticipate that being able to capture this additional source of variability may lead to stronger fits and correlation."

And
"We also suggest further refinement of our fit equations, as further variables (such as photolysis rates) and better quantification of interfire variability (such as variable emission rates) are anticipated to improve these fits."

We have now added more discussion on this issue, particularly in response to the new comment #4 from reviewer 2. Please see that response for an extended discussion of this issue, and we copy relevant portions of that response here.

"This is an interesting question, and we have provided a more detailed line of reasoning below and modified the text to clarify this point.

In the two paragraphs above, the reviewer posits that the covariance of $\Delta OA_{initial}$ with Δf_{60} and Δf_{44} is primarily due to correlations of the OA emission factor with Δf_{60} and Δf_{44} at the time of emission (due to variabilities in burn conditions) and not due to evaporation and chemistry between the time of emission and the time of the first measurement. For this to be correct, variability in the emission factor of OA would need to be a significant contributor to the variability in $\Delta OA_{initial}$ (if the relative variability in the OA emission factor is much smaller than the relative variability in $\Delta OA_{initial}$, other factors contributing to variability in $\Delta OA_{initial}$ will wash out this emissions-based covariance between $\Delta OA_{initial}$ with Δf_{60} and Δf_{44}).

In Figure 2 of our manuscript, $\Delta OA_{initial}$ varies by nearly 2 orders of magnitude (factor of 100), with multiple transects/percentiles on the high and low ends (i.e., not just a single outlier driving the upper or lower bound). In the Andreae, (2019) biomass burning emissions review paper, the OC emission factors have standard deviations that are about ½ of the mean values, so a factor of 3 variability in emission factors in the $-1\boldsymbol{\sigma}$ to $+1\boldsymbol{\sigma}$ range. Hence, variability in emission factors should not likely explain a large fraction of the variability in $\Delta OA_{initial}$. We note that (1) the emission fluxes from fires are the product of the emission factor and the fuel consumption rate (kg fuel per area per time) with fuel consumption rates varying greatly between fires (e.g., the difference between a surface fire and a crown fire), and (2) even for a fixed emission flux, variability in dilution rates from differences in fire size or atmospheric stability can lead to orders-of-magnitude differences in $\Delta OA_{initial}$, even after just 15 minutes (see Figures 6c and 7c in Bian et al., 2017).

The variability in $\Delta OA_{initial}$ is thus likely driven much more by variability in dilution and fuel consumption rates, not emission factors. It is possible that OA emission factors are correlated with fuel consumption rates because flaming wildfires (with high modified combustion efficiency, MCE) may be correlated with fast fuel consumption. However, OA emission factors are lower during flaming, high-MCE conditions (McMeeking et al., 2009), so it would be an anticorrelation rather than a correlation (the lower OA emissions factors during flaming would counter the higher fuel-consumption rates during flaming, so the OA emission fluxes would be damped by this relationship and create less variability in $\Delta OA_{initial}$).

In Figure 2, much of the $\Delta OA_{initial}$ variability comes from including both the core and edge of the same plume. Would we expect the difference in $\Delta OA_{initial}$ to come from differences in the OA emission factor? This would require (1) no additional dilution at the edge relative to the core, which is inconsistent with how diffusion works and with the CO and CO_2 concentrations between the edge and core, and (2) the edge of the plume to be emissions from flaming conditions (low OA emission factors) and the core of the plume to come from smoldering conditions (high OA emission factors), which, while possible, does not seem like it would be the

dominant (or even a common) scenario. The improbability of the two conditions above (especially #1) is further evidence that OA emission factors are not a large contributor to the variability in $\Delta OA_{initial}$.

Preliminary work (June et al., in *prep*) from the FIREX-AQ campaign is showing $\Delta OA_{initial}$ to be uncorrelated with MCE, lending further evidence that the variability in burn conditions and emissions factors do not drive much of the variability in $\Delta OA_{initial}$. FIREX-AQ was another biomass burning field campaign in which pseudo-Lagrangian research flights tracked wildfire plumes, similar to the BBOP field campaign.

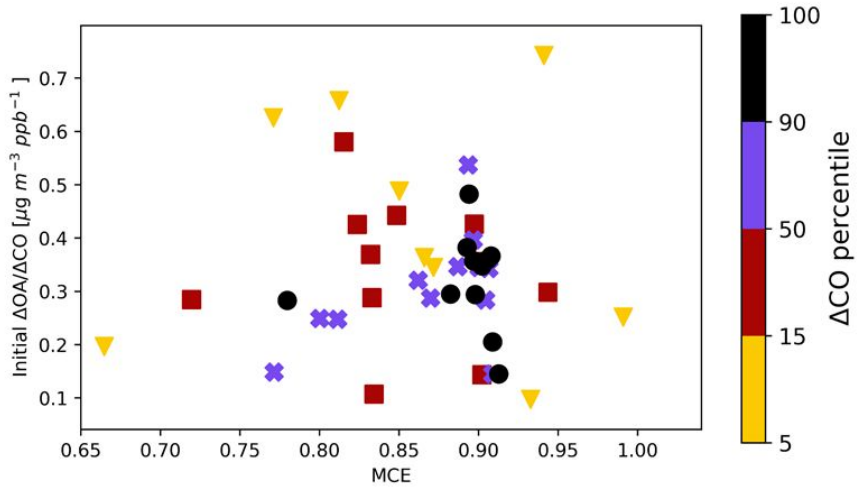

(Nicole June, et al, *in prep*)

Hence, there are multiple lines of reasoning that lead to the conclusion that OA emission factors are not a large contributor to the variability in $\Delta OA_{initial}$ (making relationships between OA emission factors with Δf_{60} and Δf_{44} unlikely to significantly contribute to the observed relationships between $\Delta OA_{initial}$ with Δf_{60} and Δf_{44}). On the other hand, theoretical studies (Bian et al., 2017; Hodshire et al., 2019a), lab analyses (Hodshire et al., 2019b), and an independent field analysis (Palm et al., 2020), have shown that we expect evaporation and chemistry before the first transect and that the extend of these processes depends on the plume concentrations.

This reasoning for ruling out the role of variability of emission factors driving relationships between $\Delta OA_{initial}$ to and Δf_{60} and Δf_{44} should have been explicit in previous versions of the manuscript, particularly after the confusion in the first round of comments. We now have added the following text to the manuscript:

"Prior studies have shown that f_{60} and f_{44} at the time of emissions correlate with OA emissions factors through variability in burn conditions (Hennigan et al. 2011; Cubison et al. 2011; McClure et al. 2020), and this relationship might also contribute to our observed correlation

between Δf_{60} and Δf_{44} with $\Delta OA_{initial}$. For this emissions relationship to be an important factor, the variability in the OA emission factor needs to be a significant contributor to the variability in $\Delta OA_{initial}$. If the relative variability in the OA emission factor is much smaller than the relative variability in $\Delta OA_{initial}$, other factors contributing to variability in $\Delta OA_{initial}$ will negate an emissions-based covariance between $\Delta OA_{initial}$ with Δf_{60} and Δf_{44}. While our observed $\Delta OA_{initial}$ in Figure 2 spans nearly a factor of 100, Andreae (2019) shows that the OA emission factors have a $-1\boldsymbol{\sigma}$ to $+1\boldsymbol{\sigma}$ range of around a factor 3. Hence, variability in fuel consumption rates and dilution prior to the first transect likely dominate the variability in $\Delta OA_{initial}$, and the relationships of Δf_{60} and Δf_{44} with $\Delta OA_{initial}$ are unlikely to be influenced much by variability in burn conditions. We conclude that evaporation and/or chemistry prior to the first measurement appears to drive the initial relationship between Δf_{60} and Δf_{44} with $\Delta OA_{initial}$, consistent with (1) the theoretical work of Hodshire et al. (2019a), (2) an analysis of what chemistry would be missed in laboratory experiments if the initial 10-60 minutes of chemistry was not considered, following field experiments (Hodshire et al., 2019b), and (3) the recent field analysis (Palm et al., 2020)."

McMeeking et al., Emissions of trace gases and aerosols during the open combustion of biomass in the laboratory, 114, D19210, doi:10.1029/2009JD011836, 2009.

Bian, Q., Jathar, S. H., Kodros, J. K., Barsanti, K. C., Hatch, L. E., May, A. A., Kreidenweis, S. M., and Pierce, J. R.: Secondary organic aerosol formation in biomass-burning plumes: Theoretical analysis of lab studies and ambient plumes, Atmos. Chem. Phys., 17, 5459-5475, doi:10.5194/acp-2016-949, 2017.

Andreae, M., Atmos. Chem. Phys., 19, 8523–8546, https://doi.org/10.5194/acp-19-8523-2019, 2019.

A. L. Hodshire, Q. Bian, E. Ramnarine, C. R. Lonsdale, M. J. Alvarado, S. M. Kreidenweis, S. H. Jathar, J. R. Pierce: More than emissions and chemistry: Fire size, dilution, and background aerosol also greatly influence near-field biomass burning aerosol aging, J. Geophys. Res., 124, https://doi.org/10.1029/2018JD029674, 2019.

Anna L. Hodshire, Ali Akherati, Matthew J. Alvarado, Benjamin Brown-Steiner, Shantanu H. Jathar, Jose L. Jimenez, Sonia M. Kreidenweis, Chantelle R. Lonsdale, Timothy B. Onasch, Amber M. Ortega, Jeffrey R. Pierce: Aging Effects on Biomass Burning Aerosol Mass and Composition: A Critical Review of Field and Laboratory Studies, Env. Sci. Tech., https://doi.org/10.1021/acs.est.9b02588, 2019b.

Palm et al., Quantification of organic aerosol and brown carbon evolution in fresh wildfire plumes, https://doi.org/10.1073/pnas.2012218117, 2020."

E4) There are several instances, where language is inaccurate or not appropriate. Some examples are included in the following, but please check the complete manuscript for similar expressions. (Please note that the line numbers were cut off in the uploaded manuscript file and only the last two digits are legible. In the following, I refer to these line numbers as they appear in the pdf.)

We agree that the manuscript will benefit from careful editing. We have addressed the editor and reviewer comments on this issue and have gone through the manuscript again to attempt to catch any poor phrasing.

E5) p. 7, l. 19: 'for many of the individual metrics' – be more specific here.

We have changed this sentence to read
"The remaining variables plotted also show some noise and few clear trends, but it is apparent that the 5-15 and 90-100 percentiles do show a separation for some of the individual metrics, in particular Δf_{44} and $\Delta O/\Delta C$."

E6) Ep. 8, l. 43: 'each variable ages downwind' should be rephrased

We have changed this sentence to read
"The Spearman tests show correlation coefficients for each flight set (Table S1) with the initial ΔOA of a flight set ($\Delta OA_{initial}$) against $\Delta OA/\Delta CO$, $\Delta f60$, $\Delta f44$, $\Delta H/\Delta C$, and $\Delta O/\Delta C$ as the smoke aerosol age downwind."

E7) p. 11, l. 54: 'our fits were made during daytime conditions' Wouldn't it be more accurate to say 'our fits were made FOR daytime conditions' ?

Changed.

E8) p. 8, l. 68: 'deltaf60 may be evaporating ' should be rephrased

We have rephrased this to:
"...consistent with the hypotheses that compounds containing species that can fragment to m/z 60 may be evaporating…"

Reviewer #2 second round of comments

Review of "Dilution impacts on smoke aging: Evidence in BBOP data"

By Anna L. Hodshire et al. Anonymous Reviewer Summary:

This manuscript derives empirical relationships for aerosol chemical age, number concentration, and mean mobility diameter which are useful for modeling the climate impact of biomass-burning aerosols. New insight from the BBOP measurement campaign is used to show that the rate of chemical aging of aerosol is affected by the "concentration" of the plume, presumably through decreasing photolytic rates with increased aerosol optical depth, and plume size, presumably because the core of larger plumes and are more protected from mixing with clean ambient air.

Ultimately, this is an interesting study but has a number of key assumptions that need to be further investigated or justified. Although the authors have weakened their language since the original draft due to comments from reviewers, they have not addressed the underlying concerns of the reviewers. This manuscript will require major revisions prior to considering publication.

General Comments:

R1) In general, the language has improved but is still not very precise and there are grammatical issues.

We agree that the manuscript has benefited from careful editing. We have addressed the editor and reviewer comments on this issue and have gone through the manuscript again to attempt to catch any poor phrasing and grammatical issues.

R2) There is a lack of details regarding SP-AMS measurements (as well as description of other instruments). There are only scattered references to the operating conditions/settings used for measuring OA in these plumes. Although the instrumentation is fully described in another manuscript, there is a minimum amount of information required for the SP-AMS measurement:

vaporizers equipped and modes used (switching between modes, temperature of thermal vaporizer), calibration, description of CE determination, ToF mode (HR-ToF, C-ToF, V-mode, W-mode), MS sampling timing (Open, closed, PToF, ePToF, pulser period, etc)

There also needs to be a description of the mass spectra analysis. What software was used. Are you reporting UMR or HR results? Is f60 based on m/z=60 or the specific ion C2H4O2+? How is gas phase subtracted? Assuming constant [CO2] gas phase concentrations of 400 ppm?

Since the vaporizer modes were switched (presumably intermittently) it is concerning how the authors choose to combine the data from the different modes. These modes measure inherently different components of the aerosol mass and fractionate the molecules in different ways. While Lee et al (2020) show that molecule fractionation in the different vaporizer modes is similar for the C2H4O2+ ion (used to calculate f60, although that is not stated by the authors), the fractionation is significantly different for the organic fraction of CO2+ (used to calculate f44) (see also Onasch et al 2012, Canagaratna et al 2015, etc).

We have greatly expanded the supplementary details of the SP-AMS, responding to all points here, including 2 new figures (Figs S29 and S30). We have also added a sentence in this main text pointing to this supplementary text. The revised supplementary text is as follows:

"The Soot Particle – Aerosol Mass Spectrometer (SP-AMS) operating on the DOE G1 aircraft during BBOP has been described in detail by Collier et al. (2016), Sedlacek et al. (2018), and Kleinman et al. (2020). The SP-AMS sampled PM1 through a constant pressure inlet operating at a pressure of ~620 Torr (Bahreini et al., 2008). The SP-AMS was equipped with dual vaporizers: (1) standard resistively heated tungsten vaporizer; and (2) 1064 nm intracavity laser vaporizer (Onasch et al., 2012). The standard tungsten vaporizer was operated at a nominal value of 600ºC for the full data set. The SP-AMS operating with the laser vaporizer OFF is effectively the same as a standard HR-AMS, measuring non-refractory particulate matter (NR-PM). The SP-AMS operating in dual vaporizer mode, with both the standard tungsten vaporizer and the laser vaporizer ON measures the NR-PM and is additionally sensitive to refractory black carbon (rBC).

Flight data was collected at a rapid rate using "Fast-MS" in V-mode (i.e., mass spectral resolution ~2000) with 1 second sample time, with negligible particle time-of-flight (PTOF) data (DeCarlo et al., 2006; Lack et al., 2009). The pulsed, orthogonal extraction time-of-flight mass spectrometer (TOF-MS) was operated with a 60 µs pulser period and collected mass spectra from m/z 11 to m/z 955. "Fast-MS" data was collected in open (i.e., sample) mode for 52 seconds and in closed (i.e., background) mode for 8 seconds every minute. The laser vaporizer was operated by either automatically alternated laser ON and OFF each minute or manually

sampling with the laser ON or OFF for long periods of time, such as full plume transects. The majority of the data (>76%) was collected in dual vaporizer mode (i.e., laser on).

The SP-AMS was calibrated for NR-PM with ammonium nitrate and for rBC with Regal black 8 independent times during BBOP. The average ionization efficiency (IE) with respect to ammonium nitrate was measured to be 8.1e-8 and the relative ionization efficiency (RIE) of rBC was measured to be 0.28, although the rBC from the SP-AMS was not used in this study.

Collier et al. (2016) determined the SP-AMS laser OFF collection efficiency (CE) to be 0.5 through comparisons with an independent HR-AMS located at the Mount Bachelor Observatory during over-flights. SP-AMS measured NR-PM values collected with the laser ON and OFF were compared for 16 different biomass burning plumes (Sedlacek et al., 2018; Kleinman et al., 2020). In each case, the plume was sampled with the laser ON and with the laser OFF, independently, and the measured plume NR-PM was normalized to CO to account for potential changes in the plume dilution between transects. The average ratio for NR-PM laser ON to laser OFF was 1.52. From these results, the average CE of NR-PM measured with the laser ON to be 0.76 with a standard deviation of 0.07 (Sedlacek et al., 2018; Kleinman et al., 2020). There is substantial evidence in the published literature for the CE of the tungsten vaporizer (Lim et al., 2019) and the laser vaporizer (Willis et al., 2014) to change as a function of chemical composition and rBC coating thickness. Unfortunately for various reasons, instrument comparisons of measurements of PM1 mass loading concentrations were very limited during BBOP, such that there does not exist a useful estimate of a changing CE for either SP-AMS vaporizer with changing plume conditions.

The SP-AMS data was analyzed using ToF-AMS Analysis Toolkit 1.61B and ToF-AMS HR Analysis 1.21B in Igor Pro. Gas phase carbon dioxide (CO_2) was directly measured on the G1 aircraft and was used to subtract gas phase contributions to CO_2^+ ion signal in the SP-AMS. SP-AMS standard NR-PM chemical species (i.e., Org, SO_4, NO_3, NH_4, Chl) were calculated using high resolution (HR) fits. f_{44} and f_{60} are unit mass resolution (UMR) ratios, whereas O:C ratios were derived using HR fits. Although it was not directly characterized for uncertainties during the BBOP campaign, we estimate uncertainties as follows. The AMS uncertainty is estimated following the methods in (Bahreini et al. 2009) (first equation of their supplemental information), leading to 37% uncertainty for organics. The laser vaporizer adds additional uncertainty up to 20%. Thus summing the uncertainties in quadrature leads to a 42% uncertainty in organics.

We further analyzed the UMRs and the potential for laser ON specific ion signals to interfere with laser OFF NR-PM ion signals with the SP-AMS data. The chemical composition of the measured wildfire plumes during BBOP were > 90% NR-PM organic material (Collier et al., 2016; Kleinman et al., 2020). rBC mass fractions were typically below 2% (Kleinman et al., 2020), though the number fractions were higher (Sedlacek et al., 2018). Despite these low concentrations, the SP-AMS laser ON (relative to laser OFF) was observed to generate C_n^+ ion signals with an identifiable fragmentation pattern for rBC material and the laser ON to OFF

NR-PM signal was observed to increase by ~50% on average. Similar results have been published for ambient urban aerosol (e.g., Lee et al. 2015). Recent laboratory work to investigate these issues has eliminated laser alignment issues and indirect heating as potential causes for these observations (Avery et al., 2020). Thus, these observations are likely due to a combination of different collection efficiencies (CEs) and relative ionization efficiencies (RIEs) for the two vaporizers when used in dual vaporizer mode (i.e., laser ON).

The HR ion signals at m/z 44 are dominated by CO_2^+ and $C_2H_4O^+$ ions (Fig. S29). The ratio of $C_2H_4O^+/CO_2^+$ increases with plume mass loading (i.e., concentration) and decreases with distance from the fire (Fig. S29), inline with the observations reported here for decreases in oxidation levels as a function of dilution. The HR ion signals at m/z 60 are dominated by $C_2H_4O_2^+$ and C_5^+ (Fig. S30). HR fitting of C_5^+ indicated that it averaged ~6% of the $C_2H_4O_2^+$ ion signal, independent of the laser vaporizer state (i.e., ON or OFF). For large $C_2H_4O_2^+$ ion signals in relatively undiluted biomass burning plumes, this ratio is likely controlled by the errors in fitting a small peak in the wings of a larger peak (Corbin et al., 2015). At lower ion signal levels, the $C_5^+/ C_2H_4O_2^+$ becomes significantly noisier, but the average does not change significantly. Laser ON may slightly increase the average ratio at lower $C_2H_4O_2^+$ ion signals, which could overestimate f_{60} for relatively dilute plumes. If this were true, the observed decrease in f_{60} with plume dilution (i.e., due to fire size and atmospheric age) would be slightly smaller than reported here.

Past research on SP-AMS ion signals from the laser vaporizer and the standard tungsten vaporizer have identified several complicating factors when operating the SP-AMS in dual vaporizer mode. First, organic material coating rBC particles and detected using the laser vaporizer have noted different fragmentation patterns (Onasch et al., 2012) and chemical compositions (Canagaratna et al., 2015) compared with the same organic material detected using the standard tungsten vaporizer. Further, there are reports of SP-AMS laser vaporizer detecting refractory CO_2^+ ions from rBC particles (Corbin et al., 2014). Currently, we have not assessed the potential for refractory CO_2^+ ion signals during BBOP as both the rBC and Org signals are highly correlated in biomass burning plumes, making minor changes to these ratios difficult to ascertain. To address the question of whether the laser vaporizer generated different ion signals from similar organic compounds, we analyzed the laser ON and OFF plume transect pairs that were used for determining laser ON CE values relative to laser OFF.

As shown in Fig. S31, the HR O:C, UMR f_{44}, and UMR f_{60} ratios are highly correlated between laser ON and OFF conditions, though differ by apparent factors. Laser ON HR O:C ratios are approximately 4% lower than laser OFF. In large part, this is due to the UMR f_{44} ratios, which are dominated by CO_2^+ ions, being 17% lower for laser ON. UMR f_{60} ratios are 18% higher in laser ON than OFF. These observations are in line with the published results from Canagaratna et al., (2015), which observed that laser vaporizer only HR O:C ratios were ~17% lower than tungsten vaporizer only HR O:C ratios for the same organic material and the HR H:C ratios were ~16% higher. In the case of BBOP, the laser vaporizer signals represented

approximately 1/3 of the total organic signal with dual vaporizers. The BBOP measured 4% lower HR O:C ratios are similar in magnitude to 5.6% (i.e., 0.33*17%) expected if the Canagaratna et al. (2015) results applied to BBOP measurements.

The BBOP SP-AMS data used in this manuscript is used to measure trends in OA. O:C, f_{44}, and f_{60} with plume dilution, either at different plume ages and/or different concentration percentiles across a biomass plume (i.e., edge vs. center). A question is whether the mixing of laser ON and OFF data here somehow biases the results due to the different absolute values between the two different states. A quick extension of the above plume pair analysis (Fig. S31) includes several "background" measurements made between the plumes (i.e., below 150 ppbv CO) and compared for laser ON vs. OFF to investigate if this ratio changes substantially between plume (i.e., high level) and background (i.e., low level) levels. The laser ON:OFF ratios of measured HR O:C averaged 0.95±0.049 in background and 0.96±0.029 in plume, UMR f_{44} averaged 0.89±0.085 in background and 0.85±0.068 in plume, and UMR f_{60} averaged 1.17±0.23 in background and 1.15±0.13 in plume. These results suggest that the observed laser ON/OFF ratios do not change from low to high signal levels, such that the trends observed for laser OFF should hold for laser ON, and vice versa. Further, the laser ON vs. OFF data points are randomly distributed throughout the measurements rather than systematically distributed to near- vs. far-field measurements or core vs. edge measurements. Hence, there should be no systematic bias due to the use of the combined laser ON and OFF data, although this combination of laser-on and -off data may contribute to noise in the observed trends."

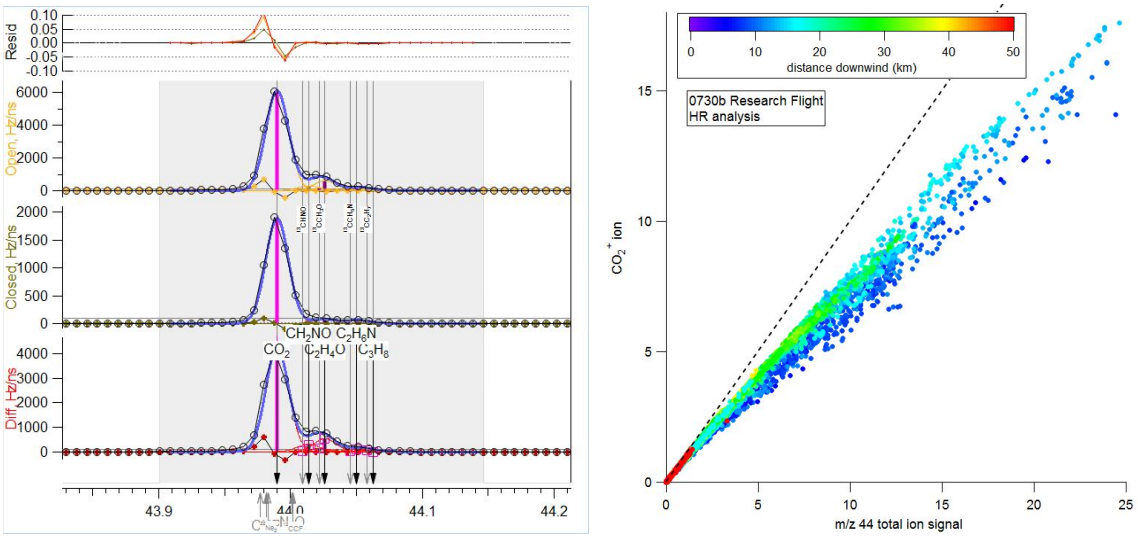

Figure S29. (a) High resolution fits at m/z 44 for a biomass burning plume during 0730b research flight with laser ON. (b) Correlation of HR CO_2^+ ion and HR total ion signal at m/z 44, colored by distance downwind (km) from fire.

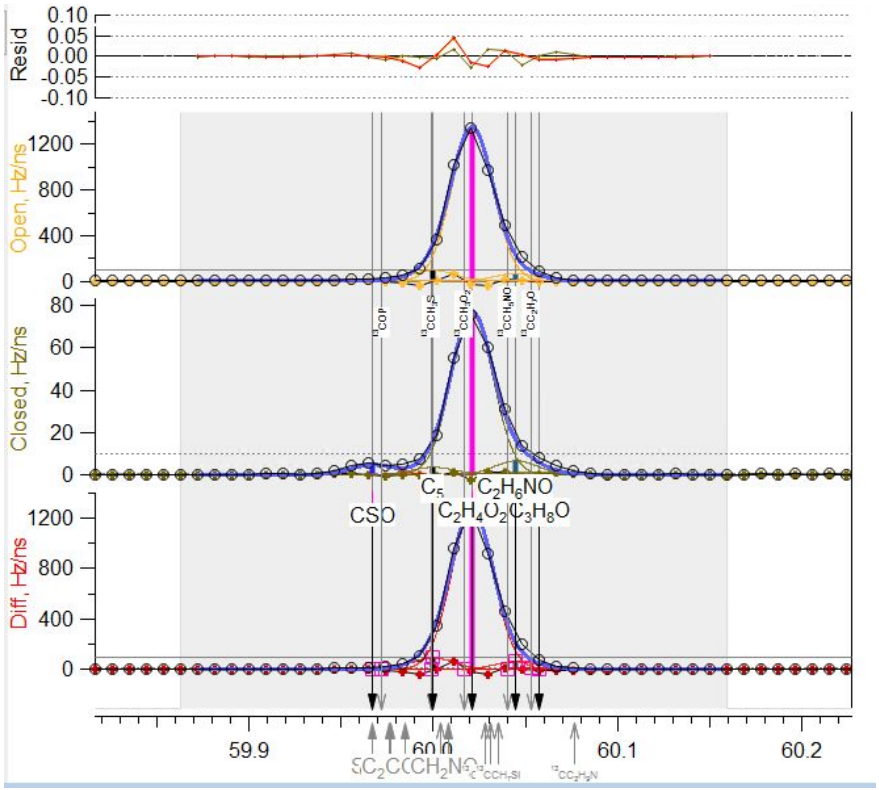

Figure S30. High resolution fits at m/z 60 for a biomass burning plume during 0730b research flight with laser ON.

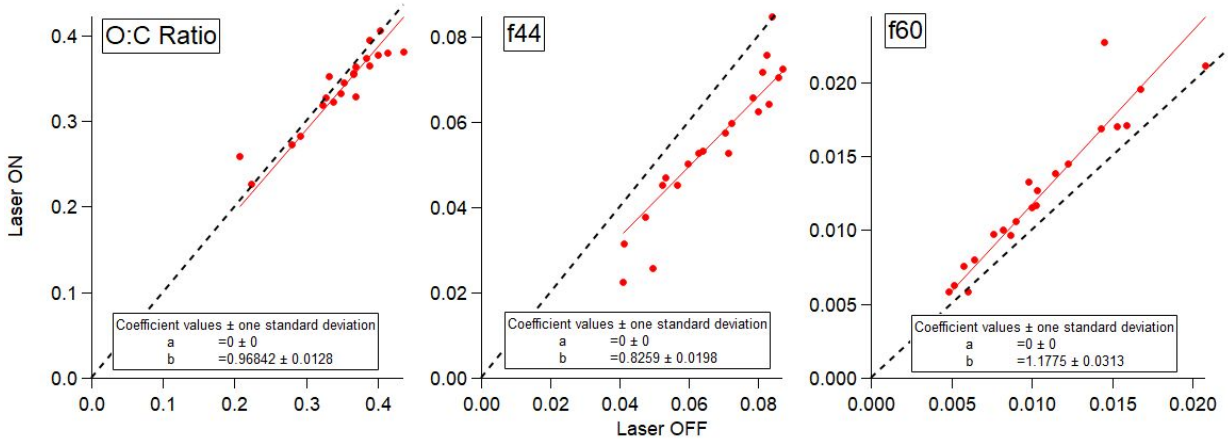

Figure S31. Laser ON versus laser OFF SP-AMS HR O:C, UMR f44, and UMR f60 ratios.

R3) Data are binned by physical age and further into edge-vs-core (such as shown in Figure 1). Each binned datum represents multiple measurements and therefore, in figure 1 and 2, should include error bars representing the variance of those measurements. This could be independent of measurement uncertainty, but would be better if it did include propagated instrument uncertainty.

We have not added these error bars due to the time constraints of the lead author as described above, as adding errors bars requires multiple analysis for each instrument and flight used in this work. We are not making any statements about systematic variance with age based on Figure 1 and the trend statistics in Figure 2 and elsewhere would be done using the mean-value datapoints (that are currently plotted) regardless.

However, we have explicitly addressed the lack of error bars in the text:

"Note that in Figure (and Figures S14-S18), the points represent the mean values for each transect and do not include error bars for uncertainty in the mean or measurement uncertainty as characterization of systematic variance (within plume percentiles) with age is beyond the scope of this study."

"As with Figure 1, the points in Figure 2 represent the mean values for each transect and percentile, and we do not include error bars as we do not attempt to characterize systematic variance (within plume percentiles) with age in this study."

R4) A key assumption of the authors is that DOAinitial, Df60, and Df44 can be used to identify dilution of the plume. However, these parameters are known to vary in primary emissions.

This is similar to question E3) from the editor. We respond in full here and copy relevant sections to question E3). To clarify, while we use $\Delta OA_{initial}$ as a proxy for dilution, we do not use Δf_{60} and Δf_{44} to identify dilution in the plume. Rather, we investigate if Δf_{60} and Δf_{44} (and other variables) systematically vary with $\Delta OA_{initial}$. To help make this more clear, we have added the following at the beginning of section 3.1 (underline new material):
"We color each line by the mean ΔOA within a ΔCO percentile bin from the transect closest to the fire, $\Delta OA_{initial}$, in order to examine whether each variable ($\Delta OA/\Delta CO$, Δf_{60}, Δf_{44}, $\Delta H/\Delta C$, and $\Delta O/\Delta C$) vary with $\Delta OA_{initial}$."

In the manuscript, the authors support the assumption regarding DOAinitial with the measured Df60 and Df44. However, these parameters are all more likely related to variations in POA between fires and within a fire as fire conditions change. The Df60 and Df44 measurements are the only support the authors provide for their main conclusion.

In the author's revisions, they have tried to further justify this assumption by making a flawed argument that their interpretation is only invalid if f60 and f44 covary with OA emissions. First this argument is flawed, as Df60initial and Df44initial are more reasonably attributed to

differences in POA. Second, it has actually been shown that f60 and f44 of POA can covary with OA emission factors (see Corbin et al 2015; Ortega et al 2015; and Lee et al 2010).

This is an interesting question, and we have provided a more detailed line of reasoning below and modified the text to clarify this point.

In the two paragraphs above, the reviewer posits that the covariance of $\Delta OA_{initial}$ with Δf_{60} and Δf_{44} is primarily due to correlations of the OA emission factor with Δf_{60} and Δf_{44} at the time of emission (due to variabilities in burn conditions) and not due to evaporation and chemistry between the time of emission and the time of the first measurement. For this to be correct, variability in the emission factor of OA would need to be a significant contributor to the variability in $\Delta OA_{initial}$ (if the relative variability in the OA emission factor is much smaller than the relative variability in $\Delta OA_{initial}$, other factors contributing to variability in $\Delta OA_{initial}$ will wash out this emissions-based covariance between $\Delta OA_{initial}$ with Δf_{60} and Δf_{44}).

In Figure 2 of our manuscript, $\Delta OA_{initial}$ varies by nearly 2 orders of magnitude (factor of 100), with multiple transects/percentiles on the high and low ends (i.e., not just a single outlier driving the upper or lower bound). In the Andreae, (2019) biomass burning emissions review paper, the OC emission factors have standard deviations that are about ½ of the mean values, so a factor of 3 variability in emission factors in the $-1\boldsymbol{\sigma}$ to $+1\boldsymbol{\sigma}$ range. Hence, variability in emission factors should not likely explain a large fraction of the variability in $\Delta OA_{initial}$. We note that (1) the emission fluxes from fires are the product of the emission factor and the fuel consumption rate (kg fuel per area per time) with fuel consumption rates varying greatly between fires (e.g., the difference between a surface fire and a crown fire), and (2) even for a fixed emission flux, variability in dilution rates from differences in fire size or atmospheric stability can lead to orders-of-magnitude differences in $\Delta OA_{initial}$, even after just 15 minutes (see Figures 6c and 7c in Bian et al., 2017).

The variability in $\Delta OA_{initial}$ is thus likely driven much more by variability in dilution and fuel consumption rates, not emission factors. It is possible that OA emission factors are correlated with fuel consumption rates because flaming wildfires (with high modified combustion efficiency, MCE) may be correlated with fast fuel consumption. However, OA emission factors are lower during flaming, high-MCE conditions (McMeeking et al., 2009), so it would be an anticorrelation rather than a correlation (the lower OA emissions factors during flaming would counter the higher fuel-consumption rates during flaming, so the OA emission fluxes would be damped by this relationship and create less variability in $\Delta OA_{initial}$).

In Figure 2, much of the $\Delta OA_{initial}$ variability comes from including both the core and edge of the same plume. Would we expect the difference in $\Delta OA_{initial}$ to come from differences in the OA

emission factor? This would require (1) no additional dilution at the edge relative to the core, which is inconsistent with how diffusion works and with the CO and CO_2 concentrations between the edge and core, and (2) the edge of the plume to be emissions from flaming conditions (low OA emission factors) and the core of the plume to come from smoldering conditions (high OA emission factors), which, while possible, does not seem like it would be the dominant (or even a common) scenario. The improbability of the two conditions above (especially #1) is further evidence that OA emission factors are not a large contributor to the variability in $\Delta OA_{initial}$.

Preliminary work (June et al., in *prep*) from the FIREX-AQ campaign is showing $\Delta OA_{initial}$ to be uncorrelated with MCE, lending further evidence that the variability in burn conditions and emissions factors do not drive much of the variability in $\Delta OA_{initial}$.

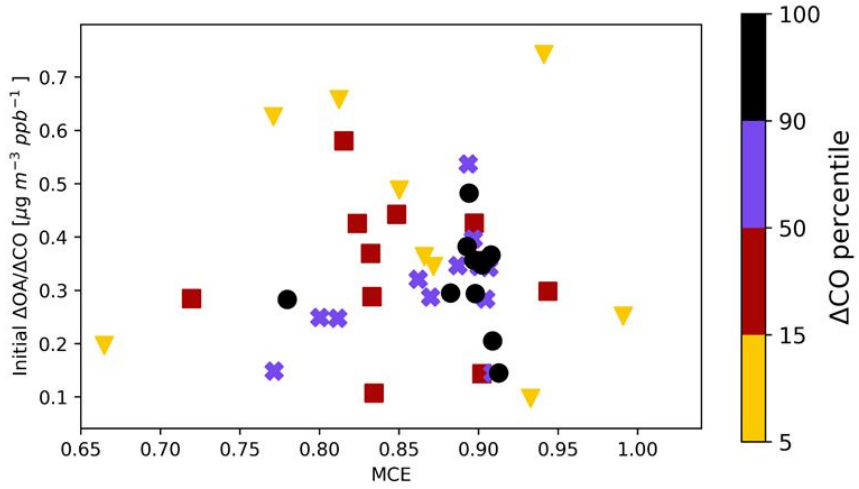

(Nicole June, et al, *in prep*)

Hence, there are multiple lines of reasoning that lead to the conclusion that OA emission factors are not a large contributor to the variability in $\Delta OA_{initial}$ (making relationships between OA emission factors with Δf_{60} and Δf_{44} unlikely to significantly contribute to the observed relationships between $\Delta OA_{initial}$ with Δf_{60} and Δf_{44}). On the other hand, theoretical studies (Bian et al., 2017; Hodshire et al., 2019a), lab analyses (Hodshire et al., 2019b), and an independent field analysis (Palm et al., 2020), have shown that we expect evaporation and chemistry before the first transect and that the extent of these processes depends on the plume concentrations.

This reasoning for ruling out the role of variability of emission factors driving relationships between $\Delta OA_{initial}$ to and Δf_{60} and Δf_{44} should have been explicit in previous versions of the manuscript, particularly after the confusion in the first round of comments. We now have added the following text to the manuscript:

"Prior studies have shown that f_{60} and f_{44} at the time of emissions correlate with OA emissions factors through variability in burn conditions (Hennigan et al. 2011; Cubison et al. 2011; McClure et al. 2020), and this relationship might also contribute to our observed correlation between Δf_{60} and Δf_{44} with $\Delta OA_{initial}$. For this emissions relationship to be an important factor, the variability in the OA emission factor needs to be a significant contributor to the variability in $\Delta OA_{initial}$. If the relative variability in the OA emission factor is much smaller than the relative variability in $\Delta OA_{initial}$, other factors contributing to variability in $\Delta OA_{initial}$ will negate an emissions-based covariance between $\Delta OA_{initial}$ with Δf_{60} and Δf_{44}. While our observed $\Delta OA_{initial}$ in Figure 2 spans nearly a factor of 100, Andreae (2019) shows that the OA emission factors have a $-1\boldsymbol{\sigma}$ to $+1\boldsymbol{\sigma}$ range of around a factor 3. Hence, variability in fuel consumption rates and dilution prior to the first transect likely dominate the variability in $\Delta OA_{initial}$, and the relationships of Δf_{60} and Δf_{44} with $\Delta OA_{initial}$ are unlikely to be influenced much by variability in burn conditions. We conclude that evaporation and/or chemistry prior to the first measurement appears to drive the initial relationship between Δf_{60} and Δf_{44} with $\Delta OA_{initial}$, consistent with (1) the theoretical work of Hodshire et al. (2019a), (2) an analysis of what chemistry would be missed in laboratory experiments if the initial 10-60 minutes of chemistry was not considered, following field experiments (Hodshire et al., 2019b), and (3) the recent field analysis (Palm et al., 2020)."

McMeeking et al., Emissions of trace gases and aerosols during the open combustion of biomass in the laboratory, 114, D19210, doi:10.1029/2009JD011836, 2009.

Bian, Q., Jathar, S. H., Kodros, J. K., Barsanti, K. C., Hatch, L. E., May, A. A., Kreidenweis, S. M., and Pierce, J. R.: Secondary organic aerosol formation in biomass-burning plumes: Theoretical analysis of lab studies and ambient plumes, Atmos. Chem. Phys., 17, 5459-5475, doi:10.5194/acp-2016-949, 2017.

Andreae, M., Atmos. Chem. Phys., 19, 8523–8546, https://doi.org/10.5194/acp-19-8523-2019, 2019.

A. L. Hodshire, Q. Bian, E. Ramnarine, C. R. Lonsdale, M. J. Alvarado, S. M. Kreidenweis, S. H. Jathar, J. R. Pierce: More than emissions and chemistry: Fire size, dilution, and background aerosol also greatly influence near-field biomass burning aerosol aging, J. Geophys. Res., 124, https://doi.org/10.1029/2018JD029674, 2019.

Anna L. Hodshire, Ali Akherati, Matthew J. Alvarado, Benjamin Brown-Steiner, Shantanu H. Jathar, Jose L. Jimenez, Sonia M. Kreidenweis, Chantelle R. Lonsdale, Timothy B. Onasch, Amber M. Ortega, Jeffrey R. Pierce: Aging Effects on Biomass Burning Aerosol Mass and Composition: A Critical Review of Field and Laboratory Studies, Env. Sci. Tech., https://doi.org/10.1021/acs.est.9b02588, 2019b.

Palm et al., Quantification of organic aerosol and brown carbon evolution in fresh wildfire plumes, https://doi.org/10.1073/pnas.2012218117, 2020.

R5) Interpretation of Spearman's correlation coefficients and the strength of these coefficients is hindered by the authors choice to combine all data from all flights together for their regressions without normalization despite showing that both aerosol age and emission factors affect the parameter of interest (e.g. Df60). This multi-variate dependence is even stated several times by the authors. For example, with 1 exception, all transect sets predictably show that Df60 decreases with physical age, but because different transect sets started with different f60 values the combined data set does not monotonically decrease with physical age and the regression results in a weak relationship (RSpearman = -0.26).

This is an example of where the authors should rethink their analytical approach but have instead weakened the language of their results.

We thank the reviewer for their suggestions here. It prompted careful consideration, but we have determined to keep the current approach. Our aim with the Spearman's correlation coefficients as used in the manuscript is to answer the question, "If all you know is the time and if all you know is the $\Delta OA_{initial}$, how well could you predict the variability between plumes?", and we now state this more clearly in the manuscript. We also are drawing more attention to the multivariate fits in Figure 3 earlier in the manuscript (details on the changes to the manuscript below). Further, we want the correlation between $\Delta OA_{initial}$ and the initial values of the variables in Figure 2 to be included in the overall $R_{\Delta OA,initial}$ as these relations are highly unlikely to be driven by covaration of emissions (see the response to R4).

There are several possibilities that the authors could consider. Continuing to use Df60 as an example, the authors could:

- Normalizing the data to the initial measured value (e.g. Df60- Df60initial) prior to combining the data. This allows you to remove the processes driving variability in the initial Df60 (essentially the emission factor) so you can isolate the effects of physical age on Df60.

There is information in the initial values that we do not want to remove. And because a relationship between the initial values of some variables with $\Delta OA_{initial}$ exists even though OA emission factors is not a major driver of $\Delta OA_{initial}$ variability, the initial values of e.g. Δf_{60} and Δf_{44} is very likely not due to the emission factor (see the response to R4)

- A multivariate analysis with predictors of DOAinitial and physical age. You could do this in any programming language, but using Excel as an example you would use the Data>Data_Analysis>regressions gui. It appears that you use this in your model in section 3.1 in equation 4. Since you did this, why do you even show the single-variable Rpearson and Rspearman values?

These separate analyses address different questions (see above), and we have added discussion on this to the manuscript.

- Lastly, you could analyze each transect set separately to get a Rspearman value of Df60 versus physical age and then average those values together. If this approach is chosen, then averaging should weighted by the number of transects in the transect set. Also, you should use a jack-knife-like approach, repeating the averaging by systematically excluding 1-2 transects sets to see how dependent the results are on any individual set.

This approach is not consistent with the question we sought to answer with these coefficients, and rather, the multivariate fit in Figure 3 with coefficients in Table S3 serves to separate the role of the two predictors.

We note that we did do a leave-one-out analysis (Table S2) after the first round of reviewer comments, following suggestions made in reviewer comments and responses R1.21 and R2.59.

We believe that our approach is appropriate for the question we sought to answer. We have now added the following text:

"We calculate these correlation coefficients separately for Figure 2 to determine how well the variability can be predicted from the $\Delta OA_{initial}$ or age alone (and whether the data are correlated vs. anticorrelated with these predictors). To complement these independent correlation coefficients, we also perform multivariate linear regressions (Eqns. 4 and 5 and Figure 3, discussed later) to explicitly decouple the influence of the two predictors."

R6) SI section: The supplement has improved with more detail but is still lacking. More detail is needed describing the instrument set up, even if it is described fully in another paper.

We have greatly expanded the SI. Please see our response to R2.

R7) The heterogeneous chemistry calculations needs a description of the calculation and justification for the methodology used. The only information provided is that it is a "simple

calculation" and a list of what the parameters are.

This description was in Section S2 in the supplement. The main text states *"However, estimates of heterogeneous mass losses indicate that after three hours of aging (the range of time the BBOP measurements were taken in) for a range of OH concentrations and reactive uptake coefficients, less than 10% of aerosol mass is lost to heterogeneous reactions (Fig. S23; see SI text S2 for more details on the calculation)."* We have modified Section S2 in the supplement in response to this comment:

"We test the impact of heterogeneous chemistry on aerosol mass loss within the smoke plume. We performed a simple calculation of reactive uptake of OH molecules with particle-phase organics that resulted in loss of organic products. These calculations include assumed values of particle diameter, OH concentration, OH diffusion coefficient, and OH reactive uptake coefficient. The following parameters are assumed for the calculations:

- OH diffusivity = 3.5e-5 [m^2 s^{-1}]
- Particle diameter varied from 1 - 1000 [nm]
- Constant OH concentration varied from 1e5 to 5e7 [molecules cm^{-3}]
- Reactive uptake coefficients varied from 0.1 to 1 [unitless]
- Molecular weight of organics = 200 [g mol^{-1}]
- Density of organics = 1.4 [g cm^{-3}]
- Total run time = 3 [hours]

The collision rate of OH with the particle surface was calculated using the condensation equations in Seinfeld and Pandis (2006). As a calculation of the upper bound limit of evaporation due to heterogeneous chemistry, we assume each collision results in removing an organic molecule on the surface of the particle (assumed to be 200 amu), fragmenting and removing the molecule from the particle. The fragmentation products are not assumed to participate in further reaction. Figure S23a shows the resulting final:initial mass ratios after four hours of aging, indicating that for the aerosol sizes containing most of the mass in this study (>100 nm) and under expected OH concentrations (<10^7 cm^{-3}), >90% of the aerosol mass remains after 3 hours in all but the cases with a reactive uptake coefficient of 1 and an OH concentration of 10^7 cm^{-3}. Note however that (1) the reactive uptake coefficient is likely lower than 1 (Slade and Knopf, 2013), (2) not every reaction will lead to complete evaporation of all products, and (3) OH concentrations are often lower than 10^7 cm^{-3} (Juncosa Calahorrano et al., 2020)."

Juncosa Calahorrano, J. F., Lindaas, J., O'Dell, K., Palm, B. B., Peng, Q., Flocke, F., Pollack, I. B., Garofalo, L. A., Farmer, D. K., Pierce, J. R., Collett, J. L., Weinheimer, A., Campos, T., Hornbrook, R. S., Hall, S. R., Ullmann, K., Pothier, M. A., Apel, E. C., Permar, W., Hu, L., Hills, A. J., Montzka, D., Tyndall, G., Thornton, J. A. and Fischer, E. V.: Daytime Oxidized Reactive Nitrogen Partitioning in Western U.S. Wildfire Smoke Plumes, J. Geophys. Res. Atmos., 1–47, doi:10.1029/2020jd033484, 2020.

Specific Comments:

R8) L31: Here and elsewhere, are you calculating the mass mean mobility diameter or number mean mobility diameter?

Mean number diameter-we've added 'number' here and 'number' and 'mobility' elsewhere in the paper when appropriate.

R9) L38: "...undergone more decreases in a marker for primary biomass burning organic aerosol." This is an awkward statement

We have changed this to
"We further find that on the plume edges, the organic aerosol is more oxygenated while a marker for primary biomass burning aerosol emissions has decreased in relative abundance."

R10) L41-44: "Smoke from biomass burning... influencing... as well as the health of smoke-impacted communities". "Smoke-impacted" is redundant.

We have removed the second 'smoke'.

R11) L45: Dilution is a process which is a central theme of the manuscript. It should have a proper description of what that process is. I suggest something like, "Dilution is the process where the plume mixes with clean background air, reducing concentration of fire emitted aerosols and gases". The current statement, "Dilution through entrainment..." is not explicit.

We have updated this statement to be more explicit:
"Dilution of a smoke plume occurs as the plume travels downwind, mixing with regional 'background' air, reducing the concentrations of the smoke aerosols and vapors and potentially driving changes in the physical and chemical properties of the emissions (Adachi et al., 2019; Akagi et al., 2012; Bian et al., 2017; Cubison et al., 2011; Hecobian et al., 2011; Hodshire et al., 2019a, 2019b; Jolleys et al., 2012, 2015; Konovalov et al., 2019; May et al., 2015; Noyes et al., 2020; Sakamoto et al., 2015)."

R12) L50-52: Lacks explanation of why large plumes dilute slower. Since this is so important to the story, it should have a better description. Currently, it is just stated that they do. Something like "...cores of larger plumes are protected from dilution due the physical distance from background air..." Citations for this are Garofalo et al (2019) and Lee et al (2020).

We have altered this to
"Large, thick plumes dilute more slowly than small, thin plumes for similar atmospheric conditions, as the cores of larger plumes are at a greater physical distance to the background air, shielding them from dilution for longer (Akagi et al., 2012; Bian et al., 2017; Cubison et al., 2011; Hecobian et al., 2011; Hodshire et al., 2019a, 2019b; Jolleys et al., 2012, 2015; Konovalov et al., 2019; May et al., 2015; Sakamoto et al., 2015, Lee et al., 2020, Garofalo et al., 2019)."

R13) L86-87: "... evaporation of vapors." Should be "evaporation of more volatile compounds."

We have updated the text to this suggestion.

R14) L88: "; plumes with higher concentrations will undergo more coagulation..." Are you referring to number concentration, mass concentration, or both?

Aerosol number; we have added this to the text.

R15) L101: "... differences in aerosol loading serve as a proxy for differences in dilution rates..." Do you mean rates or amount of dilution prior to first measurement? I have provided other comments in more detail regarding this assumption.
'Amount' is more appropriate here. We have updated this statement to be more inclusive of other points:
"The differences in aerosol loading serve as a proxy for differences in initial fire and plume sizes, mass fluxes, and subsequent amount of dilution. The extent to which dilution has occurred prior to the first observation is not a measurable quantity, and fire sizes and mass fluxes were not estimated as a part of the BBOP campaign."

R16) L103: "...given initial plume mass and physical age..." "mass" should be "OA mass concentration".

Added.

R17) L115: More description needs to be provided regarding the settings for the SP-AMS.

Was it equipped with a tungsten thermal vaporizer? If so, what temperature was the thermal vaporizer set to? HR-ToF, C-ToF, L-ToF, quadrupole? ToF set to V-mode or W-mode? How was data analyzed? Are you reporting UMR or HR results? Is f60 the levoglucosan fraction (i.e. fC2H4O2 as is discussed by Corbin et al 2015 and Lee et al 2020) or based on the UMR m/z=60 organic fragment after subtracting C5 contributions (also m/z=60, see Cubison et al 2011 and

Lee et al 2010). What was the MS timing? Open vs closed timing? PToF or ePToF mode? Pulse period, sampling Hz? What m/z range was scanned?

Please see our response to R2.

R18) L116: "PM1 aerosol masses" should be "aerosol mass concentration of PM1 (sub-micron particulates)..."

Done

R19) L119-121: How was collection efficiency determined?

Please see our response to R2.

R20) L119-121: It looks like the laser vaporizer was switched between on and off. How frequently was the laser vaporizer switched? Is the data presented in this manuscript with the laser on, off, or both?

These measure inherently different attributes of PM1 that may not be directly comparable or combinable.

Also, because the laser vaporizer fractionates aerosols molecular species differently than the thermal vaporizer (Onasch et al 2012; Corbin et al 2014; Canagaratna et al 2015; Lee et al 2015; Lee et al 2020) single ions such as $C_2H_4O_2^+$ and Org44+ (used to calculate f60 and f44) CANNOT be compared or combined between modes.

Please see our response to R2.

R21) L121-L122: "We do not attempt to characterize whether the collection efficiency of the SP-AMS changes as the aerosol ages"

Collection efficiency has been observed to change by a factor of 2 or more as BB POA grows in size and becomes more spherical (See Middlebrook et al 2012, Willis et al 2014, Corbin et al 2015 (ACP), Massoli et al 2015, Collier et al 2018). This change in CE has been observed to bias particles of different morphology/composition differently between different vaporizer modes (laser + oven versus oven-only), specifically affecting the CE of the laser more than the CE of the thermal vaporizer.

We have modified this and the following text: "There is evidence from other studies that the CE of the tungsten vaporizer (laser off mode) (Lim et al., 2019) and the laser vaporizer (laser on mode) (Willis et al., 2014) changes as a function of chemical composition, rBC coating thickness, size, and sphericity in laboratory studies (Middlebrook et al., 2012; Willis et al., 2014; Corbin et al., 2015; Massoli et al., 2015; Collier et al., 2018) and an aircraft study (Kleinmane et al., 2007). Results pertinent to changes in CE due to aging in smoke plumes are scarce (see discussion in Kleinman et al., 2020). We assume these CEs for the laser on and off modes are constant in space and time, which is a limitation of this study."

Kleinman, L. I., et al. (2007), Aircraft observations of aerosol composition and ageing in New England and Mid‐Atlantic States during the summer 2002 New England Air Quality Study field campaign, J. Geophys. Res., 112, D09310, doi:10.1029/2006JD007786.

R22) L123: "...CE has been recently observed to decrease with aging within a laboratory study..." should be "... decrease with increasing chemical age induced by UV light exposure and OH- equivalent to 10 photochemical days..."

This change in CE is likely irrelevant to this manuscript since the physical age of aerosols described in this study is generally less than 3 hours while the cited study compares CE over the equivalent of 10 days. As mentioned in the previous comment, there are a range of studies that have shown increases in CE as particles grow in size (which presumably also increase with age in the near-field during the particle growth phase) which is more relevant to this study.

We have removed this sentence as part of the revised text given in R21.

R23) L 124: "... no consistent evidence of changing CE in field studies exist yet."

There are lots of studies which show changing CE in the field. For example, see Collier et al (2018), Massoli et al (2015), and Middlebrook et al (2012) for examples of changing CE in field studies. Also see Willis et al (2014) and Corbin et al (2015, ACP) which report the same phenomena in laboratory studies.

We have removed this sentence as part of the revised text given in R21.

R24) L124-125: "We use the f60 and f44 fractional components..."

Here and elsewhere, f60 and f44 are referred to as if they are chemical species instead of parameters describing mass fractions.

For f50, the relevant OA species group is anhydrous sugars with the dominant species being levoglucosan (C6H10O5) (Lee et al 2010; Cubison et al 2012). This species is indirectly observed by the SP-AMS as the fragment C2H4O2 (m/z=60), a fragment of the levoglucosan molecule after the OA is vaporized and the vapors are ionized by a 70 eV electron supply. Similarly, OA observed at m/z 44 is the CO2 fragment of, primarily, OOA after subtracting the gas [CO2] mass.

We have updated this imprecise language throughout regarding how we refer to f44 and f60.

R25) L128-129: "The f44 fractional component (arising from primarily CO2+...)"

This is another example of imprecise language. Suggest, "f44, the OA fractional component observed by the SP-AMS as the ion fragment CO2+, is a proxy for ..." The current wording suggests that f44 is a fraction of something else which isn't specified (i.e. f44/Org).

We've updated this as suggested
"f_{44}, the OA fractional component observed by the SP-AMS as the ion fragment CO_2+ as well as some acid groups, is a proxy for SOA arising from oxidative aging (Alfarra et al., 2004; Cappa and Jimenez, 2010; Jimenez et al., 2009; Volkamer et al., 2006)."

R26) L129: extra semicolon

Fixed

R27) L130-132: "...of semivolatile f60-containing species and addition of oxidized f44-containing..." Another example of imprecise language using f60 and f44. The aerosols contain levoglucosan and anhydrous sugars, not f60, and OOA, not f44.

We've updated this to
"...likely due to both evaporation and/or oxidation of semivolatile species that contribute to m/z 60 in the SP-AMS and addition of oxidized species that contribute to m/z 44 in the SP-AMS…"

R28) L135: "changes in O/C and H/C are also influenced by..."
These other processes also affect all of the other parameters discussed in this paper.

We have updated this to
"Changes in O/C and H/C (as well as changes in total OA mass, number, f_{44}, and f_{60}) are also influenced by mixing of different air masses and co-oxidation of different VOC precursors (Chen et al. 2015)."

R29) L140: “provided CO measurements” should be “measured CO concentration” or “measured CO mixing ratio”.

Updated to ‘measured CO concentrations’

R30) L141: “An SPN1 radiometer provided total shortwave irradiance”. The radiometer measured total shortwave irradiance, it did not provide or create the irradiance.

Updated ‘provided’ to ‘measured’

R31) L143: “(Dx)” refers to the smoke contribution and should be placed after “species X from smoke” otherwise Dx is implied to refer to the background value of x. Also, the smoke doesn’t contribute species X, it is comprised of species X. The fire emits/contributes X.

Updated to
“To determine the contribution to the concentrations of species X from smoke emissions (ΔX)...”

R32) L145-146: This sentence needs to be rewritten. Suggest something like “Variability of the normalized emission ratio (Dx/DCO) along the lagrangian flight path implies production or removal of species X in the plume.”

Changed to
“Increases or decreases of ΔX/ΔCO along the Lagrangian flight path indicate whether the total amount of X in the plume has increased or decreased (implying production or removal) since time of emission.”

R33) L147: “... average regional background for each species by using the lowest 10% of the CO data for...”

This statement reads as if you subtract a CO concentration from the number size distribution, OA, etc to get a background correction. It should say something like “... background values of X... were determined to correspond with time periods which displayed the lowest 10% of CO concentrations...”

We agree that this is confusing and have updated to
“The background concentration of X is determined as a regional average of the observed out-of-plume concentrations of X. To avoid using smoke-impacted measurements we apply a threshold of only using measurements of X that occur in regions that correspond to the lowest

10% of CO data. We determine the lowest 10% of CO concentrations from each flight during time periods with a similar altitude, latitude, and longitude as the smoke plume. We perform sensitivity calculations on our assumptions of background regions and discuss them in Sect. 3."

R34) L149: Should read "Mass concentrations of elemental O, H, and C were calculated..."

Fixed

R34.b) L152-153: It is not clear what you mean by this sentence.

We are unable to address this comment, as L152-153 in the original submission are *equation 1 (where X = O or H):*

$$\frac{\Delta X}{\Delta C} = \frac{(X_{in\ plume} - X_{out\ of\ plume})}{(C_{in\ plume} - C_{out\ of\ plume})} \qquad Eq.\ 1$$

R35) L154: "inside and outside of the plume".

Does this refer to sampling time periods/locations corresponding lowest 10% of CO or <150 ppbv? Why would you change between these definitions of background?

We have modified our explanation of how we quantify the background in R33. We use the two definitions in order to have a buffer between the plumes and background to ensure to the best of our ability that we are reporting in plume and out of plume values. We note that in our analyses where we split into different ΔCO bins we do not use the lowest 5% of the in-plume region, again to provide a buffer between in-plume and out-of-plume. We have added the following text:

"We note that we use different definitions of in-plume and background (i.e. the lowest 10% of CO measurements) in order to provide a buffer between the plume and background to ensure to the best of our abilities that we are capturing non-smoke-impacted air for the background and smoke-impacted air for in-plume cases. The regions of the lowest 10% of CO measurements always fall under 150 ppbv (Figs. S7-S11). Similarly, we exclude the lowest 5% of CO data in the in-plume measurements in our analyses to provide a further buffer between smoke-impacted and background air."

R36) L157-158: "We only consider data to be in-plume if the absolute CO>=150 ppbv, as comparisons of CO and the number concentration show that in-plume data has CO>150 ppbv and out of plume (background) data has CO < 150 ppbv."

Why did you change the definition of background from time/location corresponding to lowest 10% of CO to <150 ppbv?

See response to R35.

What do you mean by "comparisons of CO and the number concentrations"? What independent metric are you defining as "background" here? If number concentration is used to define time/location of background air, why not use that instead of CO <10% or CO < 150 ppbv? The logic here is circular or incomplete.

This statement was misleading, and we have removed it.

R37) L 162: "concentrations" should be singular.

We are unable to address this comment as line 162 does not include the word concentrations. We have looked for incorrect usage elsewhere and have not found any.

R38) L163: Should be "mobility" diameters.

Fixed

R39) L164: "...as the bulk of observed newly formed particles observed fell below 40 nm" Grammar.

Fixed

R40) How do you identify "newly formed particles" independent of the particle size? This implies that you observed newly formed particles >40 nm.

This statement is confusing and we have updated to
"Frequently, the background-corrected, normalized number concentration in the FIMS size range between 20-40 nm increases by 1-2 orders of magnitude relative to typical plume conditions, indicating possible nucleation events, primarily at the edges or in between smoke plumes (Figs. S7-S11)."

R41) L165-166: Grammar in sentence structure.

Changed to

"Smoke plumes contain particles with diameters larger than 262 nm (Janhäll et al., 2009): thus, we cannot provide total number concentrations, but we can infer how the evolution of ΔN/ΔCO within our observed size range evolves."

R42) L187-188: "The centerline..." This sentence needs to be rewritten for clarity.

Rewritten to

"The centerline is subjectively chosen to approximately capture the most-concentrated portion of each plume pass (as estimated using total aerosol number concentrations)."

R43) L190: "...and this physical age is assumed to be constant across the transect, as the crossings took between 50-500 seconds."

While crossing the plume occurred in only a short time, were the transects always perfectly across flow? If not, then wouldn't the aerosol at different sampling times along a transect have different physical ages with larger uncertainty than just 50-500 seconds?

Good point, we have modified the sentence as follows:

"...and this physical age is assumed to be constant across the transect, as the crossings took between 50-500 seconds; however, transects that were not perfectly tangential to the mean wind would have sampled different plume ages on the opposite sides of the plume."

R44) L195: missing comma
Fixed

R45) L201-202: "thinnest (least CO-dense)... thickest (most CO-dense)..." Use either of the commonly accepted nomenclature of "CO mixing ratio" or "CO concentration".
Changed to "lowest CO mixing ratio" and "highest CO mixing ratio"

R46) L207: missing a verb between "plumes" and "from"
The original sentence is (section in question bolded, underlined)
"We note that some plumes show more than one maxima in CO concentrations within a given plume crossing, which implies that there may be more than one fire or fire front, and that these ***plumes from*** *separate fires or fronts are not mixing perfectly."*
We do not find a missing verb.

R47) L205-207: could the multiple peaks during a transect be explained by spatial variations in the plume structure, such as the core of the plume was higher in some areas than others causing the flight to dip below/above the core and then back into it?
This is a reasonable point. We have added the following:
"Multiple maxima could also imply vertical variations in the location of the core of the plumes that the flights did not sample."

R48) L213: It is hard to tell what the variability in DBC/DCO are since they are plotted on a log scale. They appear to vary by an order of magnitude, i.e. not constant as the authors suggest.

Yes. We have modified the text to be as follows:

"Figure 1 shows that for this specific plume, ΔOA/ΔCO and ΔBC/ΔCO systematically vary little with age for both the 5-15 and 90-100 percentile of ΔCO (p-values>0.5), yet both show non-systematic variability between transects."

R49) L213: I pointed this out in my general comments. Each dot in figure 1 is a single value that represents multiple measurements in space and time. How well does the value of any single datum in this figure represent the range of data it is derived from? You need to have error bars to show that variability.

See the response to R3.

R50) L215: "for each transect" should be "each transect set".
Fixed

R51) L218-219: "...it is apparent that the 5-15 and 9-90 percentiles do show a separation..."

This statement cannot be verified or supported without some idea of error bars, either representing propagated measurement uncertainty, variability of binned data, or both.

We have modified the text as follows:

"The remaining variables plotted also show some noise and few clear trends, but it is apparent that the transect-mean values 5-15 and 90-100 percentiles do show a separation for some of the individual metrics, in particular Δf_{44} and ΔO/ΔC."

R52) L227-231: This is one of the key assumptions of the research, that the initial, background-corrected OA mass concentration can be used as a proxy for the degree of dilution of the plume. The authors provide no support for why DOAinitial would represent the degree of dilution even though this is the main storyline of their paper.

First, I do agree that the cores of larger plumes are likely protected from mixing with background air because of the distance between the core and the background air and it is well understood that some plume chemistry and mixing occurs very early after combustion+pyrolysis and prior to measurement. However, this needs to be presented differently. Start with the hypothesis that cores of larger plumes mix slower with background air and then use the observations to prove it by showing something like the rate of change in f60 and f44 as a function of physical age for plumes with different DOAinitial.

The current presentation is problematic. Think of two hypothetical smoke plumes that are identical in terms of dilution, photolytic reaction rate etc and were measured at the same physical age, but the corresponding fires had different OA emission factors (say, flux of OA from fire B was twice that of fire A). Fire B would have ~2x the measured DOAinitial compared to Fire A. This would instead be interpreted by the authors as having half the dilution of the plume from fire B instead of twice the OA emission.

This demonstrates that the author's assumption that DOAinitial is a proxy for plume dilution only makes sense if all fires measured emit OA at the same rate and concentration.

Please see the response to R4 for an extended discussion of this topic.

Specific to this comment, the example of the 2x difference in emission factors is fitting as 2x is around the range that OA emission factors vary by (Andreae, 2019), whereas our observed range of initial OA concentrations was nearly a factor of 100. OA emissions factors can only be a minor contributor to variability. Additional reasoning is given in response to R4 (starting on Page 13 of this response).

R53) L228-229: "(as presumably larger, more intensely burning fires will have larger mass fluxes than smaller...)".

This assumption is false.
Larger and more intense fires do not necessarily correspond to higher emission rates. Emissions of OA depend on a number of factors other than fire intensity (I assume you mean temperature). Hotter, more intense fires (i.e. flaming stage) can burn more efficiently and actually emit less OA than cooler, smoldering fires (Akagi et al 2011; McMeeking et al 2009; May et al 2014). Corbin

et al (2015) found that in laboratory burn experiments the vast majority of OA emissions occurred in the "starting phase" before the logs fully caught fire.

The reviewer appears to be discussing emission factors, not emission rates (emission factor □ fuel consumption rate per area □ fire area). By intensity, we meant heat release per fire (i.e., fire radiative power [FRP] = fire radiative flux * fire area). FRP has been used to estimate smoke emissions from satellites (using assumed emissions factors), e.g. Ichoku and Ellison (2014). Further, it is unequivocal that having a larger-area fire with all else equal is going to emit more material than a smaller fire.

We have updated this to
"(as larger fires and fires with faster rates of fuel consumption per area will have larger mass fluxes than smaller fires or fires with less fuel consumption per area, all else equal)"

Ichoku, C. and Ellison, L.: Global top-down smoke-aerosol emissions estimation using satellite fire radiative power measurements, Atmos. Chem. Phys., 14, 6643–6667, https://doi.org/10.5194/acp-14-6643-2014, 2014.

R54) L243: missing a comma between items in the list. L252: delete either "systematically" or "sequentially"
Both fixed

R55) L251-257: See general comments regarding data analysis. The authors choose to combine all data together to determine the effects of aging and dilution on plume characteristics. However, they do not normalize the data in anyway or try another technique to separate these two effects. Normalizing a parameter to the first measured value (say f60) acknowledges that there are differences in f60 between plumes (maybe related to DOAinitial) and would allow for analysis of temporal trends after emission. One result maybe that the photolytic age of the aerosol mass (as measured by f60 or f44) is slower plumes with higher DOAinitial , i.e. there is less of a change/unit time of f60 or f44 or DN/DCO, etc.

Currently, the analysis is a regression comparing apples and oranges and the results are not meaningful.

Please see our response to R5.

R56) L262-266: Include citations to Cubison et al (2011), Garofalo et al (2019), Forrister et al (2015), Lee et al (2020) for constant DOA/DCO as plumes age.

We are citing Cubison and Garofalo here. We have added the other two citations.

R57) L270-270: Containing text "...estimates of heterogeneous mass losses indicate that after three hours of aging for a range of OH concentrations and reactive uptake coefficients, over 90% of aerosol mass is anticipated to remain..."

This is the basis for which the authors interpret changing f44, f60 as relating to coagulation. However, this statement is only relevant to particle evolution after ~3 hours while nearly all of the observations occur within a physical age of 3 hours.

We do not follow the reviewer's thought process here. We do not interpret changes f_{44} or f_{60} 'as relating to coagulation' in this paper. To first order, coagulation does nothing to change f_{44} or f_{60} (there may be some minor indirect effects due to reducing particle surface area, hence changing condensation/evaporation fluxes), and to the sensitivity we have with the measurements, it only changes particle number.

The point of this statement is to say that little mass/composition changes should occur from het. chem over the 3 hours timespan that the measurements were taken. To make that more clear, we have updated this to
...estimates of heterogeneous mass losses indicate that after three hours of aging (the range of time the BBOP measurements were taken in) for a range of OH concentrations and reactive uptake coefficients...

R58) L281: "with more concentrated plumes". Be more specific by what you mean by more concentrated. Do you mean less diluted, higher mass concentrations of OA, higher CO mixing ratios?

Updated to "with plumes with higher $\Delta OA_{initial}$"

R59) L282-284: "(2) Differences in Δf60 and Δf44 for the nearest-to-source measurements indicate that evaporation and/or chemistry likely occurred before the time of these first measurements..."

It is well documented that the f60 and f44 of POA varies between fires (Cubison et al 2011; Jolleys et al 2015; Ortega et al 2013; McClure et al 2020). Since differences of POA emissions can explain variability in Δf60 and Δf44 for the nearest-to-source measurements, variability of these parameters can NOT be used as evidence of chemistry/evaporation in the smoke plume without knowing the actual f60 and f44 values of fresh POA.

See our extensive response to R4 (Page 13 of this response). As well, the sentence in quotes has been rewritten:

"(2) The differences in Δf_{60} and Δf_{44} are apparent even for the nearest-to-source measurements that are ~15 minutes after the time of emission."

R60) L282-284 "...(assuming that emitted Δf60 and Δf44 do not correlate with ΔOAinitial; there is currently no evidence for this alternative hypothesis)."

There is actually a lot of evidence that f60 and f44 can correlate with OA emissions. In laboratory studies, the evolution of emissions as fires progress from starting-to-flaming-to-smoldering has shown that levoglucosan emissions occur primarily at the starting phase by combustion of hemicellulose material which is also when the majority of OA emissions occur (Corbin et al 2015). Ortega et al (2015) and Lee et al (2010) also observed increased values of f60 in lab burns with higher OA emission factors. These laboratory studies support observations of smoke in ambient troposphere (e.g. Lee et al 2010; Aiken et al 2009; Lee et al 2020).

As you note, it is hard to measure the f60 of POA in ambient smoke. However, the lifetime of levoglucosan in the free troposphere is much longer than the age of aerosol in this study (<3 hours) which is probably why there is only a weak trend to lower f60 values with increasing physical age. So, your measurements of Df60 should be fairly representative of POA and your study (and your first point on lines 280-282 and repeated on line 319) are evidence that f60 is correlated with OA emission factors in wildfires.

See our extensive response to R4 (Page 13 of this document). As well, the sentence in quotes has been rewritten and extended:

"Prior studies have shown that f_{60} and f_{44} at the time of emissions correlate with OA emissions factors through variability in burn conditions (Hennigan et al. 2011; Cubison et al. 2011; McClure et al. 2020), and this relationship might also contribute to our observed correlation between Δf_{60} and Δf_{44} with $\Delta OA_{initial}$. For this emissions relationship to be an important factor, the variability in the OA emission factor needs to be a significant contributor to the variability in $\Delta OA_{initial}$. If the relative variability in the OA emission factor is much smaller than the relative variability in $\Delta OA_{initial}$, other factors contributing to variability in $\Delta OA_{initial}$ will negate an emissions-based covariance between $\Delta OA_{initial}$ with Δf_{60} and Δf_{44}. While our observed $\Delta OA_{initial}$ in Figure 2 spans nearly a factor of 100, Andreae (2019) shows that the OA emission factors have a $-1\boldsymbol{\sigma}$ to $+1\boldsymbol{\sigma}$ range of around a factor 3. Hence, variability in fuel consumption rates and dilution prior to the first transect likely dominate the variability in $\Delta OA_{initial}$, and the relationships of Δf_{60} and Δf_{44} with $\Delta OA_{initial}$ are unlikely to be influenced much by variability in burn conditions. We

conclude that evaporation and/or chemistry prior to the first measurement appears to drive the initial relationship between Δf_{60} and Δf_{44} with $\Delta OA_{initial}$, consistent with (1) the theoretical work of Hodshire et al. (2019a), (2) an analysis of what chemistry would be missed in laboratory experiments if the initial 10-60 minutes of chemistry was not considered, following field experiments (Hodshire et al., 2019b), and (3) the recent field analysis (Palm et al., 2020)."

R61) L284: "Amounts" should be singular.

Fixed

R62) L291: Add citation Jolleys et al (2015).

Unable to determine the location asked for this reference placement.

R63) L313-314: delete "tends to be fairly constant or slightly decreasing with physical age and". Saying that it is poorly correlated is enough.

Removed

R64) L319-320: Evaporation does not happen from dilution. Evaporation will happen if the air is undersaturated (less than predicted vapor pressure of species X compared to equilibrium predicted by Henry's law). Here and elsewhere, please don't say that dilution causes evaporation, instead that dilution promotes evaporation.

Fixed

R65) L334: "NME is more variable..." Do you mean larger or higher? The NME is more variable between parameters, but that is meaningless.

Changed to larger

R66) L336: too many open brackets.
Fixed

R67) L337: What do you mean by "biomass burning modeling"? Are you referring to models of BB emissions, aerosol aging, fire spread?

Changed to "modeling of aging biomass burning aerosol"

R68) L343-345: Since you present a mulit-variate analysis here, what was the point of the past several pages discussing single variable correlation coefficients? Especially after you show that "Both physical age and DOAinitial appear to influence Df60, Df44, and DO/DC..." (Line 319 and a similar statement on L280-282).

Please see our response to R5. We have added text to discuss the synergy between the analysis on Figure 2 with that of Figure 3.

R69) L360-363: This statement needs more explanation and needs citations. Why would you expect plume regions with higher DOAinitial to have lower normalized number concentrations? As stated in the text, the driving process for this should be coagulation. ("*Although we would anticipate that plume regions with higher initial ΔOA would have lower normalized number concentrations due to coagulation"*) Coagulation is proportional to the square of the particle concentration for particles of the same size, and Sakamoto et al., (2016) showed that mass concentrations can be used to estimate the rates that the median diameter increases due to coagulation in biomass burning plumes.
Sakamoto, K. M., Laing, J. R., Stevens, R. G., Jaffe, D. A. and Pierce, J. R.: The evolution of biomass-burning aerosol size distributions due to coagulation: Dependence on fire and meteorological details and parameterization, Atmos. Chem. Phys., 16(12), 7709–7724, doi:10.5194/acp-16-7709-2016, 2016.
We have added that citation to this statement

To a first order, I would expect the opposite. That higher number concentrations would be observed with higher DOAinitial because the OA vapor pressure is higher and this promotes new particle nucleation because vapors are more likely to collide with other vapor molecules to nucleate than with existing particles to condense on (Lim et al 2019; and work from Neil Donahue's group).

High particle mass concentrations generally suppress nucleation because high mass concentrations correspond to a high condensation sink (Westervelt et al., 2014). A high condensation sink cuts down new particle formation through lowering condensable vapor supersaturations (reducing nucleation and growth rates) and increasing the coagulational losses of any clusters that form. Further, high concentrations of particles mean fast coagulation of the primary particles, reducing number concentrations.

We don't follow the rationale about the OA vapor pressure being higher when OA concentrations are high. Under high aerosol concentrations, the low-volatility OA material forming in the gas phase (that could be involved in nucleation) will have a lower ambient vapor pressure than under

low aerosol concentrations because the condensation sink is faster. Higher concentrations of pre-existing particles do not promote new particle formation (there are documented cases where high concentrations of particles do not appear to suppress new particle formation, hypothesized to be to particle-phase mass transfer limitations on condensation, but we are not aware of any cases where high concentration of particles promotes new particle formation).

Westervelt, D.M., Pierce, J.R., Adams, P.J.: Analysis of feedbacks between nucleation rate, survival probability, and cloud condensation nuclei formation, Atmos. Chem. Phys., 14, 5577-5597, doi:10.5194/acp-14-5577-2014, 2014.

R70) L371-372: Decreasing normalized number concentrations are ascribed to coagulation. This contradicts the model that changes in f60 and f44 are due to evaporation of solid particulate balanced by condensation of more oxidized-OA described on line 277-279.

As stated in our response to R57) coagulation is not related to changes in f44 and f60. Coagulation reduces particle number and increases the average particle size. There is no contradiction between these statements: the first focuses on coagulation and the second on evaporation-chemistry-condensation.

R71) L381-382: Awkward and redundant sentence.

Unsure what sentence is in question here.

R72) L384-393: Discussion of nucleation-mode particles seems out of place here. Maybe move towards beginning of section 3.

After careful consideration, we have kept this subsection here. This subsection discusses particle number concentrations, and nucleation-mode particles are a part of that discussion.

Nucleation-mode particles are defined as 20-40nm. This needs a citation.
We are not defining the nucleation-mode particles to be 20-40 nm. We are inferring that nucleation is occurring due to the 'banana' behavior in the data that is observed in this size range. (The FIMS does not measure below 20 nm). Updated to
"Particles appear in the 20-40 nm size range in the FIMS measurements independently of plume OA concentrations (Figs S7-S11), implying that nucleation events may be occuring for some of the transects."

Earlier, a statement was made “bulk of observed newly formed particles observed fell below 40 nm” which implies that a fraction of newly formed particles were larger 40 nm. Was that a mis-statement? This would contradict your definition that nucleation-mode particles are 20-40 nm?

This phrase has been removed.

R73) L388: “one day” should be one transect or transect set. L405-406: Awkward or redundant sentence.

Fixed to ‘one set of transects’.
Updated to
Differences in initial values of Δf_{60}, Δf_{44}, and $\Delta O/\Delta C$ are evidence that evaporation and/or chemistry has likely occurred before the time of initial measurement and that plumes or plume regions with lower initial aerosol loading can undergo these changes more rapidly than thicker plumes.

R74) L408-409: “indicate that evaporation and/or chemistry has likely occurred before the time of initial measurement...” See previous comments questioning validity of this statement.

We changed “indicate” to “are evidence”; see our earlier responses.

R75) L437: Format of some citations need to be cleaned up.

We have checked and corrected the citations.

R76) Figure 1:

- See comments regarding adding error bars to show data variability of bin. There are a few points that are very different from the rest of the data set (such as in the DOA/DCO and DN/DCO datasets) which makes me think the single value representing the bin is inadequate.

- Please change DBC/DCO to a linear scale

Changed.

- Your values of f60 are pretty low for fresh BBOA. I am wondering if this is an issue with the SP-AMS settings or how the data was handled.

The f60 values in Figure 1 and Figure 2 are within the range of the closest transect of prior biomass burning field studies (Garofalo et al., 2019; Cubison et al., 2011) and lab studies (Hennigan et al., 2011).

Hennigan, C. J., Miracolo, M. A., Engelhart, G. J., May, A. A., Presto, A. A., Lee, T., Sullivan, A. P., McMeeking, G. R., Coe, H., Wold, C. E., Hao, W.-M., Gilman, J. B., Kuster, W. C., de Gouw, J., Schichtel, B. A., Collett Jr., J. L., Kreidenweis, S. M., and Robinson, A. L.: Chemical and physical transformations of organic aerosol from the photo-oxidation of open biomass burning emissions in an environmental chamber, Atmos. Chem. Phys., 11, 7669–7686, https://doi.org/10.5194/acp-11-7669-2011, 2011.

Cubison, M. J., Ortega, A. M., Hayes, P. L., Farmer, D. K., Day, D., Lechner, M. J., Brune, W. H., Apel, E., Diskin, G. S., Fisher, J. A., Fuelberg, H. E., Hecobian, A., Knapp, D. J., Mikoviny, T., Riemer, D., Sachse, G. W., Sessions, W., Weber, R. J., Weinheimer, A. J., Wisthaler, A., and Jimenez, J. L.: Effects of aging on organic aerosol from open biomass burning smoke in aircraft and laboratory studies, Atmos. Chem. Phys., 11, 12049–12064, https://doi.org/10.5194/acp-11-12049-2011, 2011.

Garofalo, L. A., Pothier, M. A., Levin, E. J. T., Campos, T., Kreidenweis, S. M., & Farmer, D. K. (2019). Emission and evolution of submicron organic aerosol in smoke from wildfires in the western United States. Acs Earth And Space Chemistry, 3, 1237-1247. doi:10.1021/acsearthspacechem.9b00125

- Need units for Dp axis, “[nm]”.

Added.

R77) Figure 2:

- If you insist on combining all of the data together for a single regression, than you should not be drawing lines between points. Instead this should be a scatter plot with markers.

After careful consideration, we have determined to keep the lines. Without these lines the reader would not be able to follow individual sets of transects because some points from different sets would be colored similarly.

- Legend is inconsistent with figure 1. Either use “edge” or 5%<D[CO]<15%.

We have updated the figure to dCO to be consistent with the text and figure legend.

- Use of “[CO]” is inconsistent with text.

We have updated the figure to dCO to be consistent with the text and figure legend.

- Need units for Dp axis

Updated.

- Caption says that panels (d) and (g) have log axis but are plotted on linear axis. Panels (a) and (f) are plotted on log axis (also in corresponding figures in SI).

Fixed

- Font of “Dp” in caption is different than rest of fonts.

This was to get the overbar in Word. We anticipate that during the switch to LaTeX for typesetting, fonts will be homogenized.

- I think you should also provide a scatter plot of the first measurement of these parameters as a function DOAinitial.

We have made this figure as Figure S24 in the SI and added the following text to the main text: “We include in the supporting information scatter plots of each parameter of Fig. 1 as a function of $\Delta OA_{initial}$ (Fig. S24), and observe no trends other than the cores of the plumes generally having a higher $\Delta OA_{initial}$ than the edges of the plumes, as expected.”

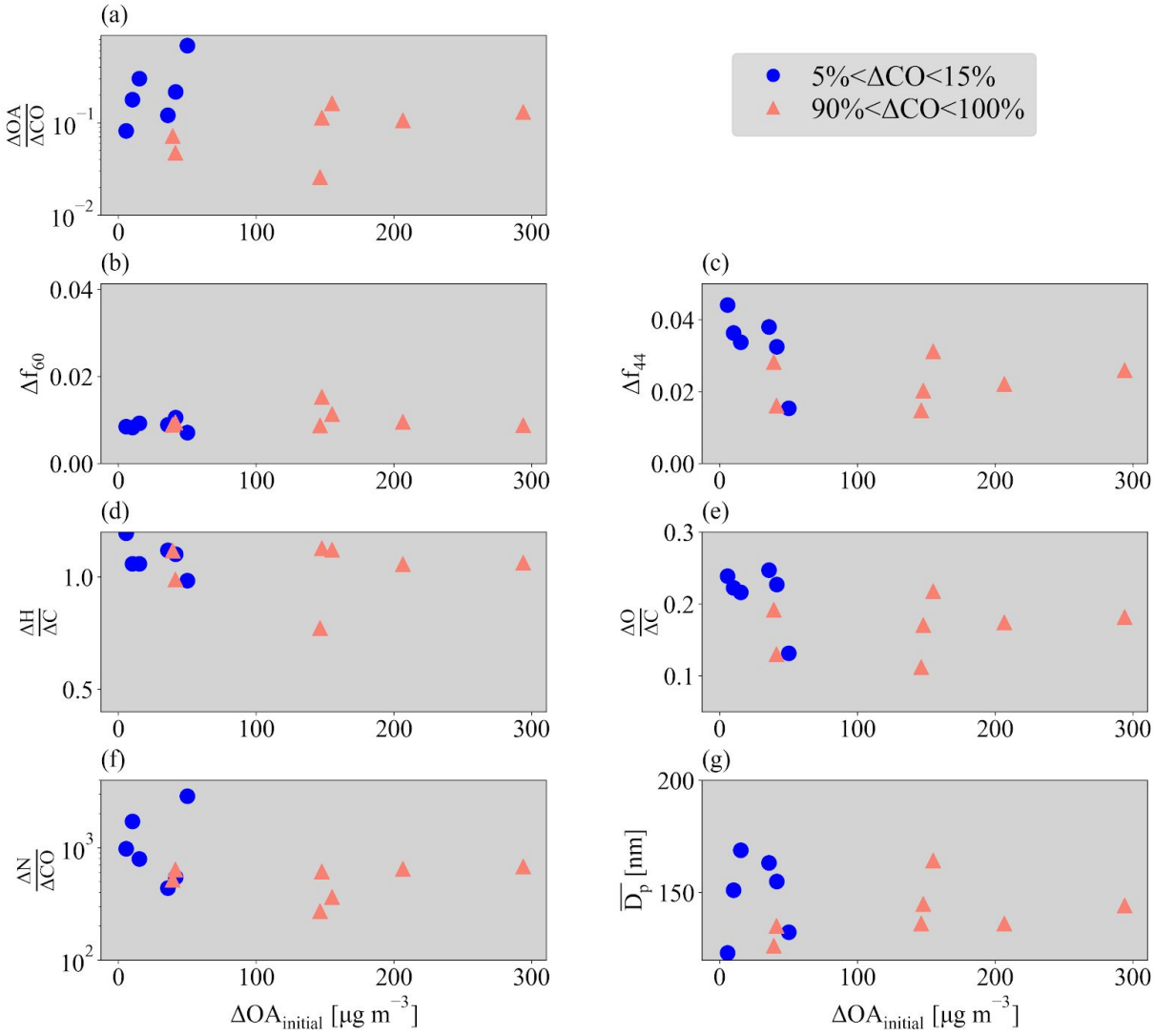

Figure S24. Scatter plot of each parameter of Figure 1 against $\Delta OA_{initial}$.

- Needs error bars

Please see our response to R3.

R78) Figure 3:

• Spearman's correlations are not needed here.

We include both correlation coefficients and see no reason to remove one.

Supplemental Information:

R79) "...electrical mobility as in SMPS..." Should be "...similar to the operating principle of the SMPS..."

Fixed

R80) "...when size distribution suggests that particles smaller than 10 nm contribute negligibly..." Neither the FIMS or CPC 3010 are efficient at counting <10nm Dm particles, so why would the existence of those particles cause differences between the two instruments?

This was a typo--it should have been 20 nm and we have fixed it.

R81) "The SPAMS is thoroughly detailed in Kleinman et al. (2020)..." This still needs to be described here. At least summarizing the operating conditions of the SP-AMS.

We have greatly expanded this supplementary discussion on the SP-AMS (see our response to R2).

R82) "An SPN1 radiometer provided total shortwave irradiance..." It probably measured total shortwave irradiance, not "provided" or "created" the irradiance. This instrument needs to be described more. Maybe what exactly the measurements are and what they represent.

Changed to 'measured'. The papers cited provide instrument details, which is a standard practice in scientific papers.

R83) "... following parameters assumed for the calculation" missing a verb.

Fixed

R84) "Heterogeneous chemistry calculations:" There is no citation to justify the calculation. Is this a common methodology used? Has this methodology passed peer review?

Explained in R7. The collision rate calculation was from Seinfeld and Pandis (2006), and we added upper-bound assumptions about mass loss per reaction.

Seinfeld, J. H. and Pandis, S. N.: Atmospheric Chemistry and Physics, 2nd edn., John Wiley and Sons, New York, 2006.

R85) Fig S1: Colorbar label is missing an "]"

Fixed

R86) Fig S7-S11: Why are x-axis on the top and bottom panels different scales?

The bottom panel is a continuation of the top panel (in time, the x axis). Added this information explicitly to the caption.

Fig S13: should be moved to just before figure S19

These figures are in the order that they are referenced in the main text.

R87) Fig S19-S22: Caption mis-identifies which panels use a log scale.

Corrected

R88) Fig S24: Could you also plot the [CO] of each transect similar to S24-S26. I want to see that the absolute concentration is higher in the center of the plume than the edges and that the [CO] of the core decreases in each successive transect of the set to show dilution.

We have made this figure, Figure S27, and have added the following text to the main text: "To more clearly see this, Fig. S28 provides the same style of figure as Figs. S26-S27 for in-plume CO concentrations. Generally CO peaks around the centerline and is highest in the most fresh transect, but shows variability across transects."

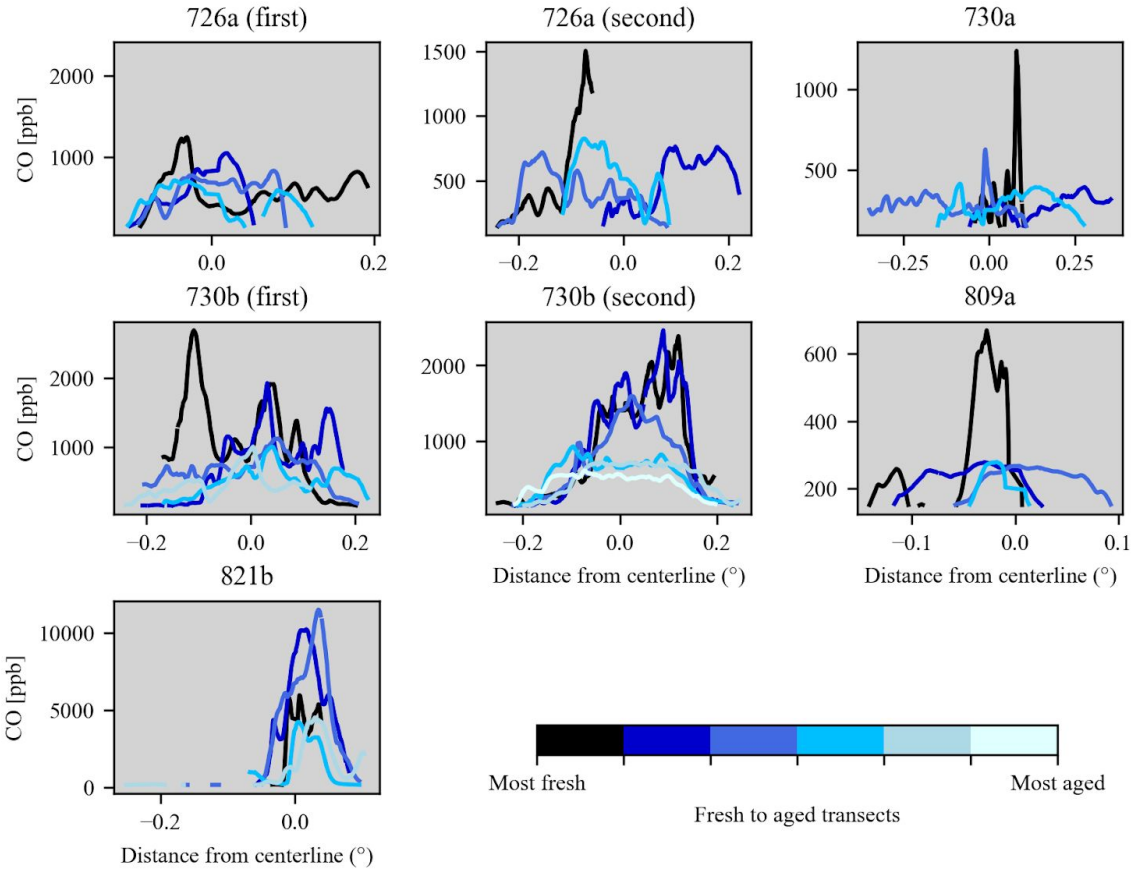

Figure S27. Total in-plume CO (ppbv) irradiance for each flight along each transect included in this study. The titles indicate the flight. The black color indicates the earliest transect, with increasingly lighter colors indicating increasingly downwind transects. The centerline was estimated from the number size distribution and the estimated center of the fire (Figures S1-S6).

R89) Fig S27: Need the 1:1, 1:2, and 0.5:1 line representing constant lines of oxidation. If it is arbitrary where the intersection of these lines is placed (as you cite from Heald et al 2010), then have an arbitrary intersection near the average of your data. The importance is the trends in H:C vs O:C. Alternatively, remove this figure.
We have removed this discussion and figure.

References:

Aiken, A., Salcedo, D., Cubison, M. J., Huffman, J. A., DeCarlo, P. F., Ulbrich, I. M., Docherty, K. S., Sueper, D., Kimmel, J. R., Worsnop, D. R., Trimborn, A., Northway, M., Stone, E. A., Schauer, J. J., Volkamer, R. M., Fortner, E., de Foy, B., Wang, J., Laskin, A.,

Shutthanandan, V., Zheng, J., Zhang, R., Gaffney, J., Marley, N. A., Paredes-Miranda, G., Arnott, W. P., Molina, L. T., Sosa, G., and Jimenez, J. L. (2009). Mexico City Aerosol Analysis During MILAGRO Using High Resolution Aerosol Mass Spectrometry at the Urban Supersite (T0)—Part 1: Fine Particle Composition and Organic Source Apportionment. Atmos. Chem. Phys. 9:6633–6653.

Akagi, S. K., Yokelson, R. J., Wiedinmyer, C., Alvarado, M. J., Reid, J. S., Karl, T., Crounse, J. D., and Wennberg, P. O.: Emission factors for open and domestic biomass burning for use in atmospheric models, Atmos. Chem. Phys., 11, 4039–4072, https://doi.org/10.5194/acp-11-4039-2011, 2011.

Canagaratna, M. R., Jimenez, J. L., Kroll, J. H., Chen, Q., Kessler, S. H., Massoli, P., et al. (2015). Elemental ratio measurements of organic compounds using aerosol mass spectrometry: Characterization, improved calibration, and implications. Atmospheric Chemistry and Physics, 15(1), 253–272. https://doi.org/10.5194/acp-15-253-2015

Collier, S., Williams, L. R., Onasch, T. B., Cappa, C. D., Zhang, X., Russell, L. M., et al. (2018). Influence of emissions and aqueous processing on particles containing black carbon in a polluted urban environment: Insights from a soot particle-aerosol mass spectrometer. Journal of Geophysical Research: Atmospheres, 123, 6648–6666. https:// doi.org/10.1002/2017JD027851

Corbin, J. C., Sierau, B., Gysel, M., Laborde, M., Keller, A., Kim, J., et al. (2014). Mass spectrometry of refractory black carbon particles from six sources: Carbon-cluster and oxygenated ions. Atmospheric Chemistry and Physics, 14(5), 2591–2603. https://doi.org/10.5194/acp-14- 2591-2014

Corbin, J. C., Lohmann, U., Sierau, B., Keller, A., Burtscher, H., and Mensah, A. A.: Black carbon surface oxidation and organic composition of beech-wood soot aerosols, Atmos. Chem. Phys., 15, 11885–11907, https://doi.org/10.5194/acp-15-11885-2015, 2015.

Cubison, M. J., Ortega, A. M., Hayes, P. L., Farmer, D. K., Day, D., Lechner, M. J., et al. (2011). Effects of aging on organic aerosol from open biomass burning smoke in aircraft and laboratory studies. Atmospheric Chemistry and Physics, 11(23), 12,049–12,064. https://doi.org/ 10.5194/acp-11-12049-2011

Forrister, H., et al. (2015), Evolution of brown carbon in wildfire plumes, Geophys. Res. Lett., 42, 4623–4630, doi:10.1002/2015GL063897.

Jolleys, M. D., Coe, H., McFiggans, G., Taylor, J. W., O'Shea, S. J., Le Breton, M., Bauguitte, S.

J.-B., Moller, S., Di Carlo, P., Aruffo, E., Palmer, P. I., Lee, J. D., Percival, C. J., and Gallagher, M. W.: Properties and evolution of biomass burning organic aerosol from Canadian boreal forest fires, Atmos. Chem. Phys., 15, 3077–3095, https://doi.org/10.5194/acp-15-3077-2015, 2015

Lauren A. Garofalo, Matson A. Pothier, Ezra J. T. Levin, Teresa Campos, Sonia M. Kreidenweis, and Delphine K. Farmer (2019): Emission and Evolution of Submicron Organic Aerosol in Smoke from Wildfires in the Western United States, ACS Earth and Space Chemistry 3 (7), 1237-1247. DOI: 10.1021/acsearthspacechem.9b00125

Taehyoung Lee, Amy P. Sullivan, Laura Mack, Jose L. Jimenez, Sonia M. Kreidenweis, Timothy B. Onasch, Douglas R. Worsnop, William Malm, Cyle E. Wold, Wei Min Hao & Jeffrey L. Collett Jr. (2010) Chemical Smoke Marker Emissions During Flaming and Smoldering Phases of Laboratory Open Burning of Wildland Fuels, Aerosol Science and Technology, 44:9, i-v, DOI: 10.1080/02786826.2010.499884

Lee, A. K. Y., Willis, M. D., Healy, R. M., Onasch, T. B., & Abbatt, J. P. D. (2015). Mixing state of carbonaceous aerosol in an urban environment: Single particle characterization using the soot particle aerosol mass spectrometer (SP‐AMS). Atmospheric Chemistry and Physics, 15(4), 1823–1841. https://doi.org/10.5194/acp-15- 1823-2015

Lee, J. E., Dubey, M. K., Aiken, A. C., Chylek, P., & Carrico, C. M. (2020). Optical and chemical analysis of absorption enhancement by mixed carbonaceous aerosols in the 2019 Woodbury, AZ, fire plume. Journal of Geophysical Research: Atmospheres, 125, e2020JD032399. https://doi.org/ 10.1029/2020JD032399

Lim, C. Y., Hagan, D. H., Coggon, M. M., Koss, A. R., Sekimoto, K., de Gouw, J., Warneke, C., Cappa, C. D., and Kroll, J. H.: Secondary organic aerosol formation from the laboratory oxidation of biomass burning emissions, Atmos. Chem. Phys., 19, 12797– 12809, https://doi.org/10.5194/acp-19-12797-2019, 2019.
Massoli, P., et al. (2015), Characterization of black carbon-containing particles from soot particle aerosol mass spectrometer measurements on the R/V Atlantis during CalNex 2010, J. Geophys. Res. Atmos., 120, 2575–2593, doi:10.1002/2014JD022834.

May, A. A., et al. (2014), Aerosol emissions from prescribed fires in the United States: A synthesis of laboratory and aircraft measurements, J. Geophys. Res. Atmos., 119, 11,826–11,849, doi:10.1002/ 2014JD021848.

McMeeking, G. R., et al. (2009), Emissions of trace gases and aerosols during the open combustion of biomass in the laboratory, J. Geophys. Res., 114, D19210,

doi:10.1029/2009JD011836.

Ann M. Middlebrook, Roya Bahreini, Jose L. Jimenez & Manjula R. Canagaratna (2012) Evaluation of Composition-Dependent Collection Efficiencies for the Aerodyne Aerosol Mass Spectrometer using Field Data, Aerosol Science and Technology, 46:3, 258-271, DOI: 10.1080/02786826.2011.620041

Onasch, T. B., Fortner, E. C., Trimborn, A. M., Lambe, A. T., Tiwari, A. J., Marr, L. C., et al. (2015). Investigations of SP-AMS carbon ion distributions as a function of refractory black carbon particle type. Aerosol Science and Technology, 49(6), 409–422. https://doi.org/ 10.1080/02786826.2015.1039959

Ortega, A. M., Day, D. A., Cubison, M. J., Brune, W. H., Bon, D., De Gouw, J. A., & Jimenez, J. L. (2013). Secondary organic aerosol for- mation and primary organic aerosol oxidation from biomass-burning smoke in a flow reactor during FLAME-3. Atmospheric Chemistry and Physics, 13(22), 11,551–11,571. https://doi.org/10.5194/acp-13-11551- 2013

Willis, M. D., Lee, A. K. Y., Onasch, T. B., Fortner, E. C., Williams, L. R., Lambe, A. T., Worsnop, D. R., and Abbatt, J. P. D.: Collection efficiency of the soot-particle aerosol mass spectrometer (SP-AMS) for internally mixed particulate black carbon, Atmos. Meas. Tech., 7, 4507–4516, https://doi.org/10.5194/amt-7-4507-2014, 2014.

Dilution impacts on smoke aging: Evidence in BBOP data

Anna L. Hodshire[1], Emily Ramnarine[1], Ali Akherati[2], Matthew L. Alvarado[3], Delphine K. Farmer[4], Shantanu H. Jathar[2], Sonia M. Kreidenweis[1], Chantelle R. Lonsdale[3], Timothy B. Onasch[5], Stephen R. Springston[6], Jian Wang[6,a], Yang Wang[7,b], Lawrence I. Kleinman[6], Arthur J. Sedlacek III[6], Jeffrey R. Pierce[1]

[1] Department of Atmospheric Science, Colorado State University, Fort Collins, CO 80523, United States
[2]Department of Mechanical Engineering, Colorado State University, Fort Collins, CO 80523, United States
[3]Atmospheric and Environmental Research, Inc., Lexington, MA 02421, United States
[4]Department of Chemistry, Colorado State University, Fort Collins, CO 80523, United States
[5]Aerodyne Research Inc., Billerica, MA 01821, United States
[6]Environmental and Climate Sciences Department, Brookhaven National Laboratory, Upton, NY 11973, United States
[7]Center for Aerosol Science and Engineering, Washington University, St. Louis, MO 63130, United States
[a]Now at Center for Aerosol Science and Engineering, Washington University, St. Louis, MO 63130, United States
[b]Now at Department of Civil, Architectural and Environmental Engineering, Missouri University of Science and Technology, Rolla, Missouri 65409, United States

Correspondence to: Anna L. Hodshire (Anna.Hodshire@colostate.edu)

Abstract. Biomass burning emits vapors and aerosols into the atmosphere that can rapidly evolve as smoke plumes travel downwind and dilute, affecting climate- and health-relevant properties of the smoke. To date, theory has been unable to explain observed variability in smoke evolution. Here, we use observational data from the BBOP field campaign and show that initial smoke organic aerosol mass concentrations can help predict changes in smoke aerosol aging markers, number concentration, and number ~~-~~mean diameter between 40-262 nm. Because initial field measurements of plumes are generally >10 minutes downwind, smaller plumes will have already undergone substantial dilution relative to larger plumes and have lower concentrations of smoke species at these observations closest to the fire. T~~However, t~~he extent to which dilution has occurred prior to the first observation is not a directly measurable quantity. Hence, initial observed plume concentrations can serve as a rough indicator of the extent of dilution prior to the first measurement, which impacts photochemistry~~, and~~ aerosol evaporation, and coagulation. Cores of plumes have higher concentrations than edges. By segregating the observed plumes into cores and edges, we find evidence~~infer~~ that particle aging, evaporation, and coagulation occurred before the first measurement. We further find that on the plume edges, the ~~oxidation state of~~ organic aerosol is more oxygenated ~~has~~

increased while a marker for primary biomass burning aerosol emissions has decreased in relative abundance than in the plume cores. and undergone more decreases in a marker for primary biomass burning organic aerosol.Finally, we attempt to decouple the roles of the initial concentrations and time since emission bybut performing multivariate linear regression of various aerosol properties (composition, size) on these two factors.

1 Introduction

Smoke from biomass burning is a major source of atmospheric primary aerosol and vapors (Akagi et al., 2011; Gilman et al., 2015; Hatch et al., 2015, 2017; Jen et al., 2019; Koss et al., 2018; Reid et al., 2005; Yokelson et al., 2009), influencing air quality, local radiation budgets, cloud properties, and climate (Carrico et al., 2008; O'Dell et al., 2019; Petters et al., 2009; Ramnarine et al., 2019; Shrivastava et al., 2017), as well as the health of smoke-impacted communities (Ford et al., 2018; Gan et al., 2017; Reid et al., 2016). Dilution of a smoke plume occurs as the plume travels downwind, mixing with regional 'background' air, reducing the concentrations of the smoke aerosols and vapors and potentially drivingallowing for rapid changes in the physical and chemical properties of the emissions Dilution of a smoke plume occurs when the plume mixes with regional 'background' air, reducing the concentrations of the smoke aerosols and vapors as the plume travels downwind. Dilution can lead to rapid changes in the physical and chemical properties of the emissions. Dilution through entrainment of regional background air can cause vapors and particles emitted from fires to rapidly evolve as smoke travels downwind (Adachi et al., 2019; Akagi et al., 2012; Bian et al., 2017; Cubison et al., 2011; Hecobian et al., 2011; Hodshire et al., 2019a, 2019b; Jolleys et al., 2012, 2015; Konovalov et al., 2019; May et al., 2015; Noyes et al., 2020; Sakamoto et al., 2015, Palm et al., 2020). Fires span an immense range in size, from small agricultural burns, which may be only a few m^2 in total area and last a few hours, to massive wildfires, which may burn 10,000s of km^2 over the course of weeks (Andela et al., 2019). This range in size leads to variability in initial plume size and extent of dilution by the time of the first measurement., as lLarge, thick plumes dilute more slowly than small, thin plumes for similar atmospheric conditions, as the cores of larger plumes are at a greater physical distance to the background air, shielding them from dilution for longer (Akagi et al., 2012; Bian et al., 2017; Cubison et al., 2011; Hecobian et al., 2011; Hodshire et al., 2019a, 2019b; Jolleys et al., 2012, 2015; Konovalov et al., 2019; May et al., 2015; Sakamoto et al., 2015, Lee et al., 2020, Garofalo et al., 2019). Plumes can dilute unevenly, with edges of the plume mixing in with surrounding air more rapidly than the core of the plume. Variability in dilution leads to variability in the evolution of smoke emissions as instantaneous plume aerosol concentrations will control shortwave radiative fluxes (and thus photolysis rates and oxidant concentrations), gas-particle partitioning, and particle coagulation rates (Akagi et al., 2012; Bian et al., 2017; Cubison et al., 2011; Hecobian et al., 2011; Hodshire et al., 2019a, 2019b; Jolleys et al., 2012, 2015; Konovalov et al., 2019; May et al., 2015; Sakamoto et al., 2015, Garofalo et al., 2019, Ramnarine et al., 2019; Sakamoto et al., 2016). Thus, capturing variability in plume aerosol concentrations and dilution between fires and within fires can aid in understanding how species change within the first few hours of emission for a range of plume sizes.

The evolution of total particulate matter (PM) or organic aerosol (OA) mass from smoke has been the focus of many studies, as PM influences both human health and climate. Secondary organic aerosol (SOA) production occurs~~may come about~~ through oxidation of gas-phase volatile organic compounds (VOCs) that can form lower-volatility products that partition to the condensed phase (Jimenez et al., 2009; Kroll and Seinfeld, 2008). SOA formation may also arise from heterogeneous and multi-phase reactions in both the organic and aqueous phases (Jimenez et al., 2009; Volkamer et al., 2009). In turn, oxidant concentrations depend on shortwave fluxes (Tang et al., 1998; Tie, 2003; Yang et al., 2009) and the composition of the plume (Yokelson et al. 2009; Akagi et al. 2012; Hobbs et al. 2003; Alvarado et al. 2015). Smoke particles contain semivolatile organic compounds (SVOCs) (Eatough et al., 2003; May et al., 2013), which may evaporate off of particles as the plume becomes more dilute (Huffman et al. 2009; May et al. 2013; Garofalo et al. 2019; Grieshop et al. 2009), leading to losses in total aerosol mass. Field observations of smoke PM and OA mass normalized for dilution (e.g. through an inert tracer such as CO) report that for near-field (<24 hours) physical aging, net PM or OA mass can increase (Cachier et al., 1995; Formenti et al., 2003; Liu et al., 2016; Nance et al., 1993; Reid et al., 1998; Vakkari et al., 2014, 2018; Yokelson et al., 2009), decrease (Akagi et al., 2012; Hobbs et al., 2003; Jolleys et al., 2012, 2015; May et al., 2015), or remain nearly constant (Brito et al., 2014; Capes et al., 2008; Collier et al., 2016; Cubison et al., 2011; Forrister et al., 2015; Garofalo et al., 2019; Hecobian et al., 2011; Liu et al., 2016; May et al., 2015; Morgan et al., 2019; Sakamoto et al., 2015; Sedlacek et al., 2018; Zhou et al., 2017). It is theorized that both losses and gains in OA mass are likely happening concurrently in most plumes through condensation and evaporation (May et al. 2015; Hodshire et al. 2019; Hodshire et al. 2019; Bian et al. 2017; Palm et al. 2020)~~(Bian et al., 2017; Hodshire et al., 2019a, 2019b; May et al., 2015)~~, with the balance between the two determining whether net increases or decreases or no change in mass occurs during near-field aging. However, there is currently no reliable predictor of how smoke aerosol mass (normalized for dilution) may change for a given fire.

Evolution of total aerosol number, size, and composition is critical for improving quantitative understanding of how biomass burn smoke plumes impact climate. These impacts include smoke aerosols' abilities to both act as cloud condensation nuclei (CCN) and to scatter/absorb solar radiation, each of which is determined by particle size and composition (Albrecht, 1989; Petters and Kreidenweis, 2007; Seinfeld and Pandis, 2006; Twomey, 1974; Wang et al., 2008). Particles can increase or decrease in size as well as undergo compositional changes through condensation or evaporation of more volatile compounds~~vapors~~. In contrast, coagulation always decreases total number concentrations and increases average particle diameter~~.~~; Pplumes with higher aerosol number concentrations will undergo more coagulation than those with lower concentrations (Sakamoto et al., 2016).

Being able to predict smoke aerosol mass, number, size, and composition accurately is an essential component in constraining the influence of fires on climate, air quality, and health. Fires in the western United States region are predicted to increase in size, intensity, and frequency (Dennison et al., 2014; Ford et al., 2018; Spracklen et al., 2009; Yue et al., 2013). In response, several large field campaigns have taken place in the last 7 years examining wildfires in this region (Kleinman et al., 2020~~Kleinman and Sedlacek 2016~~; Garofalo et al. 2019; Palm et al., 2020). Here, we present smoke plume

observations from the Biomass Burning Observation Project (BBOP) campaign of aerosol properties from five research flights sampling wildfires downwind in seven pseudo-Lagrangian sets of transects to investigate the evolution of OA mass and oxidation state, aerosol number, and aerosol number mean diameter. A range of initial (at the time of the first plume pass in the aircraft) plume OA mass concentrations were captured within these flights and ~~sufficiently~~ fast (1 second) measurements of aerosols and key vapors were taken. The time resolution of the data was great enough that we have been able to ~~We~~ segregate each transect into edge, core, or intermediate regions of the plume and examine aerosol properties within the context of both the location within the plume (edge, core, or intermediate) and the initial OA mass loading of the given location. The differences in aerosol loading serve as a proxy for differences in initial fire and plume sizes, mass fluxes, and subsequent amount of dilution. ~~rates, as t~~The extent to which dilution has occurred prior to the first observation is not a measurable quantity, and fire sizes and mass fluxes were not estimated as a part of the BBOP campaign. We create mathematical fits for predicting OA oxidation markers and mean particle diameter given initial plume OA mass concentration and physical age (time) of the smoke. These fits may be used to evaluate other smoke datasets and assist in building parameterizations for regional and global climate models to better-predict smoke aerosol climate and health impacts.

2 Methods

The BBOP field campaign occurred in 2013 and included a deployment of the United States Department of Energy Gulfstream 1 (G-1) research aircraft in the Pacific Northwest region of the United States (Kleinman and Sedlacek, 2016; Sedlacek et al., 2018) from June 15 to September 13. We analyze five cloud-free BBOP research flights that had seven total sets of across-plume transects that followed the smoke plume downwind in a Lagrangian manner (see Figs. S1-S6 for examples; Table S1) from approximately 15 minutes after emission to 2-4 hours downwind (Kleinman and Sedlacek, 2016). The G-1 sampling setup is described in (Kleinman and Sedlacek, 2016; Sedlacek et al., 2018; Kleinman et al., 2020).

Number size distributions were obtained with a Fast-integrating Mobility Spectrometer (FIMS), providing particle size distributions nominally from approximately 20-350 nm (Kulkarni and Wang, 2006; Olfert and Wang, 2009); data was available between 20-262 nm for the flights used in this study. A Soot Photometer Aerosol Mass Spectrometer (SP-AMS) provided organic and inorganic (sulfate, chlorine, nitrate, ammonium) aerosol mass concentration of PM_1 (sub-micron aerosol) ~~PM1 aerosol masses~~ (Canagaratna et al. 2007), select fractional components (the fraction of the AMS OA spectra at a given mass-to-charge ratio) (Onasch et al., 2012), and elemental analysis (O/C and H/C) (Aiken et al., 2008; Canagaratna et al., 2015). Extended details on the SP-AMS are provided in Text S1 in the supplementary information, and~~but~~ a brief~~er~~ overview is given here. The SP-AMS had its~~the~~ highest sensitivity between 70-500 nm, dropping to 50% of peak sensitivity~~transmission efficiency~~ by 1000 nm (Liu et al. 2007). It was characterized to have a collection efficiency of 0.5 when the instrument's laser was off and 0.76 when the instrument's laser was on during the BBOP campaign, and these corrections have been applied to the data. There is ~~substantial~~ evidence from other studies that the~~in the published literature~~

~~for the~~ CE of the tungsten vaporizer (laser off mode) (Lim et al., 2019) and the laser vaporizer (laser on mode) (Willis et al., 2014) to change as a function of chemical composition, rBC coating thickness, size, and sphericity in laboratory studies (Middlebrook et al., 2012; Willis et al., 2014; Corbin et al., 2015; Massoli et al., 2015; Collier et al., 2018)~~.~~ and in aircraft observations (Kleinman et al. 2007). Results pertinent to changes in CE due to aging in smoke plumes are scarce (see discussion in Kleinman et al., 2020). ~~Unfortunately for various reasons, instrument comparisons of measurements of PM1 mass loading concentrations were very limited during BBOP, such that there does not exist a useful estimate of a changing CE for either SP-AMS vaporizer with changing plume conditions, so w~~We assume these CEs for the laser on and off modes are~~to be~~ constant in space and time~~. We do not attempt to characterize whether the collection efficiency of the SP-AMS changes as the aerosol ages~~, which is a limitation of this study. ~~This may be a limitation of this study, as collection efficiency has been recently observed to decrease with aging within a laboratory study of biomass burning (Lim et al. 2019). However, no consistent evidence of changing collection efficiencies in field studies exist yet.~~ We use the calculated f_{60} and f_{44} fractions ~~al components~~ (the mass concentrations of m/z 60 and 44 normalized by the total OA mass concentration) and O/C and H/C elemental ratios of OA as tracers of smoke and oxidative aging. Elevated f_{60} values are indicative of "levoglucosan-like" species (levoglucosan and other molecules that similarly fragment in the AMS) (Aiken et al., 2009; Cubison et al., 2011; Lee et al., 2010) and are known~~shown to be~~ tracers of smoke primary organic aerosol (POA) (Cubison et al., 2011). ~~The~~ f_{44}, the OA~~-~~ fractional component observed by the SP-AMS as the ion fragment ~~(arising from primarily~~ CO_2^+ as well as some acid groups~~, ;)~~ is a proxy for~~indicative of~~ SOA arising from oxidative aging (Alfarra et al., 2004; Cappa and Jimenez, 2010; Jimenez et al., 2009; Volkamer et al., 2006). Fractional components f_{60} and f_{44} have been shown to decrease and increase with photochemical aging, respectively, likely due to both evaporation and/or oxidation of semivolatile ~~f_{60} containing~~ species that contribute to m/z 60 in the SP-AMS and addition of oxidized ~~f_{44} containing~~ species that contribute to m/z 44 in the SP-AMS (Alfarra et al., 2004; Huffman et al., 2009). O/C tends to increase with oxidative aging (Decarlo et al., 2008) whereas H/C ranges from increasing to decreasing with oxidative aging, depending on the types of reactions occurring (Heald et al., 2009). Changes in O/C and H/C (as well as changes in total OA mass, number, ~~-~~f_{44}, and f_{60}) are also influenced by mixing of different air masses and co-oxidation of different VOC precursors (Chen et al. 2015). Tracking H/C with aging may provide clues upon the types of reactions that may be occurring; however, variable oxidation timescales can make inferences of this type difficult (Chen et al. 2015). A Single-Particle Soot Photometer (SP2; Droplet Measurement Technologies) was used to measure refractory black carbon (BC) between 80-500 nm (Schwarz et al. 2010) through laser-induced incandescence (Moteki and Kondo, 2010; Schwarz et al., 2006). An Off-Axis Integrated-Cavity Output Spectroscopy instrument (Los Gatos, Model 907)~~ provided~~ measured CO concentrations~~measurements~~. An SPN1 radiometer (Badosa et al., 2014; Long et al., 2010) measured~~ provided~~ total shortwave irradiance. Kleinman et al. (2020) provides extensive details for the BBOP instruments used in this work. The supporting information also includes more details on the instruments used.

To determine the contribution to~~of~~ the concentration of species X ~~concentrations~~ from smoke emissions (ΔX), the background concentration of X is subtracted off of the measured in-plume species concentrations ~~(ΔX)~~. To correct for

dilution, we normalize ΔX by background-corrected CO (ΔCO), which is inert on timescales of near-field aging (Yokelson et al., 2009). Increases or decreases of ΔX/ΔCO along the Lagrangian flight path ~~with time~~ indicate whether the total amount of X in the plume has increased or decreased (implying production or removal) since time of emission. The background concentration of X is determined as a regional average of the observed out-of-plume concentrations of X. To avoid using smoke-impacted measurements we apply a threshold of only using measurements of X that occur in regions that correspond to the lowest 10% of CO data. We determine the lowest 10% of CO concentrations~~data only using~~ from each flight during time periods with a similar altitude, latitude, and longitude as the smoke plume ~~in order to exclude flight data taken flying to or from each plume~~. We perform sensitivity calculations on our assumptions of background regions and discuss them in Section 3. ~~We background-correct the number size distribution, OA, O, H, C, and BC data in this manner by determining an average regional background for each species by using the lowest 10% of the CO data for a given flight with a similar altitude, latitude, and longitude as the smoke plume.~~

Mass concentrations of ~~Elemental~~ O, H, and C are calculated using the O/C and H/C and OA data from the SP-AMS (assuming all of the OA mass is from O, C, and H), allowing us to calculate the background-corrected OA atomic ratios, ΔO/ΔC, and ΔH/ΔC, following equation 1 (where X = O or H):

$$\frac{\Delta X}{\Delta C} = \frac{(X_{in\ plume} - X_{out\ of\ plume})}{(C_{in\ plume} - C_{out\ of\ plume})} \qquad \text{Eq. 1}$$

We note that any non-linear changes in chemistry and composition between the plume and background will not perfectly isolate the elemental factors in smoke. We also background-correct fractional f_{60} and f_{44} (using the mass concentrations of m/z 60, m/z 44, and OA inside and outside of the plume), but we do not normalize by CO due to these values already being normalized by OA, following equation 2 (where $f = f_{60}$ or f_{44}):

$$\Delta f = \frac{(f_{in} * OA_{in}) - (f_{out} * OA_{out})}{\Delta OA} \qquad \text{Eq. 2}$$

We only consider data to be in-plume if the absolute CO >= 150 ppbv~~, as comparisons of CO and the number concentration show that in-plume data has CO >150 ppbv and out-of-plume (background) data has CO < 150 ppbv.~~ This threshold appears to be capturing clear plume features as seen in the number concentration while excluding background air (Figs. S7-S11). We note that we use different definitions of in-plume and background (i.e. ~~e.g.~~ the lowest 10% of CO measurements) in order to provide a buffer between the plume and background to ensure to the best of our abilities that we are capturing non-smoke impacted air for the background and smoke-impacted air for in-plume cases. The regions of the lowest 10% of CO measurements always fall under 150 ppbv (Figs. S7-S11). Similarly, we exclude the lowest 5% of CO data in the in-plume measurements in our analyses to provide a further buffer between smoke-impacted and background air. We perform sensitivity analyses of our results to our assumptions about background and in-plume values in Section 3. Figures S2-S6 indicate the locations of the lowest 10% of CO for each flight.

From the FIMS, we examine the background-corrected, normalized number concentrations of particles with mobility diameters between 40-262 nm, ΔN/ΔCO. This size range allows us to exclude potential influence of fresh nucleation upon the total number concentrations. Occasionally, the background-corrected, normalized number concentration

in the FIMS size rangenumber concentration between 20-40 nm increases by 1-2 orders of magnitude relative to typical plume conditions, indicating possible nucleation events, primarily at the edges or in between smoke plumes , as the bulk of observed newly formed particles observed fell below 40 nm (Figs. S7-S11). Smoke plumes contain particles with diameters larger than 262 nm (Janhäll et al., 2009),: thusand so although, we cannot provide total number concentrations, but, we can infer how the evolution of ΔN/ΔCO within our observed size range evolveswill impact number concentrations overall. We also obtain an estimate of how the number mean diameter between 40-262 nm, $\overline{D_p}$, changes with aging through:

$$\overline{D_p} = \frac{\Sigma N_i * D_{p,i}}{\Sigma N_i} \qquad \text{Eq. 3}$$

wWhere N_i and $D_{p,i}$ are the number concentration and geometric mean diameter within each FIMS size bin, respectively.

All of the data are provided at 1 Hz and all but the SP-AMS fractional component data are available on the DOE ARM web archive (https://www.arm.gov /research/campaigns/aaf2013bbop). As the plane traveled at approximately 100 m s^{-1} on average, data were collected every 100 m across the plume. The plumes spanned from approximately 5-50 km wide (Figs. S2-6). The instruments used here had a variety of time lags (all <10 seconds) relative to a TSI 3563 nephelometer used as reference. The FIMS also showed additional smearing in flushing smoky air with cleaner air when exiting the plume with maximum observed flushing timescales around 30 seconds, but generally less (Fig. S12). To test if these lags impact our results, we perform an additional analysis where we only consider the first half of each in-plume transect, when concentrations are generally rising with time (Figure S12-S13), and our main conclusions are unaffected. We do not test the impacts of other time lags and do not attempt to further correct the data for any time lags. Kleinman et al. (2020) provides further information on instrument time delays during BBOP.

We use MODIS Terra and Aqua fire and thermal anomalies detection data to determine fire locations (Giglio et al., 2006, 2008). We estimate the fire center to be the approximate center of all clustered MODIS detection points for a given sampled fire (Figs. S1-S6). The true fire location at the time of sampling is likely different than the MODIS estimates, depending on the speed of the fire front. To estimate the physical age of the plume, we use the estimated fire center as well as the total FIMS number concentration to determine an approximate centerline of the plume as the smoke travels downwind (an example is provided in Fig. S1). The centerline is subjectively chosenplaced to attempt to approximately capture the most-concentrated portion of the total number concentration for each plume pass (as estimated using total aerosol number concentrations), as we focus on aerosol properties and their relations to dilution in this study. We use the mean wind speed and this estimated centerline to calculate an estimated physical age for each transect, and this physical age is assumed to be constant across the transect, as plume crossings took between 50-500 seconds; however, transects that were not perfectly tangential to the mean wind would have sampled different plume ages on the opposite sides of the plume. We did not propagate uncertainty in fire location, wind speed, or centerline through to the physical age, which is a limitation of this study.

3 Results and discussion

As a case example, we examine the aging profiles of smoke from the Colockum fire during the first set of pseudo-Lagrangian transects foron flight 730b (Table S1). Figure 1 provides ΔOA/ΔCO, ΔBC/ΔCO, Δf_{60}, Δf_{44}, ΔH/ΔC, ΔO/ΔC, ΔN/ΔCO, and $\overline{D_p}$ as a function of the estimated physical age; Figs. S14-S18 provides this information for the other pseudo-Lagrangian transect flight sets studied. (Here, BC represents the refractory BC from the SP2; Sect. 2.) We have divided each transect into four regions: between the 5-15 (edge), 15-50 (intermediate, outer), 50-90 (intermediate, inner), and 90-100 (core) percentile of ΔCO within each transect. (As discussed above, wWe exclude the lowest 5% in order to provide a buffer between the plume edge and background air.) Note that in Figure 1 (and Figures S14-S18), the points represent the mean values for each transect/percentile and do not include error bars for uncertainty in the mean or measurement uncertainty as characterization of systematic variance (within plume percentiles) with age is beyond the scope of this study for figure simplicity. Figures S2-S6 show the locations of these CO percentile bins for each transect of individual flights. Figure 1 shows the edge and core data, both averaged per transect, andwhileith Figs. S14-18 providesproviding all four percentile bins for each flight. These percentile bins correspond with the thinnest (lowest CO mixing ratioleast CO-dense) to thickest (highest CO mixing ratiomost CO-dense) portions of the plume, respectively. If a fire has uniform emissions ratios across all regions and dilutes evenly downwind, these percentile bins would correspond to the edges, intermediate regions, and the core of the diluting plume. We use this terminology in this study but note that uneven emissions, mixing, and/or dilution lead to the percentile bins not physically corresponding to our defined regions in some cases. We note that some plumes show more than one maxima in CO concentrations within a given plume crossing, which implies that there may be more than one fire or fire front, and that these plumes from separate fires or fronts are not mixing perfectly perfectly mixing. Multiple maxima could also imply vertical variations in the location of the core of the plumes that the flights did not capture.. As well, in at least one of the fires (in flights '730a' and '730b'), the fuels vary between different sides of the fire, as discussed in Kleinman et al., (2020). However, the lowest two ΔCO bins tend more towards the physical edges of the plume, and the highest two tend more towards the physical center of the plume (Figs. S2-S6). We do not use the data from the lowest 5% of ΔCO to reduce uncertainty at the plume-background boundary. We do not know where the plane is vertically in the plume, which is a limitation as vertical location will also impact the amount of solar flux able to penetrate through the plume.

Figure 1 shows that for this specific plume, ΔOA/ΔCO and ΔBC/ΔCO systematically vary little with age for both the 5-15 and 90-100 percentile of ΔCO (p-values>0.5), yet both show non-systematic variability between transects. A true Lagrangian flight with the aircraft sampling the same portion of the plume and no measurement artifacts (e.g. coincidence errors at high concentrations) would have a constant ΔBC/ΔCO for each transect set. This flight and other flights studied here have slight variations in ΔBC/ΔCO (Fig. 1; Figs. S14-S18), which may be indicative of deviations from a Lagrangian flight path with temporal variations in emission and/or measurement uncertainties. The remaining variables plotted also show some noise and few clear trends, but it is apparent that the transect-mean values 5-15 and 90-100 percentiles do show a

separation for some~~many~~ of the individual metrics, in particular Δf_{44} and ΔO/ΔC. In order to determine the existence or lack of trends for these metrics, we spend the remainder of this study examining each metric from all of the pseudo-Lagrangian flights together.

3.1 Organic aerosol aging: ΔOA/ΔCO, Δf_{60}, Δf_{44}, ΔH/ΔC, and ΔO/ΔC

Figure 2a-e shows~~show~~ available ΔOA/ΔCO, Δf_{60}, Δf_{44} ΔH/ΔC, and ΔO/ΔC edge and core data versus physical age for each transect for each flight of this study. We color each line by the mean ΔOA within a ΔCO percentile bin from the transect closest to the fire, $\Delta OA_{initial}$, in order to examine whether each variable (ΔOA/ΔCO, Δf_{60}, Δf_{44} ΔH/ΔC, and ΔO/ΔC) vary with $\Delta OA_{initial}$. (Some transects do not have data available for specific instruments.) As with Fig.~~ure~~ 1, the points in Fig.~~ure~~ 2 represent the mean values for each transect and percentile, and we do not include error bars as we do not attempt to characterize systematic variance (within plume percentiles) with age in this study~~that would make the figure unwieldy~~. We note that $\Delta OA_{initial}$ does not actually represent the true initial emitted OA from each fire, but instead serves as a proxy for the general fire size, intensity, and emission rate (as larger fires and fires with faster rates of fuel consumption per area will have larger mass fluxes than smaller fires or fires with less fuel consumption per area, all else equal)~~as presumably larger fires and fires with faster rates of fuel consumption per area, more intensely burning fires will have larger mass fluxes than smaller, less intensely burning fires~~). Thus, $\Delta OA_{initial}$ and other "initial" metrics referred to in this study are not to be taken as emission values and direct comparison to studies with direct emissions values is not appropriate, as dilution and chemistry may occur before the initial flight transect, which we discuss further below. We show the 5-15 (edge) and 90-100 (core) ΔCO percentile bins in Fig. 2; Fig. S19 shows the same information for all four ΔCO percentiles. We use the simple 'edge' and 'core' terminology throughout the following discussion but note that the 5-15 and 90-100 ΔCO percentile bins do not necessarily correspond to the physical (spatial) edges and cores of each plume. They instead correspond to the most CO-dense and least CO-dense portions of the plume. We also note that although some of the physical ages appear to start at approximately 0 hours (e.g. over the fire), this is from a limitation of our physical age estimation method (Sect. 2), as no flights captured data before approximately 15 minutes after emission (Kleinman et al., 2016). Flights with two sets of pseudo-Lagrangian transects ('726a' and '730b') have two separate lines in Fig. 2, one for each set. As well, two transects for flight '809a' nearly overlap (Fig. S5), with the transect that is further from the fire occurring first in the flight path, leading to an apparent slight decrease in physical age for the sequential transect (see, e.g., the white dashed line in Fig. 2a).

Also included in Fig. 2 are the Spearman rank-order correlation tests (hereafter Spearman tests), which are tests for monotonicity. The Spearman tests show correlation coefficients for each flight set (Table S1) with the initial ΔOA of a flight set ($\Delta OA_{initial}$) against ΔOA/ΔCO, Δf_{60}, Δf_{44}, ΔH/ΔC, and ΔO/ΔC as the smoke aerosol ages~~each variable ages~~ downwind. We also include Spearman tests for the calculated physical age of the smoke for each flight set against these same variables. The R values are labeled $R_{\Delta OA,initial}$ and R_{age}, respectively, in Fig. 2. We calculate these correlation coefficients separately for Figure 2 to determine how well ~~the~~ variability for each variable can be predicted~~known~~ from the $\Delta OA_{initial}$ or age alone (and

whether the~~along with if the~~ data are correlated vs. anticorrelated with these predictors). To complement these independent correlation coefficients, we also perform multivariate linear regressions (Eqns. 4 and 5 and Figure 3, discussed later) to explicitly decouple the influence of the two predictors. For the correlations with $\Delta OA_{initial}$, all transects in a given pseudo-Lagrangian set of transects have the same $\Delta OA_{initial}$ value; for flights with two pseudo-Lagrangian sets of transects, each set has its own $\Delta OA_{initial}$ value. Correlating to $\Delta OA_{initial}$ provides an estimate of how the plume aerosol concentrations at the time of the initial transect impact plume aging (aging both before and after this initial transect). We define the following categories of correlation for the absolute value of R: 0.0-0.19 is 'very weak', 0.2-0.39 is 'weak', 0.4-0.59 is 'moderate', 0.6-0.79 is 'strong', and 0.8-1.0 is 'very strong' (Evans 1996) .

As individual flights show scatter in the metrics of Fig. 2 (Figs. 1, Figs. S14-S18), we also include $R_{\Delta OA,initial}$ and R_{age} for each metric of Fig. 2 ~~systematically~~ sequentially removing one flight from the statistical analysis. These results are summarized in Table S2. In general, removing single flights does not change our conclusions, particularly when correlations are moderate or stronger. S~~We note that s~~catter in $\Delta OA_{initial}$ leads to weaker R_{age} values than would be obtained if we normalized changes with aging to the first (normalized) value. However, as plume-density-dependent aging prior to the first transect is one of the potentially interesting findings of this study, we feel that it is important to not normalize our changes further. Figs. S13, S19-S22~~1~~ show the same details as Fig. 2 but provide sensitivity tests to our methodology. Figure S13 ~~uses data from transect portions in which~~ to examines potential FIMS measurement artifacts by only using data from the first 50% of each flight leg when particle concentrations are increasing, which lessons response-time-artifacts of the FIMS during transitions from high to low concentration regions. ~~(Fig. S13),~~ Figure S20 tests our assumed in-plume CO threshold value by increasing it from 150 ppbv to 200 pbbv (~~set to 150 ppbv for Figs. 1-3~~;Fig. S19~~ Sect. 2~~). ~~,~~ ~~and~~ Figure S21 tests ΔCO percentile spacing by changing the bins from 5-15%, 15-50%, 50-90%, and 90-100% to 5-25%, 25-75%, and 75-100%. Figure S22 tests assumed background region by increasing data used from the lowest 10% to the lowest 25% of CO measurements. ~~((Figs. S19-S221).~~ Although these figures show slight variability, the findings discussed below remain robust, and we constrain the rest of our discussion to the original assumptions made for the FIMS measurements, in-plume CO threshold value, and ΔCO percentiles used in Fig. 2.

In general, both the cores and edges do not show any positive or negative trend in ΔOA/ΔCO with respect to physical aging.~~,~~ The correlation coefficients,~~with~~ $R_{\Delta OA,initial}$ and R_{age}, ~~show~~ing very weak correlations of 0.02 and +0.03 (with $R_{\Delta OA,initial}$ and R_{age} ranging between -0.25 to +0.17 and 0 to 0.07, respectively, when individual flights are left out sequentially; Table S2). The absolute variability in ΔOA/ΔCO is dominated by differences between plumes. Many previous field campaigns similarly show little change in ΔOA/ΔCO with aging (Hodshire et al., 2019a and references therein; Palm et al., 2020). This may be due to a balance between evaporation and condensation over the period of time that the plume is observed (Hodshire et al., 2019a)~~, rapid chemistry leading to SOA enhancements prior to the time of the first measurement that d~~ This hypothesis is supported by the observed Δf_{60} and Δf_{44}. ~~While the observed trends in ΔOA/ΔCO with aging are small,~~ The fractional components Δf_{60} and Δf_{44} show clear signs of changes with aging, consistent with previous studies (Cubison et al. 2011; May et al. 2015; Garofalo et al. 2019; Forrister et al. 2015; Lee et al. 2020)~~(Cubison et al., 2011;~~

Garofalo et al., 2019; May et al., 2015). Δf_{60} generally decreases with plume age (R_{age} = -0.26; a weak correlation), consistent with the hypotheses that compounds containing species that can fragment to m/z 60 Δf_{60} in the SP-AMS may be evaporating because of dilution, undergoing heterogeneous oxidation to new forms that do not appear at m/z 60, and/or having a decreasing fractional contribution due to condensation of other compounds. In contrast, Δf_{44} generally increases with age (R_{age} = +0.5; a moderate correlation) for all plumes with available data. It appears for the plumes in this study that although there is little change in ΔOA/ΔCO, loss of compounds such as those that contribute to that contain f_{60} fragments (as captured by the SP-AMS) is roughly balanced by condensation of more-oxidized compounds, including those that contain compounds with f_{44} fragments, such as carboxylic acids. This observation also suggests the possibility of heterogeneous or particle-phase oxidation that would alter the balance of Δf_{60} and Δf_{44}. However, estimates of heterogeneous mass losses indicate that after three hours of aging (the range of time the BBOP measurements were taken in) for a range of OH concentrations and reactive uptake coefficients, less than 10% of aerosol mass is lost to heterogeneous reactions (Fig. S23; see SI text S2 for more details on the calculation). over 90% of aerosol mass is anticipated to remain. These calculations indicateing that heterogeneous loss has limited effect on aerosol composition or mass (Fig. S23; see SI text S2 for more details on the calculation). Hence, the evaporation of compounds that contribute to m/z 60 in the SP-AMS containing f_{60} fragments being balanced by gas-phase production of compounds that contribute to m/z 44 in the SP-AMS containing f_{44} fragments may be the more likely pathway. When individual flights are left out sequentially, R_{age} ranges from -0.21 to -0.38 and +0.4 to +0.57 for Δf_{60} and Δf_{44}, respectively (Table S2).

Two more important features of Δf_{60} and Δf_{44} can be seen within Fig. 2: (1) Δf_{60} and Δf_{44} depend on $\Delta OA_{initial}$ (moderate correlations of $R_{\Delta OA,initial}$ = +0.43 and -0.55, respectively), with plumes with higher $\Delta OA_{initial}$ with more concentrated plumes having consistently higher Δf_{60} and lower Δf_{44}. (2) The dDifferences in Δf_{60} and Δf_{44} are apparent even for the nearest-to-source measurements that are ~15 minutes after the time of emission. indicate that evaporation and/or chemistry appears to havelikely occurred before the time of these first measurements. (assuming that emitted Δf_{60} and Δf_{44} at the time of emission do not correlate with $\Delta OA_{initial}$; there is currently no evidence for this alternative hypothesis). Prior studies have shown that f_{60} and f_{44} at the time of emissions correlate with OA emissions factors through variability in burn conditions (Hennigan et al. 2011; Cubison et al. 2011; McClure et al. 2020), and this relationship might also contribute to our observed correlation between Δf_{60} and Δf_{44} with $\Delta OA_{initial}$; however, fFor this emissions relationship to be an important factor, the variability in the OA emission factor needs to be a significant contributor to the variability in $\Delta OA_{initial}$. (Hif the relative variability in the OA emission factor is much smaller than the relative variability in $\Delta OA_{initial}$, other factors contributing to variability in $\Delta OA_{initial}$ will negate anwash out this emissions-based covariance between $\Delta OA_{initial}$ with Δf_{60} and Δf_{44}). While our observed $\Delta OA_{initial}$ in Figure 2 spans nearly a factor of 100, Andreae (2019) shows that the OA emission factors have a -1σ to +1σ range of around a factor 3. Hence, variability in fuel consumption rates and dilution prior to the first transect likely dominate the variability in $\Delta OA_{initial}$, and the relationships of Δf_{60} and Δf_{44} with $\Delta OA_{initial}$ are unlikely to be influenced much by variability in burn conditions. We conclude thatHence, evaporation and/or chemistry prior to the first measurement appears to drive the initial relationship between Δf_{60} and Δf_{44} with $\Delta OA_{initial}$, consistent with (1) the theoretical

work of Hodshire et al. (2019a), (2) an analysis of what chemistry would be missed in laboratory experiments if the initial 10-60 minutes of chemistry was not considered, following field experiments (Hodshire et al., 2019b), and (3) ~~the~~ recent field analysis indicating that up to one-third of primary OA from biomass burning evaporates and subsequently reacts to form biomass burning SOA(Palm et al. 2020) ~~(Palm et al., 2020)~~. We include in the supporting information scatter plots of each parameter of Fig. 1 as a function of $\Delta OA_{initial}$ (Fig. S24), and observe no trends other than the cores of the plumes generally having a higher $\Delta OA_{initial}$ than the edges of the plumes, as expected. The amounts of evaporation and/or chemistry appear to depend on $\Delta OA_{initial}$, with higher rates of evaporation and chemistry occurring for lower values of $\Delta OA_{initial}$. This result is consistent with the hypothesis that aircraft observations are missing evaporation and chemistry prior to the first aircraft observation (Hodshire et al., 2019b). The differences in $\Delta OA_{initial}$ between plumes may be due to different emissions fluxes (e.g., due to different fuels or combustion phases) or plume widths, where larger/thicker plumes dilute more slowly than smaller/thinner plumes. These larger plumes have been predicted to have less evaporation and may undergo relatively less photooxidation (Bian et al., 2017; Hodshire et al., 2019a, 2019b). ~~We note that each fire may emit particles with variable initial f_{44} and f_{60} values, as has been observed in laboratory studies (Hennigan et al. 2011; Cubison et al. 2011; McClure et al. 2020), which adds to scatter within the data. It is possible that variability in f_{44} and f_{60} emissions may also contribute to the observed correlations with ΔOA_{intial}; however, this would require that higher f_{44} emissions of species able to contribute to m/z 44 are correlated with lower emissions rates and/or faster dilution rates (and vice versa for species able to contribute to m/z 60 f_{60}). Lacking direct emissions measurements, this hypothesis cannot be further explored in this work.~~ When individual flights are left out sequentially, $R_{\Delta OA,initial}$ ranges from +0.3 to +0.58 and -0.42 to -0.63 for Δf_{60}~~60~~ and Δf_{44}, respectively (Table S2).

Garofalo et al. (2019) segregated smoke data from the WE-CAN field campaign by distance from the center of a given plume and showed that the edges of one of the fires studied have less fractional f_{60} and more fractional f_{44} (not background-corrected) than the core of the plume. Lee et al. (2020) saw similar patterns in a southwestern United States wildfire. Similarly, we find that the 730b flight shows a very similar pattern in f_{60} and f_{44} (Figs. S254-S265) to that shown in Fig. 6 of Garofalo et al. (2019). The 821b and 809a flights also hint at elevated f_{44} and decreased f_{60} at the edges but the remaining plumes do not show a clear trend from the physical edges to cores in f_{60} and f_{44}. This could be as CO concentrations (and thus presumably other species) do not evenly increase from the edge to the core for many of the plume transects studied (Figs. S2-S6). To more clearly see this, Fig. S27 provides the same style of figure as Figs. S26-S27 for in-plume CO concentrations. Generally CO peaks around the centerline and is highest in the most fresh transect, but shows variability across transects. We do not have UV measurements that allow us to calculate photolysis rates but the in-plume SPN1 shortwave measurements in the visible show a dimming in the fresh cores that has a similar pattern to f_{44} and the inverse of f_{60} (Fig. S286; the rapid oscillations in this figure could be indicative of sporadic cloud cover above the plumes). Lee et al. (2020) similarly saw indications of enhanced photochemical bleaching at the edges of a southwestern United States wildfire when examining aerosol optical properties.

We also plot core and edge ΔH/ΔC and ΔO/ΔC as a function of physical age (Fig. 2d-e). Similar to Δf_{44}, ΔO/ΔC increases with physical age and is well correlated to both physical age and $\Delta OA_{initial}$ (moderate correlations of R_{age} =+ 0.561 and $R_{\Delta OA,initial}$ = -0.45). When individual flights are left out sequentially, R_{age} for ΔO/ΔC ranges between +0.46 and +0.63 and $R_{\Delta OA,initial}$ ranges between -0.21 and -0.54 (Table S2). Given that Δf_{44} and ΔO/ΔC are both metrics for OA aging (Sect. 2), it is unsurprising that we see similar trends between them. Conversely, ΔH/ΔC ~~tends to be fairly constant or slightly decreasing with physical age and~~ is poorly correlated to physical age and $\Delta OA_{initial}$. ~~A Van Krevelen diagram of ΔH/ΔC versus ΔO/ΔC (Fig. S27) indicates that oxygenation reactions or a combination of oxygenation and hydration reactions are likely dominant (Heald et al., 2010) (recalling that ΔH/ΔC and ΔO/ΔC are calculated by background-correcting the individual elements before ratioing; Eq. 1); however, without further information, we cannot conclude which reactions are occurring.~~

Both physical age and $\Delta OA_{initial}$ appear to influence Δf_{60}, Δf_{44}, and ΔO/ΔC: oxidation reactions and evaporation promoted by ~~from~~ dilution occur with aging, and the extent of photochemistry and dilution should depend on plume thickness. Being able to predict biomass burning aerosol aging parameters can provide a framework for interstudy-comparisons and can aid in modeling efforts. We construct mathematical fits for predicting Δf_{60}, Δf_{44}, and ΔO/ΔC:

$$X = a\ log_{10}(\Delta OA_{initial}) + b\ (Physical\ age)\ + c \qquad \text{Eq. 4}$$

where X is Δf_{60}, Δf_{44}, or ΔO/ΔC, physical age is in hours, and *a, b,* and *c* are fit coefficients. The measured versus fit data are shown in Fig. 3a-c. The values of *a, b,* and *c* are provided in Table S3. The Pearson and Spearman coefficients of determination (R_p^2 and R_s^2, respectively) are also summarized in Fig. 3 and indicate weak-moderate goodness of fits (R_p^2 and R_s^2 of 0.28 and 0.25 for Δf_{60}, R_p^2 and R_s^2 of 0.58 and 0.6 for Δf_{44}, and R_p^2 and R_s^2 of 0.45 and 0.55 for ΔO/ΔC). We show R^2 here to indicate the fraction of variability captured by these fits, whereas calculating R for the trends in Fig. 2 indicate the direction of the correlation. We do not constrain our fits to go through the origin. To provide further metrics of goodness-of-fit, we also include the normalized mean bias (NMB) and normalized mean error (NME) in percent for each metric of Fig. 3. The NMB values are very close to zero (which is anticipated as linear fits seek to minimize the sum of squared residuals). The NME is larger ~~more variable~~, at 19.8% for Δf_{60}, 14.9% for Δf_{44}, and 10.2% for ΔO/ΔC. The p-values for each fit are ~~is~~ less than 0.01. Although no models that we are aware of currently predict aerosol fractional components (e.g. f_{60} or f_{44}), O/H and H/C are predicted by some models (e.g., ~~(~~Cappa and Wilson~~,~~ (2012) and these fit parameters may assist in ~~biomass burning~~ modeling of aging biomass burning aerosol ~~emissions~~. ¶

Other functional forms for fits were explored, with the following form showing similar results as Eq. 4:

$$ln(\Delta X) = a\ ln(\Delta OA_{initial}) + b\ ln(Physical\ age)\ + c \qquad \text{Eq. 5}$$

(Fig. S2~~8~~ and Table S4 for the fit coefficients) and $\Delta N_{initial}$ in the place of $\Delta OA_{initial}$ in Eq. 4 (Fig. S3~~029~~ and Table S5 for the fit coefficients) providing similar correlation values and NMB and NME values for $\Delta f_{60,}$ $\Delta f_{44,}$ and ΔO/ΔC.

The aging values of Δf_{60}, Δf_{44}, and ΔO/ΔC show scatter (Figs. S14-18), which likely contributes to the limited predictive power of our mathematical fits. The scatter is likely due to variability in emissions due to source fuel or combustion conditions, instrument noise and responses under the large concentration ranges encountered in these smoke plumes, inhomogeneous mixing within the plume, variability in background concentrations not captured by our background correction method, inaccurate characterizations of physical age due to variable wind speed, and/or deviations from a true Lagrangian flight path. Eqs. 4-5 performed the best out of the mathematical fits that we tested. These equations do not have a direct physical interpretation but may be used as a starting point for modeling studies as well as for constructing a more physically based fit. There may be another variable not available to us in the BBOP measurements that can improve these mathematical fits, such as photolysis rates. We do not know whether these fits may well-represent fires in other regions around the world, given variability in fuels and burn conditions. We also do not know how these fits will perform under nighttime conditions, as our fits were made for~~during~~ daytime conditions with different chemistry than would happen at night. We encourage these fits to be tested with further data sets and modeling. These equations are a first step towards parameterizations appropriate for regional and global modeling and need extensive testing to separate influences of oxidation versus dilution-driven evaporation.

3.2 Aerosol size distribution properties: ΔN/ΔCO and $\overline{D_p}$

The observations of the normalized number concentration between 40-262 nm, ΔN/ΔCO (Fig. 2f), show that plume edges and cores generally show decreases in ΔN/ΔCO with physical age, with a weak correlation of R_{age} = -0.27 (-0.13 to -0.43 when individual flights are left out, sequentially; Table S2). Although we would anticipate that plume regions with higher initial ΔOA would have lower normalized number concentrations due to coagulation (Sakamoto et al. 2016), a few dense cores have normalized number concentrations comparable or higher than the thinner edges, leading to no correlation with $\Delta OA_{initial}$. We note that variability in number emissions (e.g., due to ~~e.g.~~ burn conditions) adds unexplained variability not captured by the R values.

The mean particle size between 40-262 nm, $\overline{D_p}$ (Eq. 3), is shown to statistically increase with aging when considered across the BBOP dataset (Fig. 2g) (a moderate correlation of R_{age} = +0.53, with R_{age} ranging between +0.43 to +0.63 when individual flights are left out sequentially; Table S2). Coagulation and SOA condensation will increase $\overline{D_p}$. OA evaporation will decrease $\overline{D_p}$ if the particles are in quasi-equilibrium (where evaporation is independent of surface area) (Hodshire et al. 2019b). However, if evaporation is kinetically limited, smaller particles will preferentially evaporate more rapidly than larger particles, which may lead to an increase in $\overline{D_p}$ if the smallest particles evaporate below 40 nm (Hodshire et al. 2019b). The plumes do not show significant changes in ΔOA/ΔCO (Fig. 2a), indicating that coagulation is likely

responsible for the majority of increases in $\overline{D_p}$. (We acknowledge that ΔOA/ΔCO may be impacted by measurement artifacts as discussed in Sect. 2. For instance, if the collection efficiency of the AMS is actually decreasing with age, then ΔOA/ΔCO would be increasing and the increases in number mean diameter will be due to SOA condensation as well as coagulation.) We do not have measurements for the volatility of the smoke aerosol, and so cannot refine these conclusions further. We also perform the functional fit analysis following Sect. 3.1 (Eq. 4; where X is $\overline{D_p}$ in this case). The fit can also predict greater than 30 percent of the variance in $\overline{D_p}$ (R_p^2 and R_s^2 of 0.37 and 0.33, NME of 5.5%, and p-value less than 0.01; Fig. 3d) but does not ~~well~~ predict ΔN/ΔCO well (not shown). We show the functional fit for $\overline{D_p}$ for the alternative fit equation (Eq. 5) in Fig. S2~~9~~8 and Table S4. We also show the functional fit for $\overline{D_p}$ for Eq. 4 with $\Delta N_{initial}$ in place of $\Delta OA_{initial}$ in Fig. 30~~29~~ and Table S5. Sakamoto et al. (2016) provide fit equations for modeled $\overline{D_p}$ as a function of age, but they include a known initial $\overline{D_p}$ at the time of emission in their parameterization (rather than 15 minutes or greater, as available to us in this study), which is not available here. $\Delta N_{initial}$ in the place of $\Delta OA_{initial}$ in Eq. 4 predicts $\overline{D_p}$ similarly (Fig. S30~~29~~). As discussed in Section 3.1, scatter in number concentrations limits our prediction skill.

Particles appear in the 20-40 nm size range in the FIMS measurements independently of plume OA concentrations (Figs S7-S11), implying that nucleation events may be occuring ~~Nucleation-mode particles (inferred in this study from particles appearing between 20-40 nm in the FIMS measurements) are observed~~ for some of the transects ~~(S7-S11)~~. Some pseudo-Lagrangian sets of transects also show nucleation-mode particles downwind of fires in between transects (Figs. S7, S8, S9, and S11). Nucleation-mode particles appear to be approximately one order of magnitude less concentrated than the larger particles, and primarily occur in the outer portion of plumes, although one set of transects ~~day~~ did show nucleation-mode particles within the core of the plume (Fig. S11). Nucleation at edges could be due to increased photooxidation from higher total irradiance relative to the core (Fig. S26). As well, nucleation is more favorable when the total condensation sink is lower (e.g. reduced particle surface area; Dal Maso et al., 2002), which may occur for outer portions of plumes with little aerosol loading. However, given the relatively small number of data points showing nucleation mode particles and limited photooxidation and gas-phase information, we do not have confidence in the underlying source of the nucleation-mode particles.

4 Summary and outlook

The BBOP field campaign provided high time resolution (1 s) measurements of gas- and particle-phase smoke measurements downwind of western U.S. wildfires along pseudo-Lagrangian transects. These flights have allowed us to examine near-field (<4 hours) aging of smoke particles to provide analyses on how select ~~these~~ species vary across a range of initial organic aerosol mass loadings ($\Delta OA_{initial}$; a proxy for the relative rates at which the plume is anticipated to dilute as dilution before the first observation is not a measurable quantity) as well as how the species studied ~~y~~ vary between the edges

and cores of each plume. We find that although ΔOA/ΔCO does not correlate with $\Delta OA_{initial}$ or physical age, Δf_{60} (a marker for evaporation) is moderately correlated with $\Delta OA_{initial}$ (Spearman rank-order correlation tests correlation coefficient, $R_{\Delta OA,initial}$, of +0.43) and weakly correlated with physical age (Spearman rank-order correlation tests correlation coefficient, R_{age}, of -0.26). Δf_{44} and ΔO/ΔC (markers for photochemical aging) increases with physical aging (moderate correlations of R_{age} of +0.5 and +0.56, respectively) and are inversely related to $\Delta OA_{initial}$ (moderate correlations of $R_{\Delta OA,initial}$ of -0.55 and -0.45, respectively). ΔN/ΔCO ~~likely~~ decreases with physical aging, likely through coagulation. Mean aerosol diameter increases with age primarily due to coagulation, as organic aerosol mass does not change significantly, and is moderately correlated with physical age (R_{age} = +0.53). Nucleation is observed within a few of the fires and appears to occur primarily on the edges of the plumes. Differences in initial values of Δf_{60} , Δf_{44}, and ΔO/ΔC ~~between higher- and lower-concentrated plumes~~ are evidence~~indicate~~ that evaporation and/or chemistry has ~~likely~~ occurred before the time of initial measurement and that plumes or plume regions ~~(such as the outer parts of the plume)~~ with lower initial aerosol loading can undergo these changes more rapidly than thicker plumes. We have developed fit equations that can weakly to moderately predict Δf_{60} , Δf_{44}, ΔO/ΔC, and mean aerosol diameter given a known initial (at the time of first measurement) total organic aerosol mass loading and physical age. We were unable to quantify the impact on potential inter-fire variability in the emission values of the metrics studied here (such as variable emissions of species that can contribute to m/z 60 f_{60} and m/z 44 f_{44}). We anticipate that being able to capture this additional source of variability may lead to stronger fits and correlation. We encourage future studies to attempt to quantify these chemical and physical changes before the initial measurement using combinations of modeling and laboratory measurements, where sampling is possible at the initial stages of the fire and smoke. We also suggest further refinement of our fit equations, as additional~~further~~ variables (such as photolysis rates) and better quantification of inter-fire variability (such as variable emission rates) are anticipated to improve these fits. We finally urge future near-field (<24 hours) analyses of recent and future biomass burning field campaigns to include differences in initial plume mass concentrations and location within the plume as considerations for understanding chemical and physical processes in plumes.

Acknowledgements

We would like to thank Lauren Garofalo, Emily Fischer, Jakob Lindaas, and Ilana Pollack for useful conversations. We thank Charles Long for use of irradiation data. This work is supported by the U.S. NOAA, an Office of Science, Office of Atmospheric Chemistry, Carbon Cycle, and Climate Program, under the cooperative agreement awards NA17OAR4310001 and NA17OAR4310003; the U.S. NSF Atmospheric Chemistry program, under Grants AGS−1559607 and AGS-1950327; and the US Department of Energy's (DOE) Atmospheric System Research, an Office of Science, Office of Biological and Environmental Research program, under grant DE-SC0019000. Work conducted by LIK, AJS, JW was performed under sponsorship of the U.S. DOE Office of Biological & Environmental Sciences (OBER) Atmospheric System Research Program (ASR) under contracts DE-SC0012704 (BNL; LIK, AJS) and DE-SC0020259 (JW). Researchers recognize the

DOE Atmospheric Radiation Measurement (ARM) Climate Research program and facility for both the support to carry out the BBOP campaign and for use of the G-1 research aircraft. TBO acknowledges support from the DOE ARM program during BBOP and the DOE ASR program for BBOP analysis (contract DE-SC0014287). DKF acknowledges funding from NOAA Climate Program Office's Atmospheric Chemistry, Carbon Cycle, and Climate program (Grant NA17OAR4310010). We thank the anonymous reviewers for their constructive feedback.

References

Adachi, K., Sedlacek, A. J., Kleinman, L., Springston, S. R., Wang, J. and Chand, D.: Spherical tarball particles form through rapid chemical and physical changes of organic matter in biomass-burning smoke, Proceedings of the National Academy of Sciences, 1–6, 2019.

Aiken, A. C., Decarlo, P. F., Kroll, J. H., Worsnop, D. R., Huffman, J. A., Docherty, K. S., Ulbrich, I. M., Mohr, C., Kimmel, J. R., Sueper, D., Sun, Y., Zhang, Q., Trimborn, A., Northway, M., Ziemann, P. J., Canagaratna, M. R., Onasch, T. B., Alfarra, M. R., Prevot, A. S. H., Dommen, J., Duplissy, J., Metzger, A., Baltensperger, U. and Jimenez, J. L.: O/C and OM/OC ratios of primary, secondary, and ambient organic aerosols with high-resolution time-of-flight aerosol mass spectrometry, Environmental Science and Technology, 42(12), 4478–4485, 2008.

Aiken, A. C., Salcedo, D., Cubison, M. J., Huffman, J. A., DeCarlo, P. F., Ulbrich, I. M., Docherty, K. S., Sueper, D., Kimmel, J. R., Worsnop, D. R. and Others: Mexico City aerosol analysis during MILAGRO using high resolution aerosol mass spectrometry at the urban supersite (T0)--Part 1: Fine particle composition and organic source apportionment, Atmos. Chem. Phys., 9(17), 6633–6653, 2009.

Akagi, S. K., Yokelson, R. J., Wiedinmyer, C., Alvarado, M. J., Reid, J. S., Karl, T., Crounse, J. D. and Wennberg, P. O.: Emission factors for open and domestic biomass burning for use in atmospheric models, Atmos. Chem. Phys., 11(9), 4039–4072, 2011.

Akagi, S. K., Craven, J. S., Taylor, J. W., Mcmeeking, G. R., Yokelson, R. J., Burling, I. R., Urbanski, S. P., Wold, C. E., Seinfeld, J. H., Coe, H., Alvarado, M. J. and Weise, D. R.: Evolution of trace gases and particles emitted by a chaparral fire in California, Atmos. Chem. Phys., 12, 1397–1421, 2012.

Albrecht, B. A.: Aerosols, cloud microphysics, and fractional cloudiness, Science, 245(4923), 1227–1230, 1989.

Alfarra, M. R., Coe, H., Allan, J. D., Bower, K. N., Boudries, H., Canagaratna, M. R., Jimenez, J. L., Jayne, J. T., Garforth, A. A., Li, S.-M. and Worsnop, D. R.: Characterization of urban and rural organic particulate in the Lower Fraser Valley using two Aerodyne Aerosol Mass Spectrometers, Atmos. Environ., 38(34), 5745–5758, 2004.

Andela, N., Morton, D. C., Giglio, L., Paugam, R., Chen, Y., Hantson, S., Werf, G. R. and Randerson, J. T.: The Global Fire Atlas of individual fire size, duration, speed and direction, Earth System Science Data, 11(2), 529–552, 2019.

Andreae, M. O.: Emission of trace gases and aerosols from biomass burning – an updated assessment, Atmos. Chem. Phys., 19, 8523–8546, https://doi.org/10.5194/acp-19-8523-2019, 2019.

Badosa, J., Wood, J., Blanc, P., Long, C. N., Vuilleumier, L., Demengel, D. and Haeffelin, M.: Solar irradiances measured using SPN1 radiometers: uncertainties and clues for development, Atmospheric Measurement Techniques, 7, 4267–4283, 2014.

Bian, Q., Jathar, S. H., Kodros, J. K., Barsanti, K. C., Hatch, L. E., May, A. A., Kreidenweis, S. M. and Pierce, J. R.: Secondary organic aerosol formation in biomass-burning plumes: Theoretical analysis of lab studies and ambient plumes, Atmos. Chem. Phys., 17(8), 5459–5475, 2017.

Brito, J., Rizzo, L. V., Morgan, W. T., Coe, H., Johnson, B., Haywood, J., Longo, K., Freitas, S., Andreae, M. O. and Artaxo, P.: Ground-based aerosol characterization during the South American Biomass Burning Analysis (SAMBBA) field experiment, Atmospheric Chemistry and Physics, 14(22), 12069–12083, doi:10.5194/acp-14-12069-2014, 2014.

Cachier, H., Liousse, C., Buat-Menard, P. and Gaudichet, A.: Particulate content of savanna fire emissions, J. Atmos. Chem., 22(1-2), 123–148, 1995.

Canagaratna, M. R., Jimenez, J. L., Kroll, J. H., Chen, Q., Kessler, S. H., Massoli, P., Hildebrandt Ruiz, L., Fortner, E., Williams, L. R., Wilson, K. R. and Others: Elemental ration measurements of organic compounds using aerosol mass spectrometry: characterization, improved calibration, and implications, Atmos. Chem. Phys., 15, 253–272, 2015.

Capes, G., Johnson, B., McFiggans, G., Williams, P. I., Haywood, J. and Coe, H.: Aging of biomass burning aerosols over West Africa: Aircraft measurements of chemical composition, microphysical properties, and emission ratios, J. Geophys. Res. D: Atmos., 113(23), 0–15, 2008.

Cappa, C. D. and Jimenez, J. L.: Quantitative estimates of the volatility of ambient organic aerosol, Atmos. Chem. Phys., 10(12), 5409–5424, 2010.

Cappa, C. D. and Wilson, K. R.: Multi-generation gas-phase oxidation, equilibrium partitioning, and the formation and evolution of secondary organic aerosol, Atmos. Chem. Phys., 12(20), 9505–9528, 2012.

Carrico, C. M., Petters, M. D., Kreidenweis, S. M., Collett, J. L., Jr., Engling, G. and Malm, W. C.: Aerosol hygroscopicity and cloud droplet activation of extracts of filters from biomass burning experiments, J. Geophys. Res., 113(D8), 4767, 2008.

Canagaratna, M., Jayne, J., Jimenez, J., Allan, J., Alfarra, M., Zhang, Q., Onasch, T., Drewnick, F., Coe, H., Middlebrook, A., Delia, A., Williams, L., Trimborn, A., Northway, M., DeCarlo, P., Kolb, C., Davidovits, P. and Worsnop, D.:

Chemical and microphysical characterization of ambient aerosols with the aerodyne aerosol mass spectrometer, Mass Spectrom. Rev., 26: 185-222. doi:10.1002/mas.20115, 2007

Chen, Q., Heald, C. L., Jimenez, J. L., Canagaratna, M. R., Qi, Z., Ling-Yan, H., Xiao- Feng, H., Campuzano-Jost, P., Palm, B. B., Poulain, L., Kuwata, M., Martin, S. T., Ab- batt, J. P. D., Lee, A. K. Y., and Liggio, J.: Elemental composition of organic aerosol: the gap between ambient and laboratory measurements, Geophysical Research Letters, 42, 4182-4189, https://doi.org/10.1002/2015gl063693, 2015

Collier, S., Zhou, S., Onasch, T. B., Jaffe, D. A., Kleinman, L., Sedlacek, A. J., Briggs, N. L., Hee, J., Fortner, E., Shilling, J. E., Worsnop, D., Yokelson, R. J., Parworth, C., Ge, X., Xu, J., Butterfield, Z., Chand, D., Dubey, M. K., Pekour, M. S., Springston, S. and Zhang, Q.: Regional Influence of Aerosol Emissions from Wildfires Driven by Combustion Efficiency: Insights from the BBOP Campaign, Environmental Science and Technology, 50(16), 8613–8622, 2016.

Collier, S., Williams, L. R., Onasch, T. B., Cappa, C. D., Zhang, X., Russell, L. M., Chen, C. L., Sanchez, K. J., Worsnop, D. R. and Zhang, Q.: Influence of Emissions and Aqueous Processing on Particles Containing Black Carbon in a Polluted Urban Environment: Insights From a Soot Particle-Aerosol Mass Spectrometer, J. Geophys. Res. Atmos., 123(12), 6648–6666, doi:10.1002/2017JD027851, 2018.

Corbin, J. C., Lohmann, U., Sierau, B., Keller, A., Burtscher, H., and Mensah, A. A.: Black carbon surface oxidation and organic composition of beech-wood soot aerosols, Atmos. Chem. Phys., 15, 11885–11907, https://doi.org/10.5194/acp-15-11885-2015, 2015.

Cubison, M. J., Ortega, A. M., Hayes, P. L., Farmer, D. K., Day, D., Lechner, M. J., Brune, W. H., Apel, E., Diskin, G. S., Fisher, J. A., Fuelberg, H. E., Hecobian, A., Knapp, D. J., Mikoviny, T., Riemer, D., Sachse, G. W., Sessions, W., Weber, R. J., Weinheimer, A. J., Wisthaler, A. and Jimenez, J. L.: Effects of aging on organic aerosol from open biomass burning smoke in aircraft and laboratory studies, Atmos. Chem. Phys., 11(23), 12049–12064, 2011.

Dal Maso, M., Kulmala, M., Lehtinen, K. E. J., Mäkelä, J. M., Aalto, P., and O'Dowd, C. D.: Condensation and coagulation sinks and formation of nucleation mode particles in coastal and boreal forest boundary layers, J. Geophys. Res., 107(D19), doi:10.1029/2001JD001053, 2002.

Decarlo, P. F., Dunlea, E. J., Kimmel, J. R., Aiken, A. C., Sueper, D., Crounse, J., Wennberg, P. O., Emmons, L., Shinozuka, Y., Clarke, A., Zhou, J., Tomlinson, J., Collins, D. R., Knapp, D., Weinheimer, A. J., Montzka, D. D., Campos, T. and Jimenez, J. L.: Fast airborne aerosol size and chemistry measurements above Mexico City and Central Mexico during the MILAGRO campaign., 2008.

Dennison, P. E., Brewer, S. C., Arnold, J. D. and Moritz, M. A.: Large wildfire trends in the western United States, 1984-2011, Geophysical Research Letters, 41(8), 2928–2933, doi:10.1002/2014gl059576, 2014.

Eatough, D. J., Eatough, N. L., Pang, Y., Sizemore, S., Kirchstetter, T. W., Novakov, T. and Hobbs, P. V.: Semivolatile particulate organic material in southern Africa during SAFARI 2000, J. Geophys. Res. D: Atmos., 108(D13) [online] Available from: https://agupubs.onlinelibrary.wiley.com/doi/abs/10.1029/2002JD002296%4010.1002/%28ISSN%292169-8996.SAF 1, 2003.

Evans, J. D. (1996). Straightforward statistics for the behavioral sciences. Thomson Brooks/Cole Publishing Co.

Ford, B., Val Martin, M., Zelasky, S. E., Fischer, E. V., Anenberg, S. C., Heald, C. L. and Pierce, J. R.: Future Fire Impacts on Smoke Concentrations, Visibility, and Health in the Contiguous United States, GeoHealth, doi:10.1029/2018GH000144, 2018.

Formenti, P., Elbert, W., Maenhaut, W., Haywood, J., Osborne, S. and Andreae, M. O.: Inorganic and carbonaceous aerosols during the Southern African Regional Science Initiative (SAFARI 2000) experiment: Chemical characteristics, physical properties, and emission data for smoke from African biomass burning, J. Geophys. Res. D: Atmos., 108(D13), doi:10.1029/2002JD002408, 2003.

Forrister, H., Liu, J., Scheuer, E., Dibb, J., Ziemba, L., Thornhill, K. L., Anderson, B., Diskin, G., Perring, A. E., Schwarz, J. P., Campuzano−Jost, P., Day, D. A., Palm, B. B., Jimenez, J. L., Nenes, A. and Weber, R. J.: Evolution of brown carbon in wildfire plumes, Geophys. Res. Lett., 42(11), 4623–4630, 2015.

Gan, R. W., Ford, B., Lassman, W., Pfister, G., Vaidyanathan, A., Fischer, E., Volckens, J., Pierce, J. R. and Magzamen, S.: Comparison of wildfire smoke estimation methods and associations with cardiopulmonary-related hospital admissions, GeoHealth, 1(3), 122–136, 2017.

Garofalo, L., Pothier, M. A., Levin, E. J. T., Campos, T., Kreidenweis, S. M. and Farmer, D. K.: Emission and Evolution of Submicron Organic Aerosol in Smoke from Wildfires in the Western United States, ACS Earth and Space Chemistry, acsearthspacechem.9b00125, 2019.

Giglio, L., Csiszar, I. and Justice, C. O.: Global distribution and seasonality of active fires as observed with the Terra and Aqua Moderate Resolution Imaging Spectroradiometer (MODIS) sensors, Journal of Geophysical Research: Biogeosciences, 111(G2) [online] Available from: https://agupubs.onlinelibrary.wiley.com/doi/abs/10.1029/2005JG000142, 2006.

Giglio, L., Csiszar, I., Restás, Á., Morisette, J. T., Schroeder, W., Morton, D. and Justice, C. O.: Active fire detection and characterization with the advanced spaceborne thermal emission and reflection radiometer (ASTER), Remote Sensing of Environment, 112(6), 3055–3063, doi:10.1016/j.rse.2008.03.003, 2008.

Gilman, J. B., Lerner, B. M., Kuster, W. C., Goldan, P. D., Warneke, C., Veres, P. R., Roberts, J. M., De Gouw, J. A., Burling, I. R. and Yokelson, R. J.: Biomass burning emissions and potential air quality impacts of volatile organic compounds and other trace gases from fuels common in the US, Atmos. Chem. Phys., 15(24), 13915–13938, 2015.

659 Grieshop, A. P., Logue, J. M., Donahue, N. M., and Robinson, A. L.: Laboratory investigation of photochemical oxidation of
660 organic aerosol from wood fires 1: measurement and simulation of organic aerosol evolution, Atmos. Chem. Phys.,
661 9, 1263–1277, https://doi.org/10.5194/acp-9-1263-2009, 2009.
662 Hatch, L. E., Luo, W., Pankow, J. F., Yokelson, R. J., Stockwell, C. E. and Barsanti, K. C.: Identification and quantification
663 of gaseous organic compounds emitted from biomass burning using two-dimensional gas
664 chromatography-time-of-flight mass spectrometry, Atmos. Chem. Phys., 15(4), 1865–1899, 2015.
665 Hatch, L. E., Yokelson, R. J., Stockwell, C. E., Veres, P. R., Simpson, I. J., Blake, D. R., Orlando, J. J. and Barsanti, K. C.:
666 Multi-instrument comparison and compilation of non-methane organic gas emissions from biomass burning and
667 implications for smoke-derived secondary organic aerosol precursors, Atmos. Chem. Phys., 17, 1471–1489, 2017.
668 Heald, C. L., Kroll, J. H., Jimenez, J. L., Docherty, K. S., DeCarlo, P. F., Aiken, A. C., Chen, Q., Martin, S. T., Farmer, D. K.
669 and Artaxo, P.: A simplified description of the evolution of organic aerosol composition in the atmosphere,
670 Geophys. Res. Lett., 37(8), doi:10.1029/2010GL042737, 2010.
671 Hecobian, A., Liu, Z., Hennigan, C. J., Huey, L. G., Jimenez, J. L., Cubison, M. J., Vay, S., Diskin, G. S., Sachse, G. W.,
672 Wisthaler, A., Mikoviny, T., Weinheimer, A. J., Liao, J., Knapp, D. J., Wennberg, P. O., Urten, A., Crounse, J. D.,
673 Clair, J. S., Wang, Y. and Weber, R. J.: Comparison of chemical characteristics of 495 biomass burning plumes
674 intercepted by the NASA DC-8 aircraft during the ARCTAS/CARB-2008 field campaign, Atmos. Chem. Phys., 11,
675 13325–13337, 2011.
676 Hennigan, C. J., Miracolo, M. A., Engelhart, G. J., May, A. A., Presto, A. A., Lee, T., Sullivan, A. P., McMeeking, G. R.,
677 Coe, H., Wold, C. E., Hao, W. M., Gilman, J. B., Kuster, W. C., De Gouw, J., Schichtel, B. A., Collett, J. L.,
678 Kreidenweis, S. M. and Robinson, A. L.: Chemical and physical transformations of organic aerosol from the
679 photo-oxidation of open biomass burning emissions in an environmental chamber, Atmos. Chem. Phys., 11(15),
680 7669–7686, doi:10.5194/acp-11-7669-2011, 2011.
681 Hobbs, P. V., Sinha, P., Yokelson, R. J., Christian, T. J., Blake, D. R., Gao, S., Kirchstetter, T. W., Novakov, T. and Pilewskie,
682 P.: Evolution of gases and particles from a savanna fire in South Africa, J. Geophys. Res. D: Atmos., 108(D13),
683 doi:10.1029/2002JD002352, 2003.
684 Hodshire, A. L., Akherati, A., Alvarado, M. J., Brown-Steiner, B., Jathar, S. H., Jimenez, J. L., Kreidenweis, S. M.,
685 Lonsdale, C. R., Onasch, T. B., Ortega, A. M. and Pierce, J. R.: Aging Effects on Biomass Burning Aerosol Mass
686 and Composition: A Critical Review of Field and Laboratory Studies, Environ. Sci. Technol., 53(17), 10007–10022,
687 2019a.
688 Hodshire, A. L., Bian, Q., Ramnarine, E., Lonsdale, C. R., Alvarado, M. J., Kreidenweis, S. M., Jathar, S. H. and Pierce, J.
689 R.: More than emissions and chemistry: Fire size, dilution, and background aerosol also greatly influence near−field
690 biomass burning aerosol aging, J. Geophys. Res. D: Atmos., 2018JD029674, 2019b.

Huffman, J. A., Docherty, K. S., Aiken, A. C., Cubison, M. J., Ulbrich, I. M., Decarlo, P. F., Sueper, D., Jayne, J. T., Worsnop, D. R., Ziemann, P. J. and Jimenez, J. L.: Chemically-resolved aerosol volatility measurements from two megacity field studies., 2009.

Janhäll, S., Andreae, M. O. and Pöschl, U.: Biomass burning aerosol emissions from vegetation fires: particle number and mass emission factors and size distributions, Atmos. Chem. Phys. Disc., 9(4), 17183–17217, 2009.

Jen, C. N., Hatch, L. E., Selimovic, V., Yokelson, R. J., Weber, R., Fernandez, A. E., Kreisberg, N. M., Barsanti, K. C. and Goldstein, A. H.: Speciated and total emission factors of particulate organics from burning western US wildland fuels and their dependence on combustion efficiency, Atmos. Chem. Phys., 19, 1013–1026, 2019.

Jimenez, J. L., Canagaratna, M. R., Donahue, N. M., Prevot, a. S. H., Zhang, Q., Kroll, J. H., DeCarlo, P. F., Allan, J. D., Coe, H., Ng, N. L., Aiken, a. C., Docherty, K. S., Ulbrich, I. M., Grieshop, a. P., Robinson, a. L., Duplissy, J., Smith, J. D., Wilson, K. R., Lanz, V. a., Hueglin, C., Sun, Y. L., Tian, J., Laaksonen, A., Raatikainen, T., Rautiainen, J., Vaattovaara, P., Ehn, M., Kulmala, M., Tomlinson, J. M., Collins, D. R., Cubison, M. J., Dunlea, E. J., Huffman, J. a., Onasch, T. B., Alfarra, M. R., Williams, P. I., Bower, K., Kondo, Y., Schneider, J., Drewnick, F., Borrmann, S., Weimer, S., Demerjian, K., Salcedo, D., Cottrell, L., Griffin, R., Takami, A., Miyoshi, T., Hatakeyama, S., Shimono, A., Sun, J. Y., Zhang, Y. M., Dzepina, K., Kimmel, J. R., Sueper, D., Jayne, J. T., Herndon, S. C., Trimborn, a. M., Williams, L. R., Wood, E. C., Middlebrook, a. M., Kolb, C. E., Baltensperger, U. and Worsnop, D. R.: Evolution of organic aerosols in the atmosphere, Science, 326(5959), 1525–1529, 2009.

Jolleys, M. D., Coe, H., McFiggans, G., Capes, G., Allan, J. D., Crosier, J., Williams, P. I., Allen, G., Bower, K. N., Jimenez, J. L., Russell, L. M., Grutter, M. and Baumgardner, D.: Characterizing the aging of biomass burning organic aerosol by use of mixing ratios: A meta-analysis of four regions, Environmental Science and Technology, 46(24), 13093–13102, 2012.

Jolleys, M. D., Coe, H., McFiggans, G., Taylor, J. W., O'Shea, S. J., Le Breton, M., Bauguitte, S. J. B., Moller, S., Di Carlo, P., Aruffo, E., Palmer, P. I., Lee, J. D., Percival, C. J. and Gallagher, M. W.: Properties and evolution of biomass burning organic aerosol from Canadian boreal forest fires, Atmos. Chem. Phys., 15(6), 3077–3095, 2015.

Kleinman, L. I., Daum, P. H., Lee, Y. N., Senum, G. I., Springston, S. R., Wang, J., Berkowitz, C., Hubbe, J., Zaveri, R. A., Brechtel, F. J., Jayne, J., Onasch, T. B. and Worsnop, D.: Aircraft observations of aerosol composition and ageing in New England and Mid-Atlantic States during the summer 2002 New England Air Quality Study field campaign, J. Geophys. Res. Atmos., 112(9), 1–18, doi:10.1029/2006JD007786, 2007.

Kleinman, L. and Sedlacek, A. J., III: Biomass Burning Observation Project (BBOP) Final Campaign Report, 2016.

Kleinman, L. I., Sedlacek, A. J., III, Adachi, K., Buseck, P. R., Collier, S., Dubey, M., K., Hodshire, A. L., Lewis, E., Onasch, T. B., Pierce, J. R., Schilling, J., Springston, S. R., Wang, J., Zhang, Q., Zhoui, S., Yokelson, R. J.: Rapid Evolution of Aerosol Particles and their Optical Properties Downwind of Wildfires in the Western U.S., submitted to Atmos. Chem. Phys., 2020.

Konovalov, I. B., Beekmann, M., Golovushkin, N. A. and Andreae, M. O.: Nonlinear behavior of organic aerosol in biomass burning plumes: a microphysical model analysis, Atmos. Chem. Phys. Disc., 1–44, 2019.

Koss, A. R., Sekimoto, K., Gilman, J. B., Selimovic, V., Coggon, M. M., Zarzana, K. J., Yuan, B., Lerner, B. M., Brown, S. S., Jimenez, J. L., Krechmer, J., Roberts, J. M., Warneke, C., Yokelson, R. J. and De Gouw, J.: Non-methane organic gas emissions from biomass burning: Identification, quantification, and emission factors from PTR-ToF during the FIREX 2016 laboratory experiment, Atmos. Chem. Phys., 18(5), 3299–3319, 2018.

Kroll, J. H. and Seinfeld, J. H.: Chemistry of secondary organic aerosol: Formation and evolution of low-volatility organics in the atmosphere, Atmos. Environ., 42, 3593–3624, 2008.

Kulkarni, P. and Wang, J.: New fast integrated mobility spectrometer for real-time measurement of aerosol size distribution—I: Concept and theory, J. Aerosol Sci., 37(10), 1303–1325, 2006.

Lee, J. E., Dubey, M. K., Aiken, A. C., Chylek, P., & Carrico, C. M.: Optical and chemical analysis of absorption enhancement by mixed carbonaceous aerosols in the 2019 Woodbury, AZ fire plume, J. Geophys. Res. Atmos, 125, e2020JD032399. https://doi.org/10.1029/2020JD032399, 2020.

Lee, T., Sullivan, A. P., Mack, L., Jimenez, J. L., Kreidenweis, S. M., Onasch, T. B., Worsnop, D. R., Malm, W., Wold, C. E., Hao, W. M. and Collett, J. L.: Chemical Smoke Marker Emissions During Flaming and Smoldering Phases of Laboratory Open Burning of Wildland Fuels, Aerosol Sci. Technol., 44(9), i–v, 2010.

Lim, C. Y., Hagan, D. H., Coggon, M. M., Koss, A. R., Sekimoto, K., de Gouw, J., Warneke, C., Cappa, C. D., and Kroll, J. H.: Secondary organic aerosol formation from the laboratory oxidation of biomass burning emissions, 920 Atmos. Chem. Phys., 19, 12797-12809, 10.5194/acp-19-12797-2019, 2019.

Liu, X., Zhang, Y., Huey, L. G., Yokelson, R. J., Wang, Y., Jimenez, J. L., Campuzano-Jost, P., Beyersdorf, A. J., Blake, D. R., Choi, Y., St. Clair, J. M., Crounse, J. D., Day, D. A., Diskin, G. S., Ried, A., Hall, S. R., Hanisco, T. F., King, L. E., Meinardi, S., Mikoviny, T., Palm, B. B., Peischl, J., Perring, A. E., Pollack, I. B., Ryerson, T. B., Sachse, G., Schwarz, J. P., Simpson, I. J., Tanner, D. J., Thornhil, K. L., Ullmann, K., Weber, R. J., Wennberg, P. O., Wisthaler, A., Wolfe, G. M. and Ziemba, L. D.: Agricultural fires in the southeastern U.S. during SEAC4RS: Emissions of trace gases and particles and evolution of ozone, reactive nitrogen, and organic aerosol, J. Geophys. Res., 121(12), 7383–7414, 2016.

Liu, P.S.K., Deng, R., Smith, K.A., Williams, L.R., Jayne, J.T., Canagaratna, M.R., Moore, K., Onasch, T.B., Worsnop, D.R., and Deshler, T.: Transmission Efficiency of an Aerodynamic Focusing Lens System: Comparison of Model Calculations and Laboratory Measurements for the Aerodyne Aerosol Mass Spectrometer, Aerosol Sci. Technol., 41(8):721–733, 2007Long, C. N., Bucholtz, A., Jonsson, H., Schmid, B., Vogelmann, A. and Wood, J.: A Method of Correcting for Tilt from Horizontal in Downwelling Shortwave Irradiance Measurements on Moving Platforms, The Open Atmospheric Science Journal, 4(1), 78–87, doi:10.2174/1874282301004010078, 2010.

Massoli, P., Onasch, T. B., Cappa, C. D., Nuamaan, I., Hakala, J., Hayden, K., Li, S., Sueper, D. T., Bates, T. S., Quinn, P. K., Jayne, J. T., and Worsnop, D. R.: Characterization of black carbon−containing particles from soot particle aerosol

mass spectrometer measurements on the R/V *Atlantis* during CalNex 2010. J. Geophys. Res. Atmos., 120, 2575–2593. doi: 10.1002/2014JD022834, 2015.

May, A. A., Levin, E. J. T., Hennigan, C. J., Riipinen, I., Lee, T., Collett, J. L., Jimenez, J. L., Kreidenweis, S. M. and Robinson, A. L.: Gas-particle partitioning of primary organic aerosol emissions: 3. Biomass burning, J. Geophys. Res. D: Atmos., 118(19), 11327–11338, 2013.

May, A. A., Lee, T., McMeeking, G. R., Akagi, S., Sullivan, A. P., Urbanski, S., Yokelson, R. J. and Kreidenweis, S. M.: Observations and analysis of organic aerosol evolution in some prescribed fire smoke plumes, Atmos. Chem. Phys., 15(11), 6323–6335, 2015.

McClure, C. D., Lim, C. Y., Hagan, D. H., Kroll, J. H., and Cappa, C. D.: Biomass-burning-derived particles from a wide variety of fuels – Part 1: Properties of primary particles, Atmos. Chem. Phys., 20, 1531-1547, https://doi.org/10.5194/acp- 20-1531-2020, 2020.

Middlebrook, A. M., Bahreini, R., Jimenez, J. L. and Canagaratna, M. R.: Evaluation of composition-dependent collection efficiencies for the Aerodyne aerosol mass spectrometer using field data, Aerosol Sci. Technol., 46(3), 258–271, doi:10.1080/02786826.2011.620041, 2012.

Morgan, W. T., Allan, J. D., Bauguitte, S., Darbyshire, E., Flynn, M. J., Lee, J., Liu, D., Johnson, B., Haywood, J., Longo, K. M., Artaxo, P. E. and Coe, H.: Transformation and aging of biomass burning carbonaceous aerosol over tropical South America from aircraft in-situ measurements during SAMBBA, Atmos. Chem. Phys. Discuss., doi:10.5194/acp-2019-157, 2019.

Moteki, N. and Kondo, Y.: Dependence of Laser-Induced Incandescence on Physical Properties of Black Carbon Aerosols: Measurements and Theoretical Interpretation, Aerosol Sci. Technol., 44(8), 663–675, 2010.

Nance, J. D., Hobbs, P. V. and Radkel, L. F.: Airborne Measurements of Gases and Particles From an Alaskan Wildfire, J. Geophys. Res. D: Atmos., 98(D8), 873–882, 1993.

Noyes, K. J., Kahn, R., Sedlacek, A., Kleinman, L., Limbacher, J. and Li, Z.: Wildfire Smoke Particle Properties and Evolution, from Space-Based Multi-Angle Imaging, Remote Sensing, 12(5), 769, doi:10.3390/rs12050769, 2020.

O'Dell, K., Ford, B., Fischer, E. V. and Pierce, J. R.: Contribution of Wildland-Fire Smoke to US PM2.5 and Its Influence on Recent Trends, Environmental Science & Technology, 53(4), 1797–1804, doi:10.1021/acs.est.8b05430, 2019.

Olfert, J. S. and Wang, J.: Dynamic Characteristics of a Fast-Response Aerosol Size Spectrometer, Aerosol Sci. Technol., 43(2), 97–111, 2009.

Onasch, T. B., Trimborn, A., Fortner, E. C., Jayne, J. T., Kok, G. L., Williams, L. R., Davidovits, P. and Worsnop, D. R.: Soot Particle Aerosol Mass Spectrometer: Development, Validation, and Initial Application, Aerosol Science and Technology, 46(7), 804–817, doi:10.1080/02786826.2012.663948, 2012.

Palm, B. B., Peng, Q., Fredrickson, C. D., Lee, B. H., Garofalo, L. A. and Pothier, M. A.: Quantification of organic aerosol and brown carbon evolution in fresh wildfire plumes, , doi:10.1073/pnas.2012218117, 2020.

Petters, M. D. and Kreidenweis, S. M.: A single parameter representation of hygroscopic growth and cloud condensation nucleus activity, Atmos. Chem. Phys., 7(8), 1961–1971, 2007.

Petters, M. D., Carrico, C. M., Kreidenweis, S. M., Prenni, A. J., DeMott, P. J., Collett, J. L. and Moosmüller, H.: Cloud condensation nucleation activity of biomass burning aerosol, J. Geophys. Res. D: Atmos., 114(22), 22205, 2009.

Ramnarine, E., Kodros, J. K., Hodshire, A. L., Lonsdale, C. R., Alvarado, M. J. and Pierce, J. R.: Effects of near-source coagulation of biomass burning aerosols on global predictions of aerosol size distributions and implications for aerosol radiative effects, Atmos. Chem. Phys., 19(9), 6561–6577, 2019.

Reid, C. E., Brauer, M., Johnston, F. H., Jerrett, M., Balmes, J. R. and Elliott, C. T.: Critical review of health impacts of wildfire smoke exposure, Environmental Health Perspectives, 124(9), 1334–1343, doi:10.1289/ehp.1409277, 2016.

Reid, J. S., Hobbs, P. V., Ferek, R. J., Blake, D. R., Martins, J. V., Dunlap, M. R. and Liousse, C.: Physical, chemical, and optical properties of regional hazes dominated by smoke in Brazil, J. Geophys. Res. D: Atmos., 103(D24), 32059–32080, 1998.

Reid, J. S., Eck, T. F., Christopher, S. A., Koppmann, R., Dubovik, O., Eleuterio, D. P., Holben, B. N., Reid, E. A. and Zhang, J.: A review of biomass burning emissions part III: intensive optical properties of biomass burning particles, Atmos. Chem. Phys., 5, 827–849, 2005.

Sakamoto, K. M., Allan, J. D., Coe, H., Taylor, J. W., Duck, T. J. and Pierce, J. R.: Aged boreal biomass-burning aerosol size distributions from BORTAS 2011, Atmos. Chem. Phys., 15(4), 1633–1646, 2015.

Sakamoto, K. M., Laing, J. R., Stevens, R. G., Jaffe, D. A. and Pierce, J. R.: The evolution of biomass-burning aerosol size distributions due to coagulation: Dependence on fire and meteorological details and parameterization, Atmos. Chem. Phys., 16(12), 7709–7724, 2016.

Schwarz, J. P., Gao, R. S., Fahey, D. W., Thomson, D. S., Watts, L. A., Wilson, J. C., Reeves, J. M., Darbeheshti, M., Baumgardner, D. G., Kok, G. L. and Others: Single-particle measurements of midlatitude black carbon and light-scattering aerosols from the boundary layer to the lower stratosphere, J. Geophys. Res. D: Atmos., 111(D16) [online] Available from: https://agupubs.onlinelibrary.wiley.com/doi/abs/10.1029/2006JD007076, 2006.

Schwarz, J.P., Spackman, J.R., Gao, R.S., Perring, a. E., Cross, E., Onasch, T.B., Ahern, a., Wrobel, W., Davidovits, P., Olfert, J., Dubey, M.K., Mazzoleni, C., and Fahey, D.W.:The Detection Efficiency of the Single Particle Soot Photometer, Aerosol Sci. Technol., 44(8):612–628, 2010. Sedlacek, A. J., Iii, Buseck, P. R., Adachi, K., Onasch, T. B., Springston, S. R. and Kleinman, L.: Formation and evolution of Tar Balls from Northwestern US wildfires, Atmos. Chem. Phys. Discuss., (Figure 1), 1–28, 2018.

Seinfeld, J. H. and Pandis, S. N.: Atmospheric chemistry and physics: From air pollution to climate change, John Willey & Sons, Inc. , New York, 2006.

Shrivastava, M., Cappa, C. D., Fan, J., Goldstein, A. H., Guenther, A. B., Jimenez, J. L., Kuang, C., Laskin, A., Martin, S. T., Ng, N. L. and Others: Recent advances in understanding secondary organic aerosol: Implications for global climate forcing, Rev. Geophys., 55(2), 509–559, 2017.

Spracklen, D. V., Mickley, L. J., Logan, J. A., Hudman, R. C., Yevich, R., Flannigan, M. D. and Westerling, A. L.: Impacts of climate change from 2000 to 2050 on wildfire activity and carbonaceous aerosol concentrations in the western United States, J. Geophys. Res., 114(D20), 1418, 2009.

Tang, X., Madronich, S., Wallington, T. and Calamari, D.: Changes in tropospheric composition and air quality, J. Photochem. Photobiol. B, 46(1-3), 83–95, 1998.

Tie, X.: Effect of clouds on photolysis and oxidants in the troposphere, J. Geophys. Res., 108(D20), 23,073, 2003.

Twomey, S.: Pollution and the planetary albedo, Atmos. Environ., 8(12), 1251–1256, 1974.

Vakkari, V., Kerminen, V.-M., Beukes, J. P., Titta, P., van Zyl, P. G., Josipovic, M., Wnter, A. D., Jaars, K., Worsnop, D. R., Kulmala, M. and Laakso, L.: Rapid changes in biomass burning aerosols by atmospheric oxidation, Geophys. Res. Lett., 2644–2651, 2014.

Vakkari, V., Beukes, J. P., Dal Maso, M., Aurela, M., Josipovic, M. and van Zyl, P. G.: Major secondary aerosol formation in southern African open biomass burning plumes, Nat. Geosci., 11(8), 580–583, 2018.

Volkamer, R., Jimenez, J. L., San Martini, F., Dzepina, K., Zhang, Q., Salcedo, D., Molina, L. T., Worsnop, D. R. and Molina, M. J.: Secondary organic aerosol formation from anthropogenic air pollution: Rapid and higher than expected, Geophys. Res. Lett., 33(17), 4407, 2006.

Volkamer, R., Ziemann, P. J. and Molina, M. J.: Secondary Organic Aerosol Formation from Acetylene (C2H2): seed effect on SOA yields due to organic photochemistry in the aerosol aqueous phase, Atmos. Chem. Phys., 9(6), 1907–1928, 2009.

Wang, J., -N. Lee, Y., Daum, P. H., Jayne, J. and Alexander, M. L.: Effects of aerosol organics on cloud condensation nucleus (CCN) concentration and first indirect aerosol effect, Atmospheric Chemistry and Physics, 8(21), 6325–6339, doi:10.5194/acp-8-6325-2008, 2008.

Willis, M. D., Lee, A. K. Y., Onasch, T. B., Fortner, E. C., Williams, L. R., Lambe, A. T., Worsnop, D. R., and Abbatt, J. P. D.: Collection efficiency of the soot-particle aerosol mass spectrometer (SP-AMS) for internally mixed particulate black carbon, Atmos. Meas. Tech., 7, 4507–4516, https://doi.org/10.5194/amt-7-4507-2014, 2014.

Yang, M., Blomquist, B. W. and Huebert, B. J.: Constraining the concentration of the hydroxyl radical in a stratocumulus-topped marine boundary layer from sea-to-air eddy covariance flux measurements of dimethylsulfide, Atmos. Chem. Phys., 9(23), 9225–9236, 2009.

Yokelson, R. J., Crounse, J. D., DeCarlo, P. F., Karl, T., Urbanski, S., Atlas, E., Campos, T., Shinozuka, Y., Kapustin, V., Clarke, A. D., Weinheimer, A., Knapp, D. J., Montzka, D. D., Holloway, J., Weibring, P., Flocke, F., Zheng, W., Toohey, D., Wennberg, P. O., Wiedinmyer, C., Mauldin, L., Fried, A., Richter, D., Walega, J., Jimenez, J. L.,

Adachi, K., Buseck, P. R., Hall, S. R. and Shetter, R.: Emissions from biomass burning in the Yucatan, Atmos. Chem. Phys., 9(15), 5785–5812, 2009.

Yue, X., Mickley, L. J., Logan, J. A. and Kaplan, J. O.: Ensemble projections of wildfire activity and carbonaceous aerosol concentrations over the western United States in the mid-21st century, Atmospheric Environment, 77, 767–780, doi:10.1016/j.atmosenv.2013.06.003, 2013.

Zhou, S., Collier, S., Jaffe, D. A., Briggs, N. L., Hee, J., Sedlacek, A. J., III, Kleinman, L., Onasch, T. B. and Zhang, Q.: Regional influence of wildfires on aerosol chemistry in the western US and insights into atmospheric aging of biomass burning organic aerosol, Atmos. Chem. Phys., 17(3), 2477–2493, 2017.

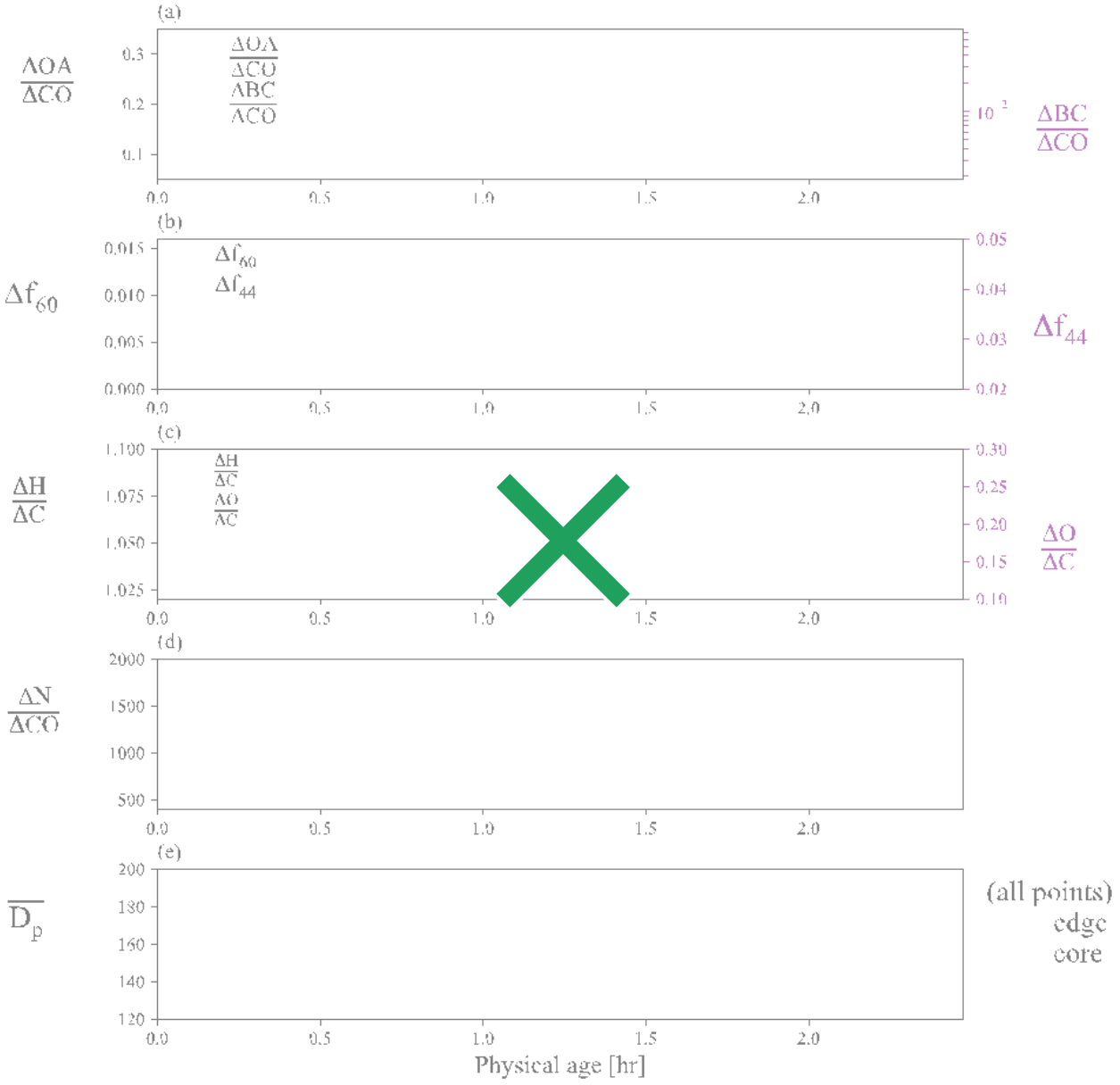
(a)
ΔOA/ΔCO
0.3
0.2
0.1
ΔOA/ΔCO
ΔBC/ΔCO
10 -2
0.0
0.5
1.0
1.5
2.0
(b)
Δf60
0.015
0.010
0.005
0.000
Δf60
Δf44
0.05
0.04
0.03
0.02
Δf44
(c)
ΔH/ΔC
1.100
1.075
1.050
1.025
ΔH/ΔC
ΔO/ΔC
0.30
0.25
0.20
0.15
0.10
ΔO/ΔC
(d)
ΔN/ΔCO
2000
1500
1000
500
(e)
Dp
200
180
160
140
120
(all points)
edge
core
Physical age [hr]

869

870

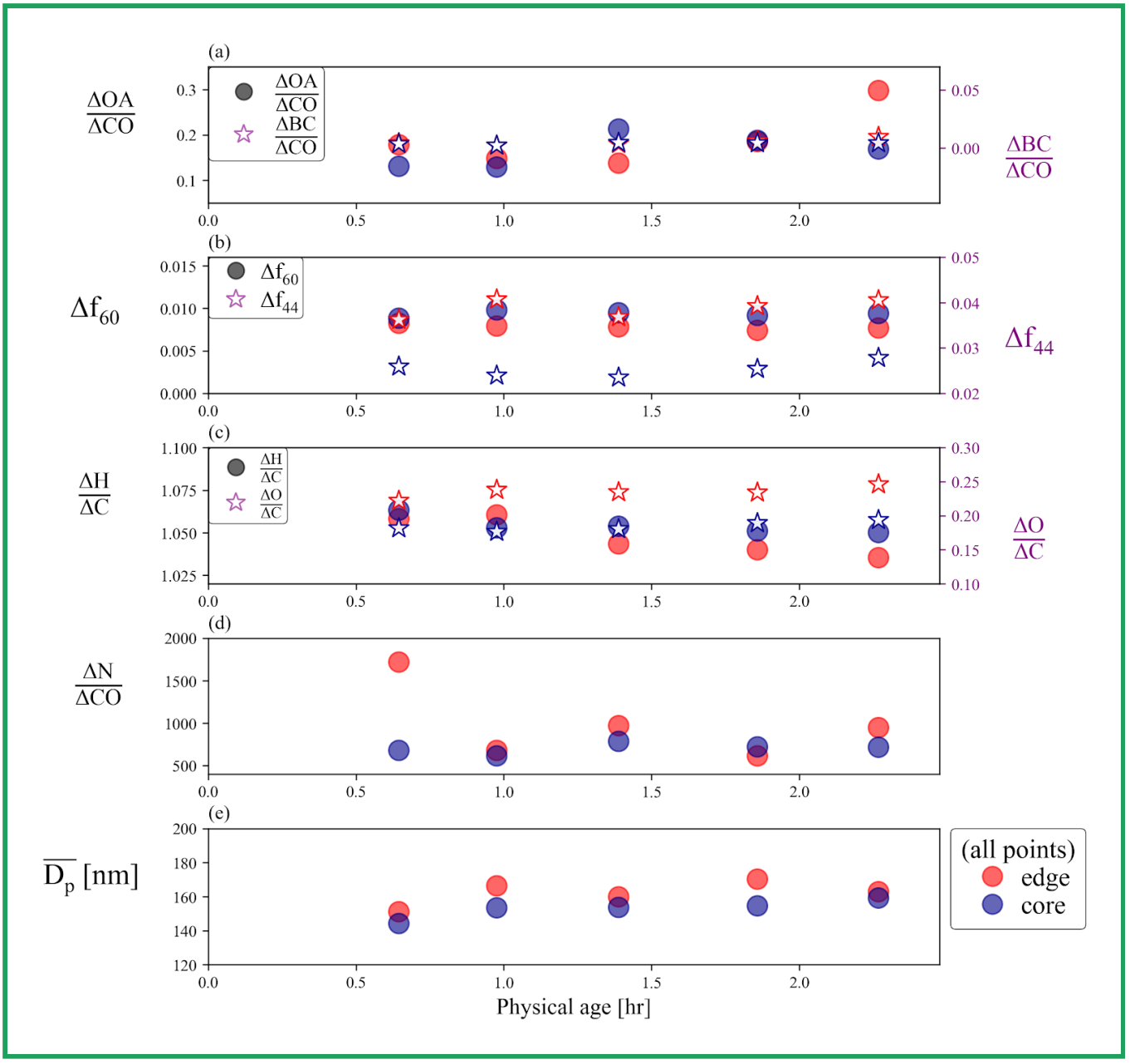

871

872 **Figure 1: Aerosol properties from the first set of pseudo-Lagrangian transects from the Colockum fire on flight '730b' (a)**
873 **ΔOA/ΔCO (right y-axis) and ΔBC/ΔCO (left y-axis), (b) Δf_{60} (right y-axis) and Δf_{44} (left y-axis), (c) ΔH/ΔC (right y-axis) and**
874 **ΔO/ΔC (left y-axis), (d) ΔN/ΔCO, and (e) $\overline{D_p}$ against physical age. For each transect, the data is divided into edge (the lowest**
875 **5-15% of ΔCO data; red points) and core (90-100% of ΔCO data; blue points). ΔBC/ΔCO is shown in log scale to improve clarity.**

876

877

878
879

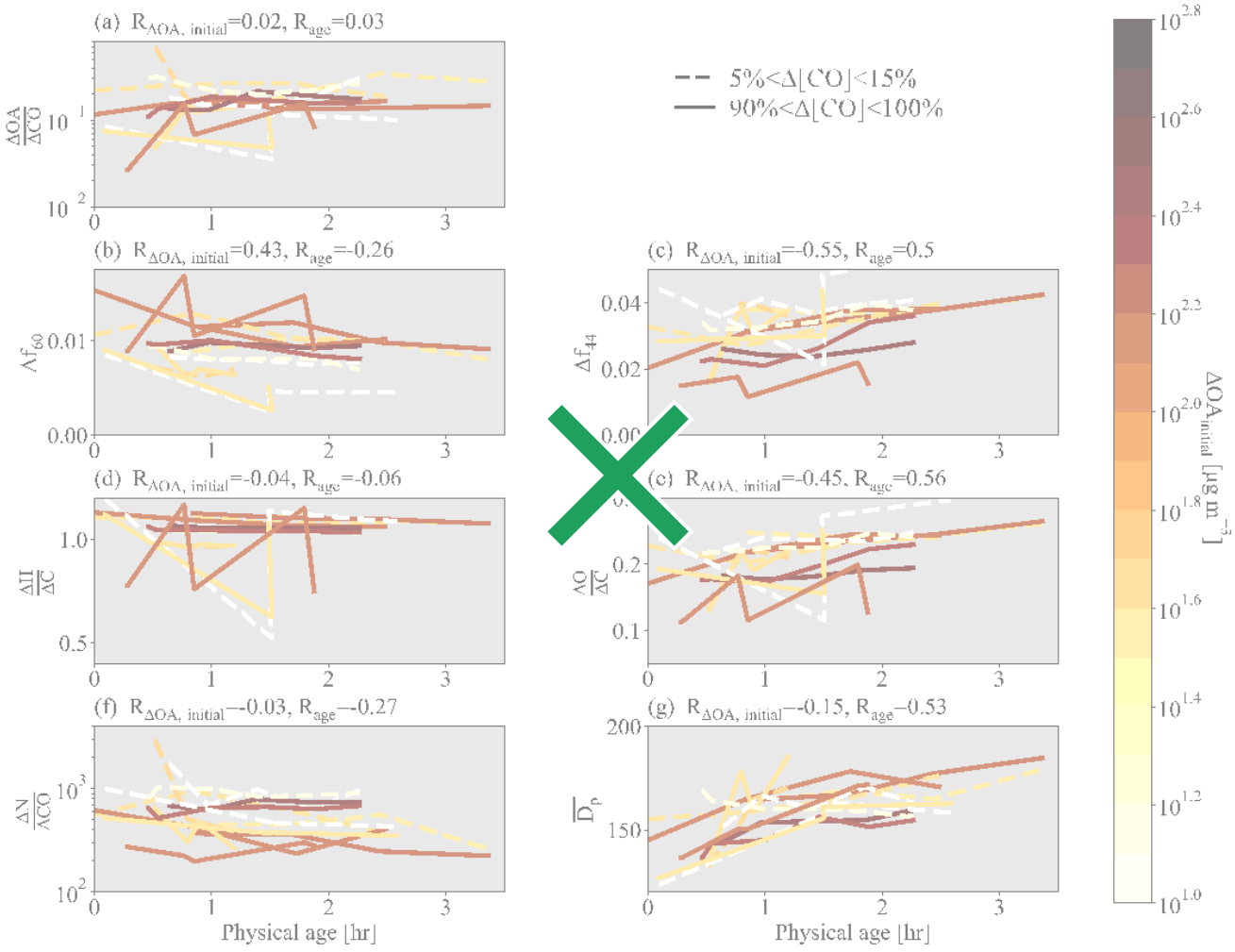

880

881
882

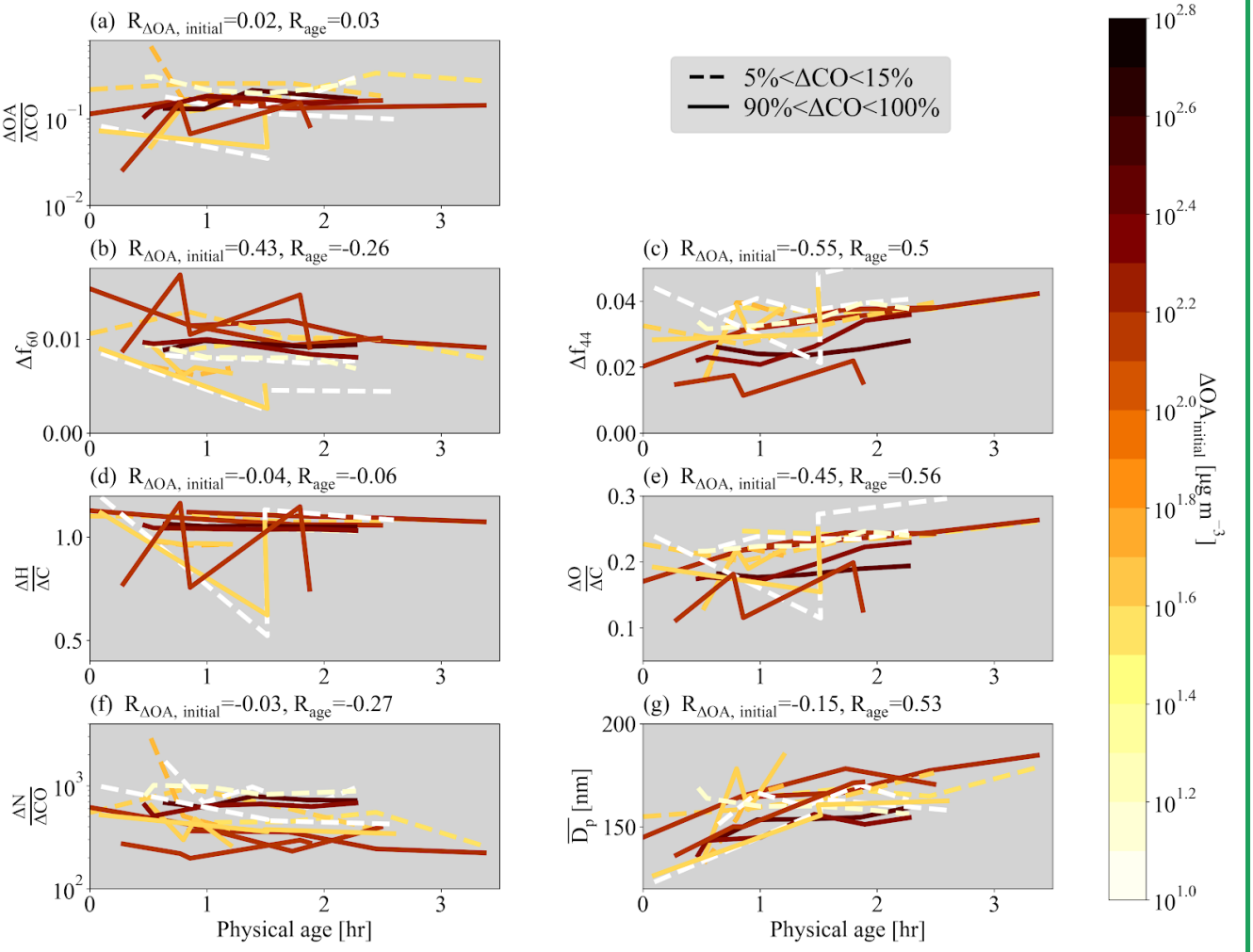

Figure 2. Various normalized parameters as a function of physical age for the 7 sets of pseudo-Lagrangian transects. Separate lines are shown for the edges (lowest 5-15% of ΔCO; dashed lines) and cores (highest 90-100% of ΔCO; solid lines). (a) ΔOA/ΔCO, (b) Δf_{60}, (c) Δf_{44}, (d) ΔH/ΔC, (e) ΔO/ΔC, (f) ΔN/ΔCO, and (g) $\overline{D_p}$ between 40-262 nm against physical age for all flights, colored by $\Delta OA_{initial}$. Some flights have missing data. Also provided is the Spearman correlation coefficient, R, between each variable and $\Delta OA_{initial}$ and physical age for each variable. Note that panels (a) and (f), ~~(d), and (g)~~ have a log y-axis.

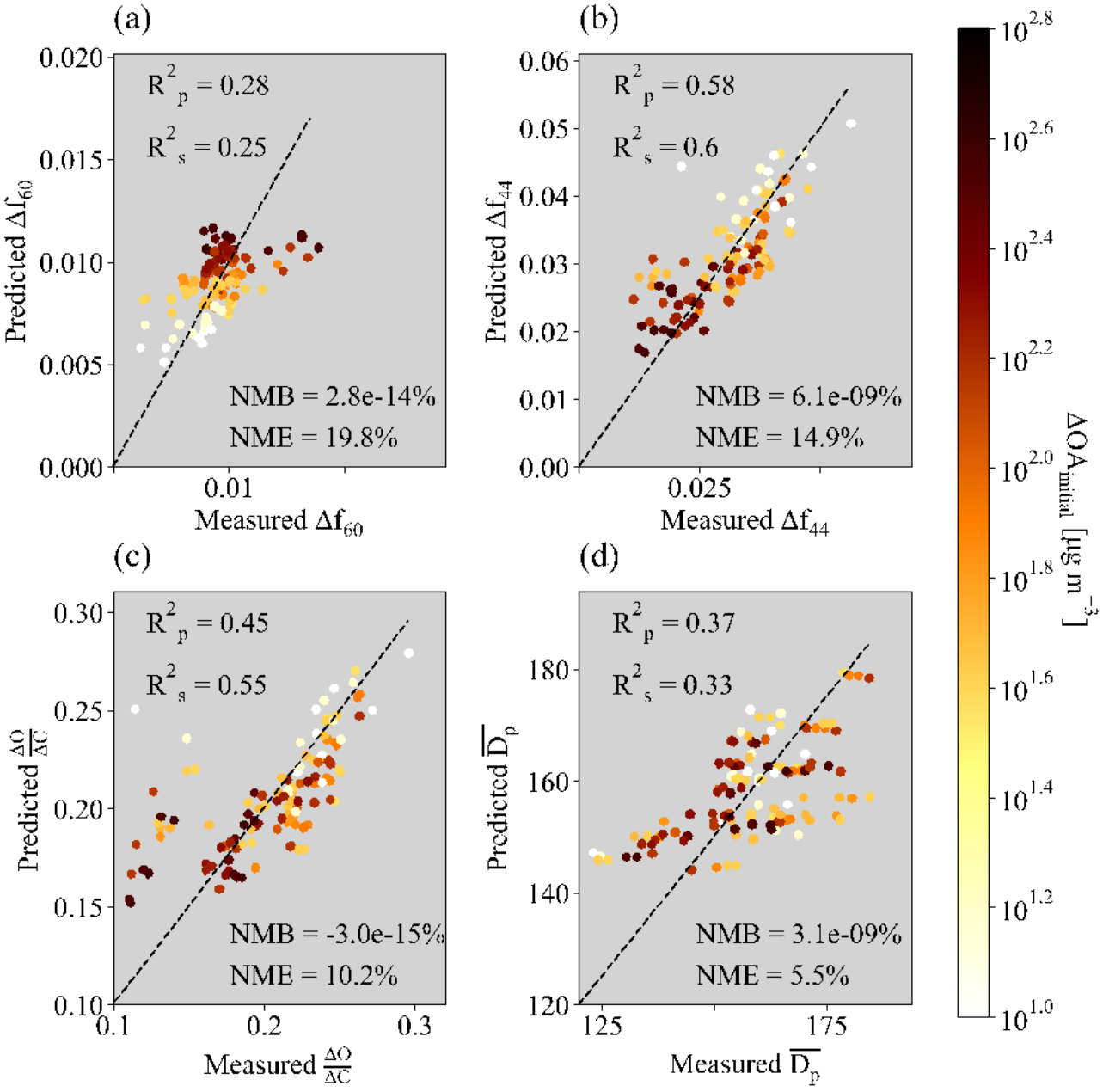

Figure 3. Measured versus predicted (a) Δf_{60}, (b) Δf_{44}, (c) ΔO/ΔC, and (d) $\overline{D_p}$ between 40-262 nm. The predicted values are from the equation $X = a\ log_{10}(OA_{initial}) + b\ (Physical\ age) + c$ where $X = \Delta f_{60}$, Δf_{44}, ΔO/ΔC, or $\overline{D_p}$. The values of *a*, *b*, and *c* are provided in Table S3. The Pearson and Spearman coefficients of determination (R_p^2 and R_s^2, respectively) are provided in each panel, along with the normalized mean bias (NMB) and normalized mean error (NME). Note that Fig. 2 provides R values rather than R^2 to

provide information upon the trend of the correlation. Included in the fit and figure are points from all four ΔCO regions within the plume (the 5-15%, 15-50%, 50-90%, and 90-100% of ΔCO), all colored by the mean $\Delta OA_{initial}$ of each ΔCO percentile range.

Supporting information for
Dilution impacts on smoke aging: Evidence in BBOP data

Anna L. Hodshire[1], Emily Ramnarine[1], Ali Akherati[2], Matthew L. Alvarado[3], Delphine K. Farmer[4], Shantanu H. Jathar[2], Sonia M. Kreidenweis[1], Chantelle R. Lonsdale[3], Timothy B. Onasch[5], Stephen R. Springston[6], Jian Wang[6,a], Yang Wang[7,b], Lawrence I. Kleinman[6], Arthur J. Sedlacek III[6], Jeffrey R. Pierce[1]

[1] Department of Atmospheric Science, Colorado State University, Fort Collins, CO 80523, United States
[2]Department of Mechanical Engineering, Colorado State University, Fort Collins, CO 80523, United States
[3]Atmospheric and Environmental Research, Inc., Lexington, MA 02421, United States
[4]Department of Chemistry, Colorado State University, Fort Collins, CO 80523, United States
[5]Aerodyne Research Inc., Billerica, MA 01821, United States
[6]Environmental and Climate Sciences Department, Brookhaven National Laboratory, Upton, NY 11973, United States
[7]Center for Aerosol Science and Engineering, Washington University, St. Louis, MO 63130, United States
[a]Now at Center for Aerosol Science and Engineering, Washington University, St. Louis, MO 63130, United States
[b]Now at Department of Civil, Architectural and Environmental Engineering, Missouri University of Science and Technology, Rolla, Missouri 65409, United States

Text S1. Further details on BBOP instrumentation

The Fast Integrated Mobility Spectrometer (FIMS) characterizes particle sizes based on electrical mobility similar to the operating principle of the ~~as in~~ scanning mobility particle sizer (SMPS). Because the FIMS measures particles of different sizes simultaneously instead of sequentially as in traditional SMPS, it provides aerosol size distribution with a much higher time resolution at 1 Hz (Wang et al., 2017). The relative humidity of the aerosol sample was reduced to below ~25% using a Nafion dryer before being introduced into the FIMS. Therefore, the measured size distributions represented that of the dry aerosol particles. The particle number concentration integrated from FIMS size distribution typically agrees with the CPC 3010 (Condensation Particle Counter) measurement (Kleinman et al., 2020) within ~ 15% when size distribution suggests that particles smaller than 20~~10~~ nm contribute negligibly to the total number concentration. Thus, we estimate the uncertainty in the FIMS number concentration to be ~15%. The uncertainty in measured particle size is about 3% (Wang et al., 2017).

The Soot Particle Aerosol Mass Spectrometer (SP-AMS) is thoroughly detailed in Kleinman et al. (2020). Although it was not directly characterized for uncertainties during the BBOP campaign, we estimate uncertainties as follows. The AMS uncertainty is estimated following the methods in (Bahreini et al. 2009) (first equation of their supplemental information), leading to 37% uncertainty for organics. The laser vaporizer adds additional uncertainty up to 20%. Thus summing the uncertainties in quadrature leads to a 42% uncertainty in organics. The Soot Photometer (SP2) had an uncertainty of 20%.

CO measurement uncertainties are detailed in Kleinmen et al. (2020): the Off-Axis Integrated Cavity Output Spectroscopy was found to have an accuracy of 1-2%, and the precision at ambient backgrounds of 90 ppb was 0.5 ppbv RMS (using a 1 second averaging).

An SPN1 radiometer (Badosa et al., 2014; Long et al., 2010) measured ~~provided~~ total shortwave irradiance, with a shaded mask applied following (Badosa et al., (2014). The data was corrected for tilt up to 10 degrees of tilt, following (Long et al., (2010). For tilt greater than 10 degrees these values are set to "bad". Instrument uncertainties are detailed in (Badosa et al. (2014).

The Soot Particle – Aerosol Mass Spectrometer (SP-AMS) operating on the DOE G1 aircraft during BBOP has been described in detail by Collier et al. (2016), Sedlacek et al. (2018), and Kleinman et al. (2020). The SP-AMS sampled PM_1 through a constant pressure inlet operating at a pressure of ~620 Torr (Bahreini et al., 2008). The SP-AMS was equipped with dual vaporizers: (1) standard resistively heated tungsten vaporizer; and (2) 1064 nm intracavity laser vaporizer (Onasch et al., 2012). The standard tungsten vaporizer was operated at a nominal value of 600°C for the full data set. The SP-AMS operating with the laser vaporizer OFF is effectively the same as a standard HR-AMS, measuring non-refractory particulate matter (NR-PM). The SP-AMS operating in dual vaporizer mode, with both the standard tungsten vaporizer and the laser vaporizer ON measures the NR-PM and is additionally sensitive to refractory black carbon (rBC).

Flight data was collected at a rapid rate using “Fast-MS” in V-mode (i.e., mass spectral resolution ~2000) with 1 second sample time, with negligible particle time-of-flight (PTOF) data (DeCarlo et al., 2006; Lack et al., 2009). The pulsed, orthogonal extraction time-of-flight mass spectrometer (TOF-MS) was operated with a 60 µs pulser period and collected mass spectra from m/z 11 to m/z 955. “Fast-MS” data was collected in open (i.e., sample) mode for 52 seconds and in closed (i.e., background) mode for 8 seconds every minute. The laser vaporizer was operated by either automatically alternated laser ON and OFF each minute or manually sampling with the laser ON or OFF for long periods of time, such as full plume transects. The majority of the data (>76%) was collected in dual vaporizer mode (i.e., laser on).

The SP-AMS was calibrated for NR-PM with ammonium nitrate and for rBC with Regal black 8 independent times during BBOP. The average ionization efficiency (IE) with respect to ammonium nitrate was measured to be 8.1e-8 and the relative ionization efficiency (RIE) of rBC was measured to be 0.28, although the rBC from the SP-AMS was not used in this study.

Collier et al. (2016) determined the SP-AMS laser OFF collection efficiency (CE) to be 0.5 through comparisons with an independent HR-AMS located at the Mount Bachelor Observatory during over-flights. SP-AMS measured NR-PM values collected with the laser ON and OFF were compared for 16 different biomass burning plumes (Sedlacek et al., 2018; Kleinman et al., 2020). In each case, the plume was sampled with the laser ON and with the laser OFF, independently, and the measured plume NR-PM was normalized to CO to account for potential changes in the plume dilution between transects. The average ratio for NR-PM laser

ON to laser OFF was 1.52. From these results, the average CE of NR-PM measured with the laser ON to be 0.76 with a standard deviation of 0.07 (Sedlacek et al., 2018; Kleinman et al., 2020). There is substantial evidence in the published literature for the CE of the tungsten vaporizer (Lim et al., 2019) and the laser vaporizer (Willis et al., 2014) to change as a function of chemical composition and rBC coating thickness. Unfortunately for various reasons, instrument comparisons of measurements of PM_1 mass loading concentrations were very limited during BBOP, such that there does not exist a useful estimate of a changing CE for either SP-AMS vaporizer with changing plume conditions.

The SP-AMS data was analyzed using ToF-AMS Analysis Toolkit 1.61B and ToF-AMS HR Analysis 1.21B in Igor Pro. Gas phase carbon dioxide (CO_2) was directly measured on the G1 aircraft and was used to subtract gas phase contributions to CO_2^+ ion signal in the SP-AMS. SP-AMS standard NR-PM chemical species (i.e., Org, SO_4, NO_3, NH_4, Chl) were calculated using high resolution (HR) fits. f_{44} and f_{60} are unit mass resolution (UMR) ratios, whereas O:C ratios were derived using HR fits. Although it was not directly characterized for uncertainties during the BBOP campaign, we estimate uncertainties as follows. The AMS uncertainty is estimated following the methods in (Bahreini et al. 2009) (first equation of their supplemental information), leading to 37% uncertainty for organics. The laser vaporizer adds additional uncertainty up to 20%. Thus summing the uncertainties in quadrature leads to a 42% uncertainty in organics. (The Soot Photometer (SP2) had an uncertainty of 20%.)

We further analyzed the UMRs and the potential for laser ON specific ion signals to interfere with laser OFF NR-PM ion signals with the SP-AMS data. The chemical composition of the measured wildfire plumes during BBOP were > 90% NR-PM organic material (Collier et al., 2016; Kleinman et al., 2020). rBC mass fractions were typically below 2% (Kleinman et al., 2020), though the number fractions were higher (Sedlacek et al., 2018). Despite these low concentrations, the SP-AMS laser ON (relative to laser OFF) was observed to generate C_n^+ ion signals with an identifiable fragmentation pattern for rBC material and the laser ON to OFF NR-PM signal was observed to increase by ~50% on average. Similar results have been published for ambient urban aerosol (e.g., Lee et al. 2015). Recent laboratory work to investigate these issues has eliminated laser alignment issues and indirect heating as potential causes for these observations (Avery et al., 2020). Thus, these observations are likely due to a combination of different collection efficiencies (CEs) and relative ionization efficiencies (RIEs) for the two vaporizers when used in dual vaporizer mode (i.e., laser ON).

The HR ion signals at m/z 44 are dominated by CO_2^+ and $C_2H_4O^+$ ions (Fig. S31~~30~~). The ratio of $C_2H_4O^+/CO_2^+$ increases with plume mass loading (i.e., concentration) and decreases with distance from the fire (Fig. S31~~30~~), inline with the observations reported here for decreases in oxidation levels as a function of dilution. The HR ion signals at m/z 60 are dominated by $C_2H_4O_2^+$ and C_5^+ (Fig. S32~~1~~). HR fitting of C_5^+ indicated that it averaged ~6% of the $C_2H_4O_2^+$ ion signal, independent of the laser vaporizer state (i.e., ON or OFF). For large $C_2H_4O_2^+$ ion signals in relatively undiluted biomass burning plumes, this ratio is likely controlled by the errors in

fitting a small peak in the wings of a larger peak (Corbin et al., 2014~~5~~). At lower ion signal levels, the C_5^+/ $C_2H_4O_2^+$ becomes significantly noisier, but the average does not change significantly. Laser ON may slightly increase the average ratio at lower $C_2H_4O_2^+$ ion signals, which could overestimate f_{60} for relatively dilute plumes. If this were true, the observed decrease in f_{60} with plume dilution (i.e., due to fire size and atmospheric age) would be slightly smaller than reported here.

Past research on SP-AMS ion signals from the laser vaporizer and the standard tungsten vaporizer have identified several complicating factors when operating the SP-AMS in dual vaporizer mode. First, organic material coating rBC particles and detected using the laser vaporizer have noted different fragmentation patterns (Onasch et al., 2012) and chemical compositions (Canagaratna et al., 2015) compared with the same organic material detected using the standard tungsten vaporizer. Further, there are reports of SP-AMS laser vaporizer detecting refractory CO_2^+ ions from rBC particles (Corbin et al., 2014). Currently, we have not assessed the potential for refractory CO_2^+ ion signals during BBOP as both the rBC and Org signals are highly correlated in biomass burning plumes, making minor changes to these ratios difficult to ascertain. To address the question of whether the laser vaporizer generated different ion signals from similar organic compounds, we analyzed the laser ON and OFF plume transect pairs that were used for determining laser ON CE values relative to laser OFF.

As shown in Fig. S33~~32~~, the HR O:C, UMR f_{44}, and UMR f_{60} ratios are highly correlated between laser ON and OFF conditions, though differ by apparent factors. Laser ON HR O:C ratios are approximately 4% lower than laser OFF. In large part, this is due to the UMR f_{44} ratios, which are dominated by CO_2^+ ions, being 17% lower for laser ON. UMR f_{60} ratios are 18% higher in laser ON than OFF. These observations are in line with the published results from Canagaratna et al., (2015), which observed that laser vaporizer only HR O:C ratios were ~17% lower than tungsten vaporizer only HR O:C ratios for the same organic material and the HR H:C ratios were ~16% higher. In the case of BBOP, the laser vaporizer signals represented approximately 1/3 of the total organic signal with dual vaporizers. The BBOP measured 4% lower HR O:C ratios are similar in magnitude to 5.6% (i.e., 0.33*17%) expected if the Canagaratna et al. (2015) results applied to BBOP measurements.

The BBOP SP-AMS data used in this manuscript is used to measure trends in OA. O:C, f_{44}, and f_{60} with plume dilution, either at different plume ages and/or different concentration percentiles across a biomass plume (i.e., edge vs. center). A question is whether the mixing of laser ON and OFF data here somehow biases the results due to the different absolute values between the two different states. A quick extension of the above plume pair analysis (Fig. S33~~2~~) includes several "background" measurements made between the plumes (i.e., below 150 ppbv CO) and compared for laser ON vs. OFF to investigate if this ratio changes substantially between plume (i.e., high level) and background (i.e., low level) levels. The laser ON:OFF ratios of measured HR O:C averaged 0.95±0.049 in background and 0.96±0.029 in plume, UMR f_{44} averaged 0.89±0.085 in background and 0.85±0.068 in plume, and UMR f_{60} averaged 1.17±0.23

in background and 1.15±0.13 in plume. These results suggest that the observed laser ON/OFF ratios do not change from low to high signal levels, such that the trends observed for laser OFF should hold for laser ON, and vice versa. Further, the laser ON vs. OFF data points are randomly distributed throughout the measurements rather than systematically distributed to near- vs. far-field measurements or core vs. edge measurements. Hence, there should be no systematic bias due to the use of the combined laser ON and OFF data, although this combination of laser-on and -off data may contribute to noise in the observed trends.

Text S2. Heterogeneous chemistry calculations

We test the impact of heterogeneous chemistry on aerosol mass loss within the smoke plume. We performed a simple calculation of reactive uptake of OH molecules with particle-phase organics that resulted in loss of organic products. These calculations include assumed values of particle diameter, OH concentration, OH diffusion coefficient, and OH reactive uptake coefficient. ~~of OH molecules collision to the surface of a single particle ranging from 1 nm to 1 μm size in diameter.~~ The following parameters are assumed for the calculations:

- OH diffusivity = 3.5e-5 [m^2 s^{-1}]
- Particle diameter varied from 1 - 1000 [nm]
- Constant OH concentration varied from 1e5 to 5e7 [molecules cm^{-3}]
- Reactive uptake coefficients varied from 0.1 to 1 [unitless]
- Molecular weight of organics = 200 [g mol^{-1}]
- Density of organics = 1.4 [g cm^{-3}]
- Total run time = 3 [hours]

The collision rate of OH with the particle surface was calculated using the condensation equations in Seinfeld and Pandis (2006). As a ~~n upper bound~~ calculation of the upper bound limit of evaporation due to heterogeneous chemistry, we assume each collision results in removing an organic molecule on the surface of the particle (assumed to be 200 amu), fragmenting and removing the molecule from the particle. The fragmentation products are not assumed to participate in further reaction. Figure S23a shows the resulting final:initial mass ratios after four hours of aging, indicating that for the~~all~~ aerosol sizes containing most of the mass ~~captured~~ in this study (>100 nm) and under expected~~a range of~~ OH concentrations ($<10^7$ cm^{-3}), >90% of the aerosol mass remains after 3 hours in all but the cases with a reactive uptake coefficient of 1 and an OH concentration of 10^7 cm^{-3}. Note however that (1) the reactive uptake coefficient is likely lower than 1 ~~As a lower bound, we also include a case in which only 10% of all OH collisions result in a mass loss of 200 amu (Figure S23c)~~ (Slade and Knopf, 2013), (2) not every reaction will lead to complete evaporation of all products, and (3) OH concentrations are often lower than 10^7 cm^{-3} (Juncosa Calahorrano et al., 2020)~~(CITATION)~~.

Avery, A.M., Williams, L.R., Fortner, E.C., Robinson, W.A., and Onasch, T.B.: Particle detection using the dual-vaporizer configuration of the soot particle Aerosol Mass Spectrometer (SP-AMS). Aerosol Sci. Technol., doi:10.1080/02786826.2020.1844132, 2020.

Bahreini, R.; Dunlea, E. J.; Matthew, B. M.; Simons, C.; Docherty, K. S.; DeCarlo, P. F.; Jimenez, J. L.; Brock, C. A.; Middlebrook, A. M.: Design and Operation of a Pressure-Controlled Inlet for Airborne Sampling with an Aerodynamic Aerosol Lens. Aerosol Sci. Technol. 42 (6), 465−471, 2008

Badosa, J., Wood, J., Blanc, P., Long, C. N., Vuilleumier, L., Demengel, D. and Haeffelin, M.: Solar irradiances measured using SPN1 radiometers: uncertainties and clues for development, Atmospheric Measurement Techniques, 7, 4267–4283, 2014.

Bahreini, R., Ervens, B., Middlebrook, a. M., Warneke, C., de Gouw, J. a., DeCarlo, P.F., Jimenez, J.L., Brock, C. a., Neuman, J. a., Ryerson, T.B., Stark, H., Atlas, E., Brioude, J., Fried, A., Holloway, J.S., Peischl, J., Richter, D., Walega, J., Weibring, P., Wollny, a. G., and Fehsenfeld, F.C.: Organic aerosol formation in urban and industrial plumes near Houston and Dallas, Texas. J. Geophys. Res., 114:D00F16, 2009.

Canagaratna, M.R., Massoli, P., Browne, E.C., Franklin, J.P., Wilson, K.R., Onasch, T.B., Kirchstetter, T.W., Fortner, E.C., Kolb, C.E., Jayne, J.T., Kroll, J.H., and Worsnop, D.R.: Chemical Compositions of Black Carbon Particle Cores and Coatings via Soot Particle Aerosol Mass Spectrometry with Photoionization and Electron Ionization. J. Phys. Chem. A, 119(19):4589–4599, 2015.

Collier, S., Zhou, S., Onasch, T.B., Jaffe, D.A., Kleinman, L., Sedlacek, A.J., Briggs, N.L., Hee, J., Fortner, E., Shilling, J.E., Worsnop, D., Yokelson, R.J., Parworth, C., Ge, X., Xu, J., Butterfield, Z., Chand, D., Dubey, M.K., Pekour, M.S., Springston, S., and Zhang, Q.: Regional Influence of Aerosol Emissions from Wildfires Driven by Combustion Efficiency: Insights from the BBOP Campaign. Environ. Sci. Technol., 50(16):acs.est.6b01617, 2016.

Corbin, J.C., Sierau, B., Gysel, M., Laborde, M., Keller, A., Kim, J., Petzold, A., Onasch, T.B., Lohmann, U., and Mensah, A. A.: Mass spectrometry of refractory black carbon particles from six sources: carbon-cluster and oxygenated ions. Atmos. Chem. Phys., 14(5):2591–2603, 2014.

Corbin, J., Othman, A., D. Allan, J., R. Worsnop, D., D. Haskins, J., Sierau, B., Lohmann, U., and A. Mensah, A. (2015). Peak-fitting and integration imprecision in the Aerodyne aerosol mass spectrometer: effects of mass accuracy on location-constrained fits. Atmos. Meas. Tech., 8(11):4615–4636.
DeCarlo, P.F., Kimmel, J.R., Trimborn, A., Northway, M.J., Jayne, J.T., Aiken, A.C., Gonin, M., Fuhrer, K., Horvath, T., Docherty, K.S., Worsnop, D.R., and Jimenez, J.L.: Field-Deployable, High-Resolution, Time-of-Flight Aerosol Mass Spectrometer. Anal. Chem., 78(24):8281–8289, 2006.

Juncosa Calahorrano, J. F., Lindaas, J., O'Dell, K., Palm, B. B., Peng, Q., Flocke, F., Pollack, I. B., Garofalo, L. A., Farmer, D. K., Pierce, J. R., Collett, J. L., Weinheimer, A., Campos, T., Hornbrook, R. S., Hall, S. R., Ullmann, K., Pothier, M. A., Apel, E. C., Permar, W., Hu, L., Hills, A. J., Montzka, D., Tyndall, G., Thornton, J. A. and Fischer, E. V.: Daytime Oxidized Reactive Nitrogen Partitioning in Western U.S. Wildfire Smoke Plumes, J. Geophys. Res. Atmos., 1–47, doi:10.1029/2020jd033484, 2020.

Kleinman, L. I., Sedlacek, A. J., III, Adachi, K., Buseck, P. R., Collier, S., Dubey, M. K., Hodshire, A. L., Lewis, E., Onasch, T. B., Pierce, J. R., Shilling, J., Springston, S. R., Wang, J., Zhang, Q., Zhou, S. and Yokelson, R. J.: Rapid Evolution of Aerosol Particles and their Optical Properties Downwind of Wildfires in the Western U.S, Aerosols/Field Measurements/Troposphere/Physics (physical properties and processes), doi:10.5194/acp-2020-239, 2020.

Lack, D. A.; Corbett, J. J.; Onasch, T.; Lerner, B.; Massoli, P.; Quinn, P. K.; Bates, T. S.; Covert, D. S.; Coffman, D.; Sierau, B.; Herndon, S.; Allan, J.; Baynard, T.; Lovejoy, E.; Ravishankara, A. R.; Williams, E.: Particulate emissions from commercial shipping: Chemical, physical, and optical properties. J. Geophys. Res. 114 (D7), D00F04, 2009.

Lee, A.K.Y., Willis, M.D., Healy, R.M., Onasch, T.B.B., and Abbatt, J.P.D.: Mixing state of carbonaceous aerosol in an urban environment: single particle characterization using the soot particle aerosol mass spectrometer (SP-AMS). Atmos. Chem. Phys., 15(4):1823–1841, 2015.

Lim, C.Y., Hagan, D.H., Coggon, M.M., Koss, A.R., Sekimoto, K., de Gouw, J., Warneke, C., Cappa, C.D., and Kroll, J.H.: Secondary organic aerosol formation from the laboratory oxidation of biomass burning emissions. Atmos. Chem. Phys., 19(19):12797–12809, 2019.

Long, C. N., Bucholtz, A., Jonsson, H., Schmid, B., Vogelmann, A. and Wood, J.: A Method of Correcting for Tilt from Horizontal in Downwelling Shortwave Irradiance Measurements on Moving Platforms, The Open Atmospheric Science Journal, 4(1), 78–87, doi:10.2174/1874282301004010078, 2010.

Onasch, T. B., Trimborn, A., Fortner, E. C., Jayne, J. T., Kok, G. L., Williams, L. R., Davidovits, P. and Worsnop, D. R.: Soot particle aerosol mass spectrometer: Development, validation, and initial application, Aerosol Sci. Technol., 46(7), 804–817, doi:10.1080/02786826.2012.663948, 2012.

Sedlacek III, A.J., Buseck, P.R., Adachi, K., Onasch, T.B., Springston, S.R., and Kleinman, L.: Formation and evolution of tar balls from northwestern US wildfires. Atmos. Chem. Phys., 18(15):11289–11301, 2018.

Seinfeld, J. H. and Pandis, S. N.: Atmospheric Chemistry and Physics, 2nd edn., John Wiley and Sons, New York, 2006.

Slade, J. H. and Knopf, D. A.: Heterogeneous OH oxidation of biomass burning organic aerosol surrogate compounds: assessment of volatilisation products and the role of OH concentration on the reactive uptake kinetics, Phys. Chem. Chem. Phys., 15(16), 5898–5915, 2013.

Wang, J., Pikridas, M., Spielman, S. R. and Pinterich, T.: A fast integrated mobility spectrometer for rapid measurement of sub-micrometer aerosol size distribution, Part I: Design and model evaluation, J. Aerosol Sci., 108, 44–55, 2017.

Willis, M.D., Lee, A.K.Y., Onasch, T.B., Fortner, E.C., Williams, L.R., Lambe, A.T., Worsnop, D.R., and Abbatt, J.P.D.: Collection efficiency of the soot-particle aerosol mass spectrometer (SP-AMS) for internally mixed particulate black carbon. Atmos. Meas. Tech., 7(12):4507–4516, 2014.

Table S1. Flight description table.

Flight name, date	Number of sets of pseudo-Lagrangian transects	Fire name	Fuel[1]	~~Missing data~~[2]
‘726a’, 07-26-2013	2	Mile Marker 28	grasslands, shrub brush,	

			timber, and timber litter	
‘730a’, 07-30-2013	1	Colockum Tarps	grass, trees	
‘730b’, 07-30-2013	2	Colockum Tarps	grass, trees	
‘809a’, 08-09-2013	1	Colockum Tarps	grass, trees	~~NO_{yx}~~
‘821b’, 08-21-2013	1	Government Flats		~~O_3~~

[1]When known
[2]Instruments relevant to this study

Table S2. Calculated $R_{\Delta OA,initial}$ and R_{age} values for ΔOA/ΔCO, Δf_{60}, Δf_{44} ΔH/ΔC, ΔO/ΔC, ΔN/ΔCO, and D_p when one flight is left out of the statistical analysis. We include the original R values as the first row for comparison. Red values indicate that the correlation has improved compared to all flights in the statistical analysis (closer to ±1). Blue values indicate that the correlation has worsened (closer to 0) compared to all flights in the statistical analysis. Black values denote no change in the correlation compared to all flights in the statistical analysis. Note that for flights ‘726a’ and ‘730b’ both sets of Lagrangian transects have been left out.

ΔOA/ΔCO		
Flight left out, date	Resulting $R_{\Delta OA,\ initial}$	Resulting R_{age}
None	+0.02	+0.03
‘726a’, 07-26-2013	+0.12	0.0
‘730a’, 07-30-2013	+0.02	+0.07
‘730b’, 07-30-2013	+0.17	0.0
‘809a’, 08-09-2013	-0.25	+0.02
‘821b’, 08-21-2013	+0.05	+0.03
Δf_{60}		
Flight left out, date	Resulting $R_{\Delta OA,\ initial}$	Resulting R_{age}
None	+0.43	-0.26
‘726a’, 07-26-2013	+0.58	-0.38
‘730a’, 07-30-2013	+0.39	-0.37
‘730b’, 07-30-2013	+0.52	-0.19
‘809a’, 08-09-2013	+0.3	-0.21
‘821b’, 08-21-2013	+0.4	-0.26
Δf_{44}		
Flight left out, date	Resulting $R_{\Delta OA,\ initial}$	Resulting R_{age}
None	-0.55	+0.5
‘726a’, 07-26-2013	-0.63	+0.4
‘730a’, 07-30-2013	-0.62	+0.54
‘730b’, 07-30-2013	-0.45	+0.46
‘809a’, 08-09-2013	-0.54	+0.54
‘821b’, 08-21-2013	-0.42	+0.57
ΔH/ΔCO		

Flight left out, date	Resulting $R_{\Delta OA,\ initial}$	Resulting R_{age}
None	-0.04	-0.06
‘726a’, 07-26-2013	-0.04	-0.12
‘730a’, 07-30-2013	-0.13	-0.2
‘730b’, 07-30-2013	0.0	-0.16
‘809a’, 08-09-2013	0.02	-0.01
‘821b’, 08-21-2013	-0.01	-0.05
ΔO/ΔCO		
Flight left out, date	Resulting $R_{\Delta OA,\ initial}$	Resulting R_{age}
None	-0.45	+0.56
‘726a’, 07-26-2013	-0.54	+0.46
‘730a’, 07-30-2013	-0.52	+0.55
‘730b’, 07-30-2013	-0.21	+0.54
‘809a’, 08-09-2013	-0.5	+0.61
‘821b’, 08-21-2013	-0.32	+0.63
ΔN/ΔCO		
Flight left out, date	Resulting $R_{\Delta OA,\ initial}$	Resulting R_{age}
None	-0.03	-0.27
‘726a’, 07-26-2013	-0.03	-0.13
‘730a’, 07-30-2013	-0.03	-0.3
‘730b’, 07-30-2013	-0.21	-0.43
‘809a’, 08-09-2013	-0.07	-0.2
‘821b’, 08-21-2013	0.0	-0.37
$\overline{D_p}$		
Flight left out, date	Resulting $R_{\Delta OA,\ initial}$	Resulting R_{age}

None	-0.15	+0.53
'726a', 07-26-2013	-0.18	+0.43
'730a', 07-30-2013	-0.17	+0.57
'730b', 07-30-2013	+0.19	+0.63
'809a', 08-09-2013	-0.28	+0.52
'821b', 08-21-2013	-0.18	+0.52

Table S3. Fit coefficients *a, b,* and *c* for the fits shown in Fig. 3 , equation 4. The units of *a* are (metric), but note that the units of $\Delta OA_{initial}$ must be μg m^{-3}; the units of *b* are (metric)/hr, and the units of *c* are (metric), where (metric) = the units of $\Delta f_{60,}$ Δf_{44}, ΔO/ΔC, or $\overline{D_p}$, respectively.

Metric	*a*	*b*	*c*
Δf_{60}	2.8e-03	-6.4e-04	4.7e-03
Δf_{44}	-1.1e-02	5.8e-03	4.4e-02

ΔO/ΔC	-3.6e-02	2.6e-02	0.24
$\overline{D_p}$	-1.5	10	150

Table S4. Fit coefficients *a, b,* and *c* for the fits shown in Fig. S28 , equation 5. The units of *a* are (metric); the units of *b* are (metric)/hr, and the units of *c* are (metric), where (metric) = the units of $\Delta f_{60,}$ Δf_{44}, ΔO/ΔC, or $\overline{D_p}$, respectively.

Metric	*a*	*b*	*c*
Δf_{60}	0.14	-6.6e-02	-5.3
Δf_{44}	-0.14	0.11	-2.9
ΔO/ΔC	-7.3e-02	6.1e-02	-1.3

$\overline{D_p}$	-6.3e-03	4.0e-02	5.1

Table S5. Fit coefficients *a, b,* and *c* for the fits shown in Fig. S29 , equation 4 (but with $\Delta N_{initial}$ in place of $\Delta OA_{initial}$). The units of *a* are (metric); the units of *b* are (metric)/hr, and the units of *c* are (metric), where (metric) = the units of $\Delta f_{60,}$ Δf_{44}, $\Delta O/\Delta C$, or $\overline{D_p}$, respectively.

Metric	*a*	*b*	*c*
Δf_{60}	2.0e-03	-5.4e-04	-1.5e-03
Δf_{44}	-1.1e-02	5.3e-03	8.4e-02
$\Delta O/\Delta C$	-4.1e-02	2.4e-02	0.4
$\overline{D_p}$	-3.5	10	160

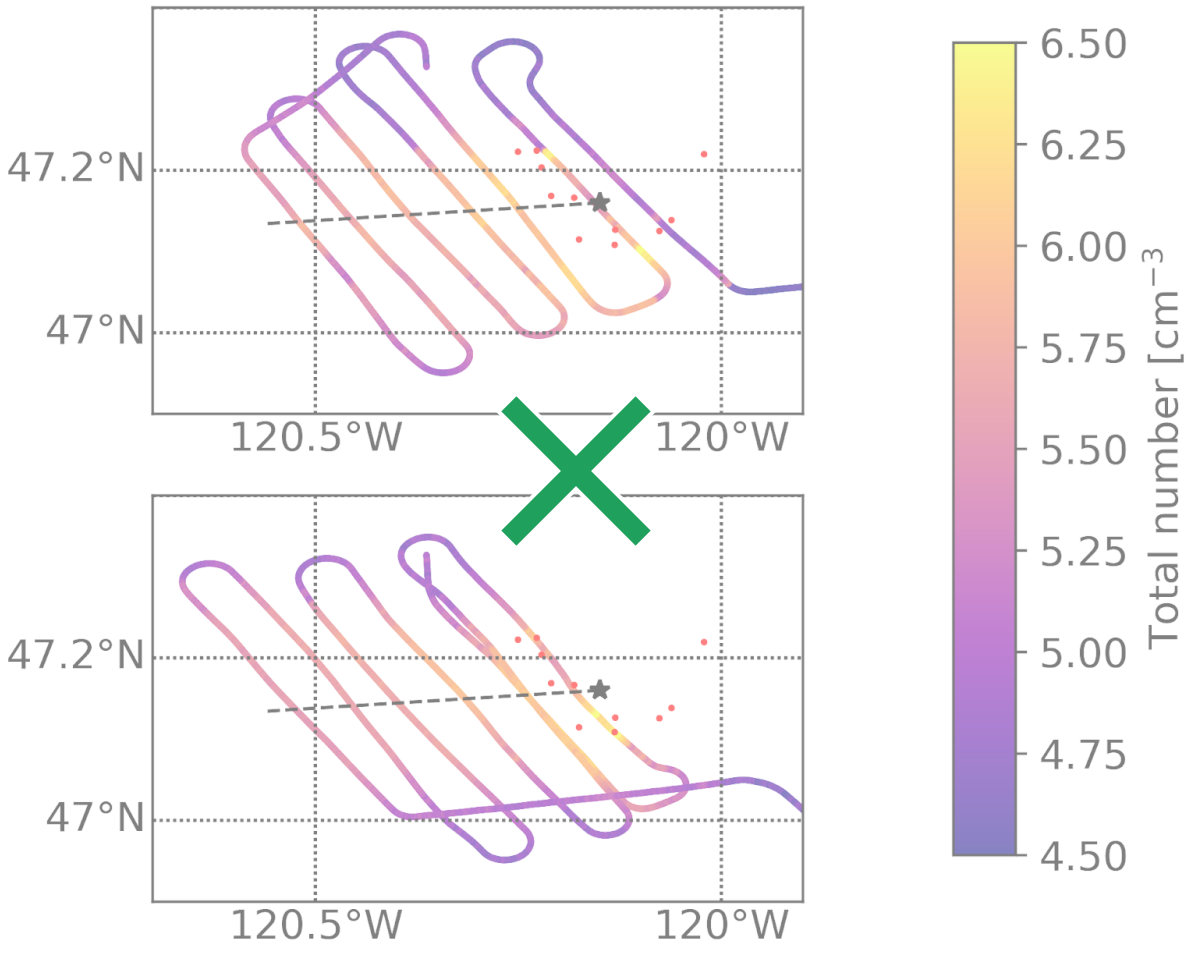
47.2°N
47°N
120.5°W
120°W
47.2°N
47°N
120.5°W
120°W
6.50
6.25
6.00
5.75
5.50
5.25
5.00
4.75
4.50
Total number [cm^{-3}]

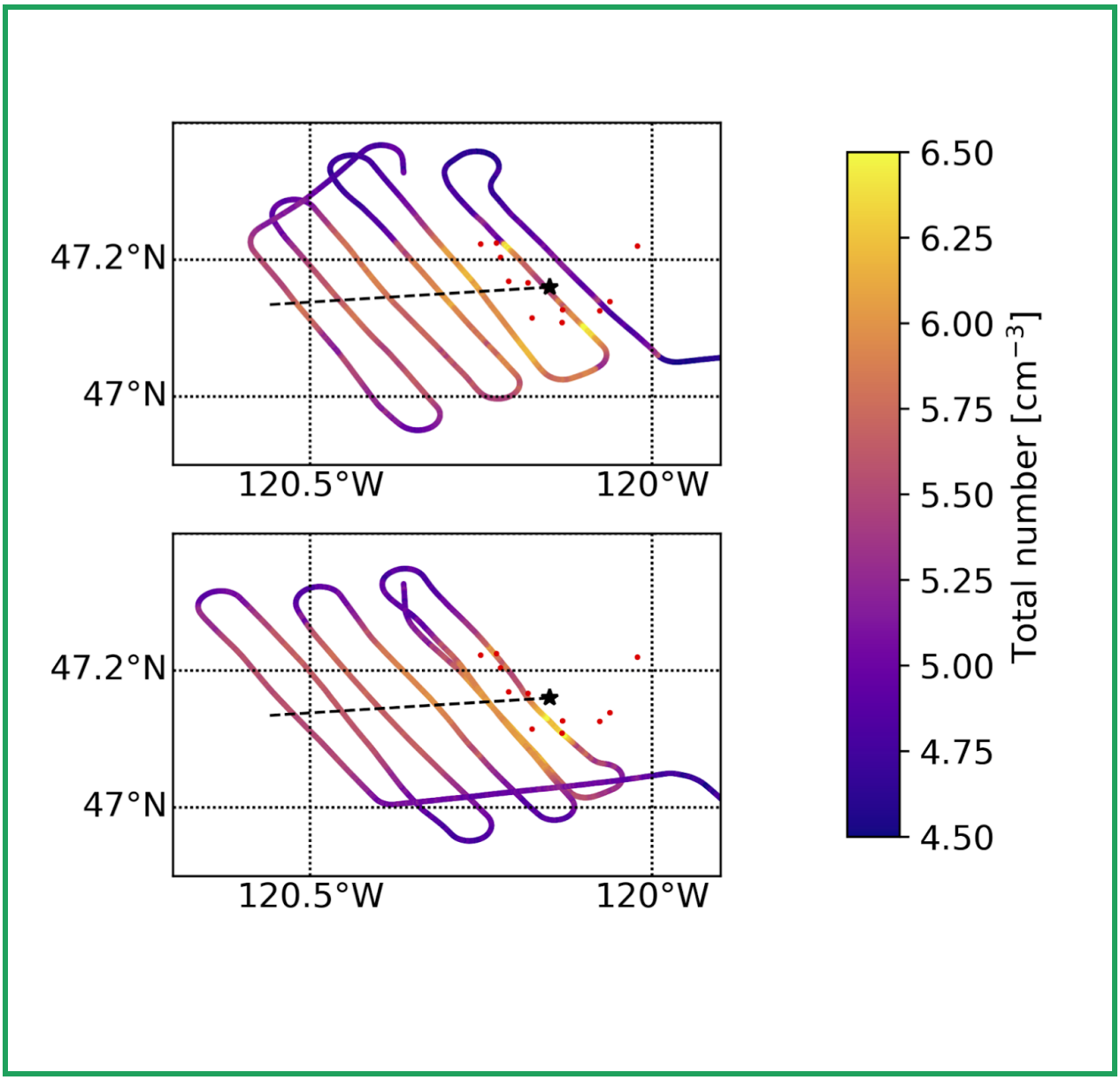

Figure S1. The flight path for flight '730b', colored by the FIMS total number concentration. The red dots are MODIS fire/thermal anomalies. The black star indicates the approximate center of the fire and the black dashed line indicates the approximate centerline of the plume, estimated by the number concentration.

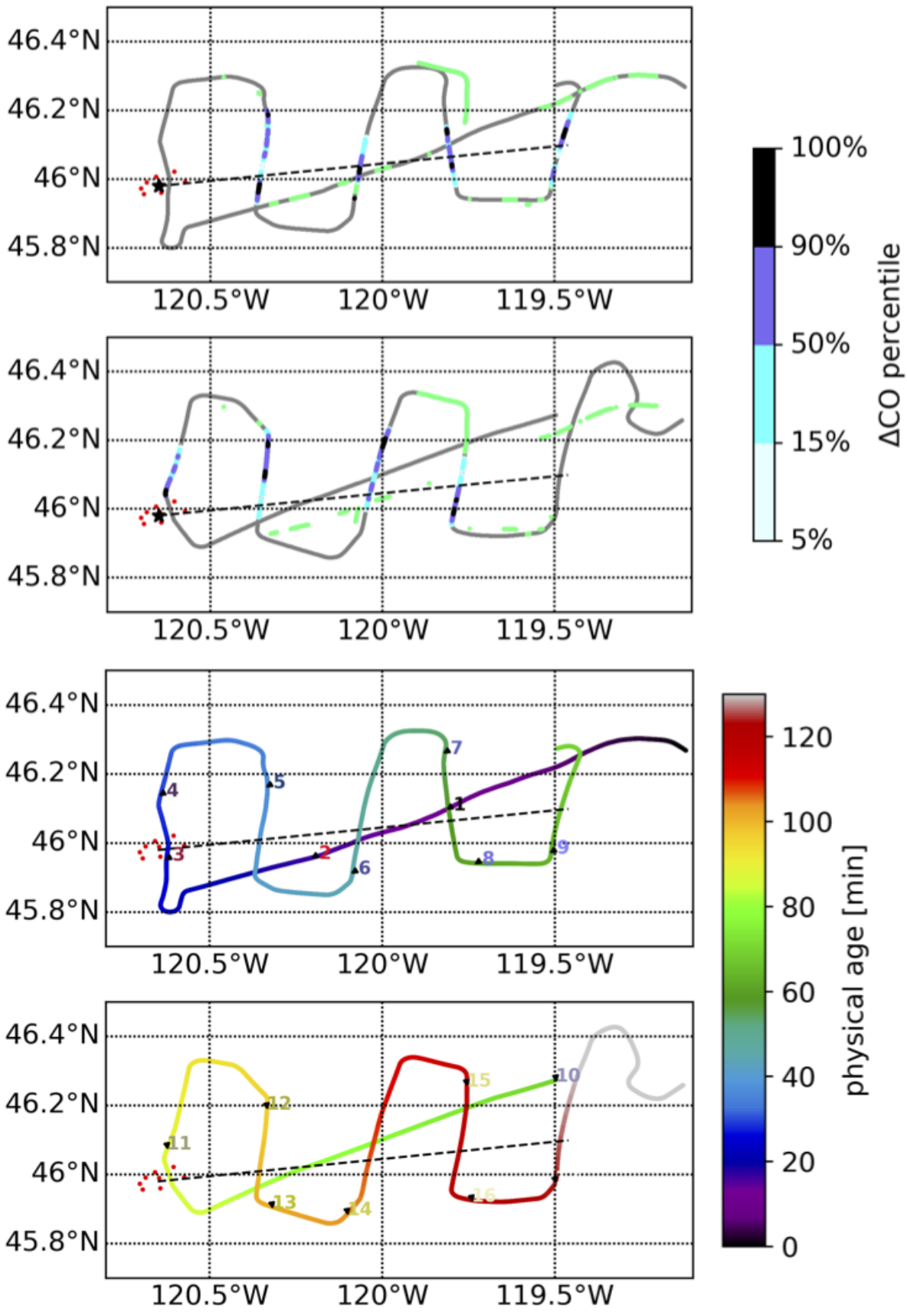
46.4°N
46.2°N
46°N
45.8°N
120.5°W
120°W
119.5°W
100%
90%
50%
15%
5%
ΔCO percentile
1
2
3
4
5
6
7
8
9
10
11
12
13
14
15
16
120
100
80
60
40
20
0
physical age [min]

Figure S2. The flight path for ‘726a’. Top two panels: the legs used in this study are colored by each ΔCO percentile bin used in the main text analyses. The green traces indicate the locations of the lowest 10% of CO, used to compute averaged backgrounds for this flight. Bottom two panels: the flight track colored by time since take-off in minutes. The numbers indicate the leg numbers as identified in the BBOP database. There were two complete flight paths for this day. The red dots are MODIS fire/thermal anomalies. The black star indicates the approximate center of the fire and the black dashed line indicates the approximate centerline of the plume, estimated by the number concentration.

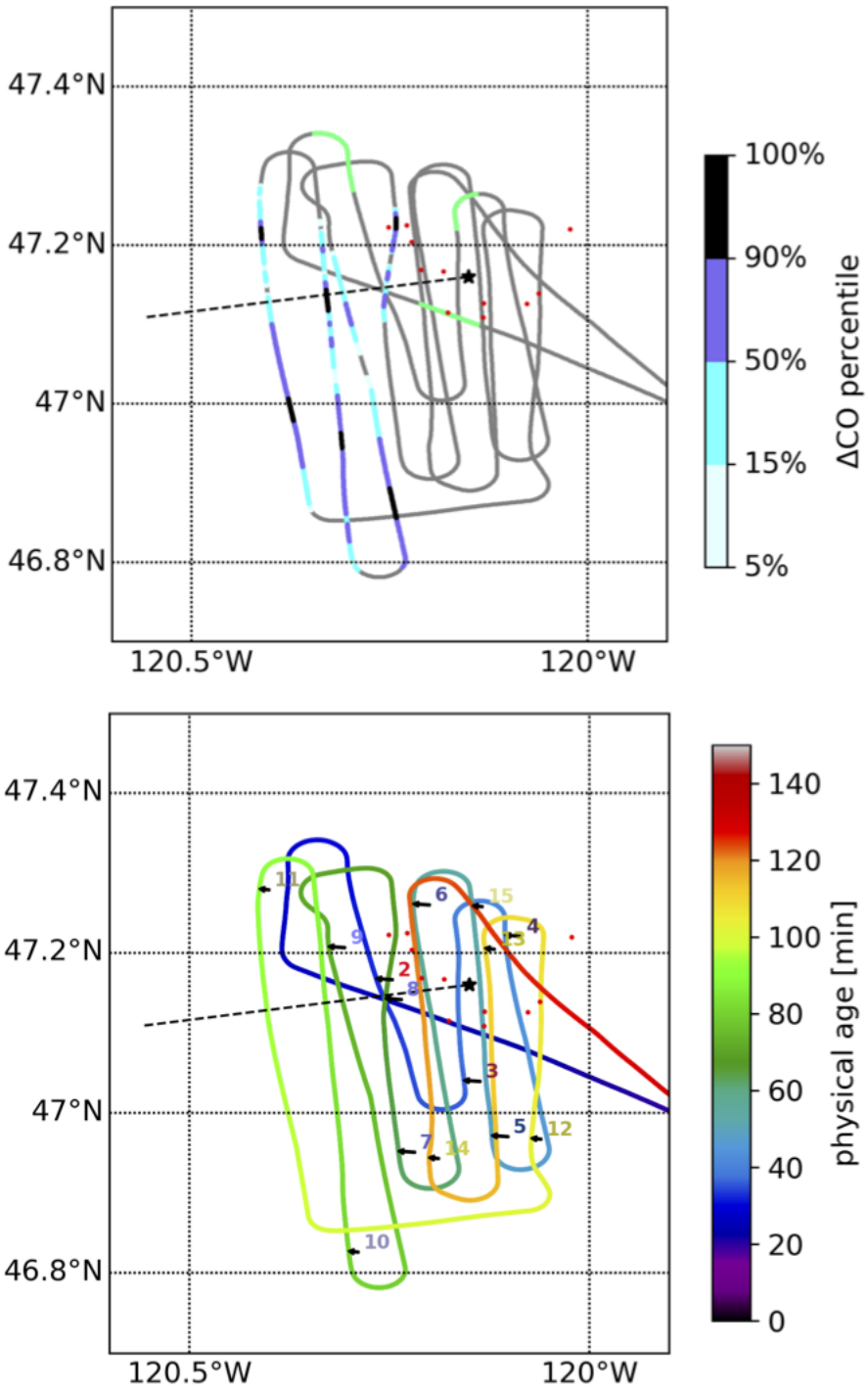

Figure S3. The flight path for '730a'. Top panel: the legs used in this study are colored by each ΔCO percentile bin used in the main text analyses. The green traces indicate the locations of the lowest 10% of CO, used to compute averaged backgrounds for this flight. Bottom panel: the flight track colored by time since take-off in minutes. The numbers indicate the leg numbers as

identified in the BBOP database. The red dots are MODIS fire/thermal anomalies. The black star indicates the approximate center of the fire and the black dashed line indicates the approximate centerline of the plume, estimated by the number concentration.

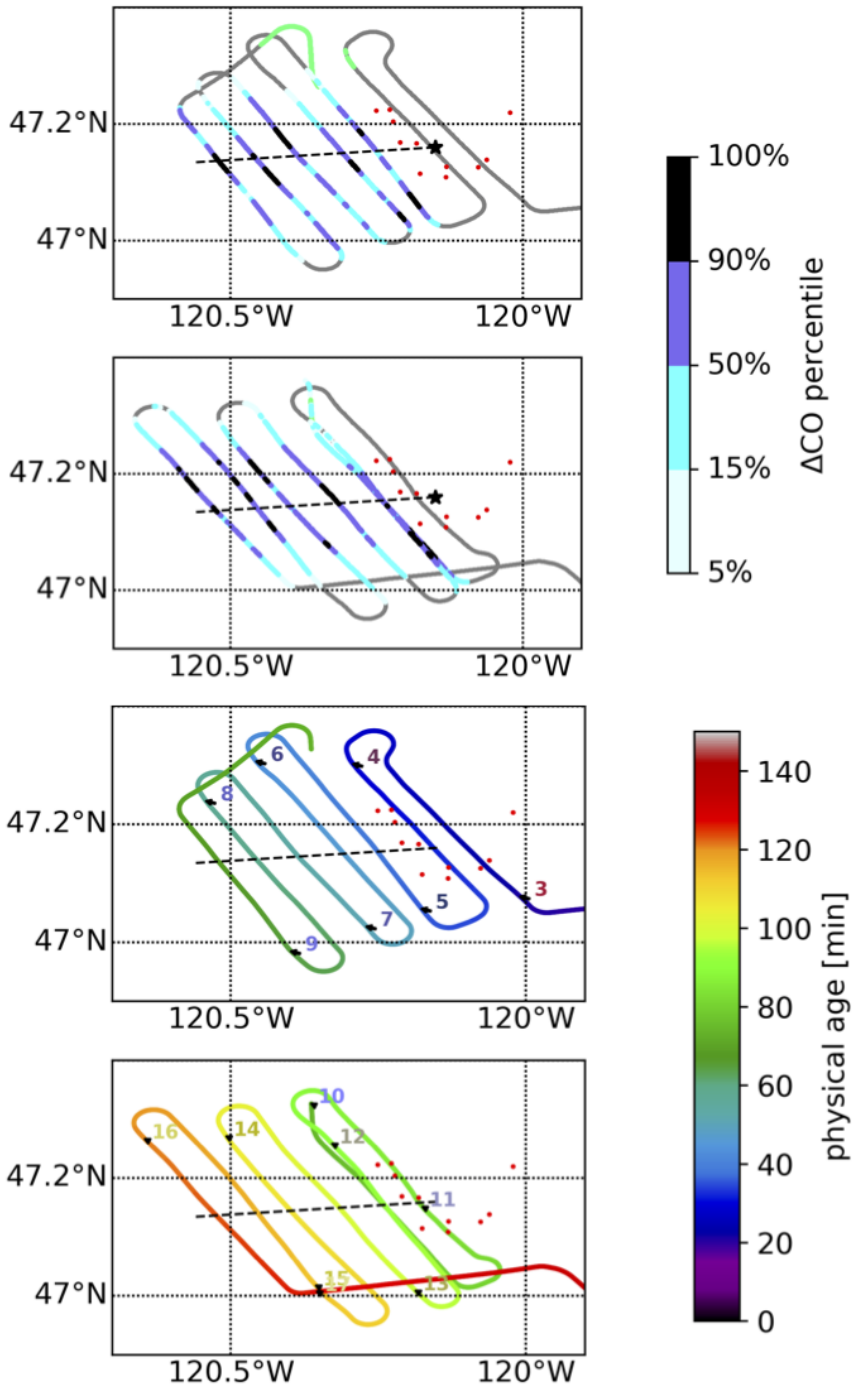

Figure S4. The flight path for '730b'. Top two panels: the legs used in this study are colored by each ΔCO percentile bin used in the main text analyses. The green traces indicate the locations of the lowest 10% of CO, used to compute averaged backgrounds for this flight. Bottom two panels: the flight track colored by time since take-off in minutes. The numbers indicate the leg numbers as identified in the BBOP database. There were two complete flight paths for this flight. The red dots are MODIS fire/thermal anomalies. The black star indicates the approximate center

of the fire and the black dashed line indicates the approximate centerline of the plume, estimated by the number concentration.

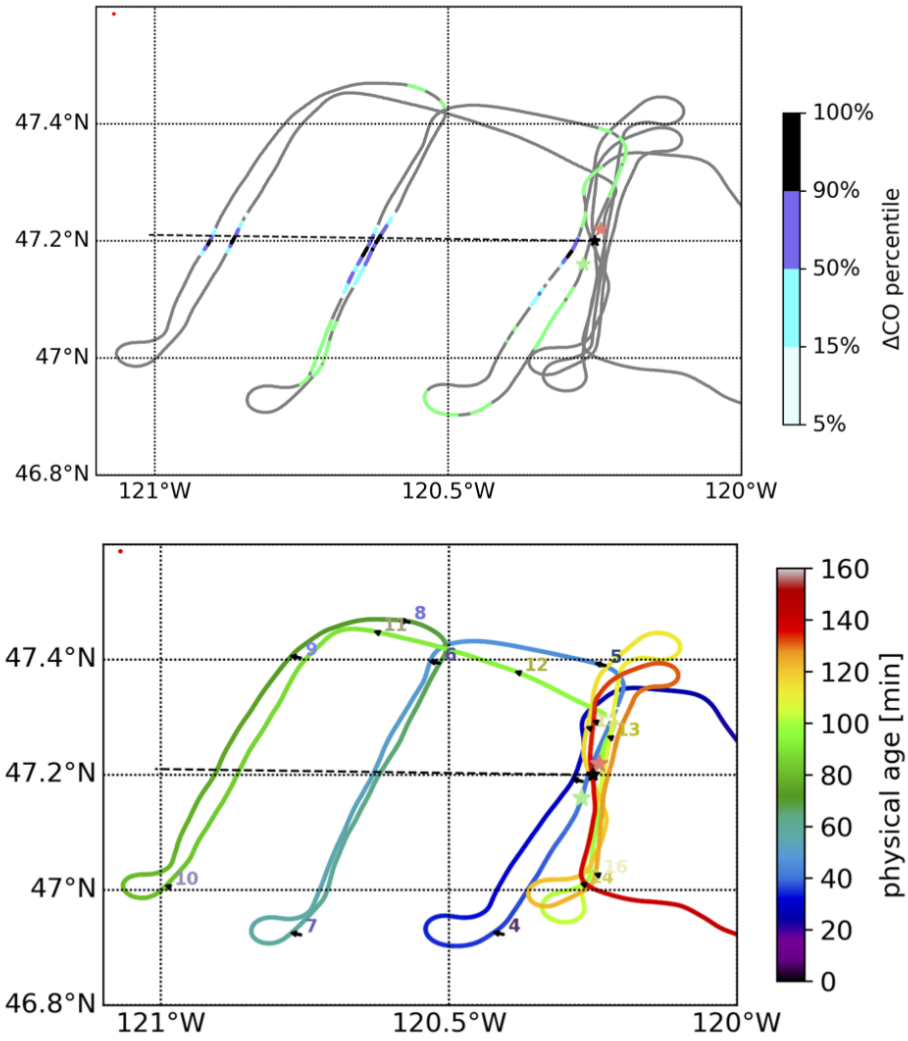

Figure S5. The flight path for '809a'. Top panel: the legs used in this study are colored by each ΔCO percentile bin used in the main text analyses. The green traces indicate the locations of the lowest 10% of CO, used to compute averaged backgrounds for this flight. Bottom panel: the flight track colored by time since take-off in minutes. The numbers indicate the leg numbers as identified in the BBOP database. The Worldview image for this day had clouds over the fire location at the time of the satellite passover. Thus we estimate a fire center using Worldview and MODIS images for this region on the previous day (8-08-2013) (light green star) and the following day (8-10-2013) (salmon-colored star). The black star indicates our estimated center of the fire on 8-09-2013 and the black dashed line indicates the approximate centerline of the plume, estimated by the number concentration.

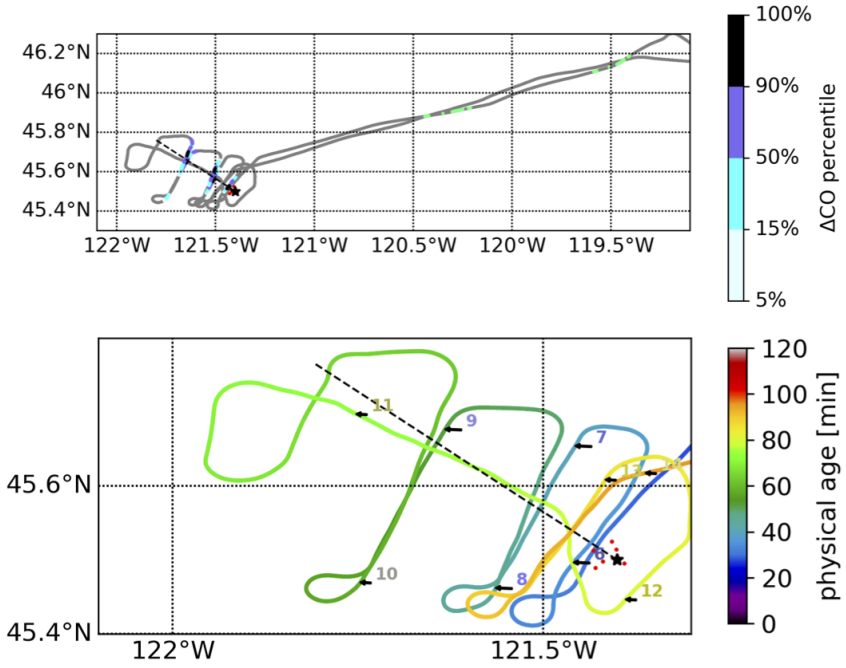

Figure S6. The flight path for '821b'. Top panel: the legs used in this study are colored by each ΔCO percentile bin used in the main text analyses. The green traces indicate the locations of the lowest 10% of CO, used to compute averaged backgrounds for this flight. Bottom panel: the flight track colored by time since take-off in minutes. The numbers indicate the leg numbers as identified in the BBOP database. The red dots are MODIS fire/thermal anomalies. The black star indicates the approximate center of the fire and the black dashed line indicates the approximate centerline of the plume, estimated by the number concentration.

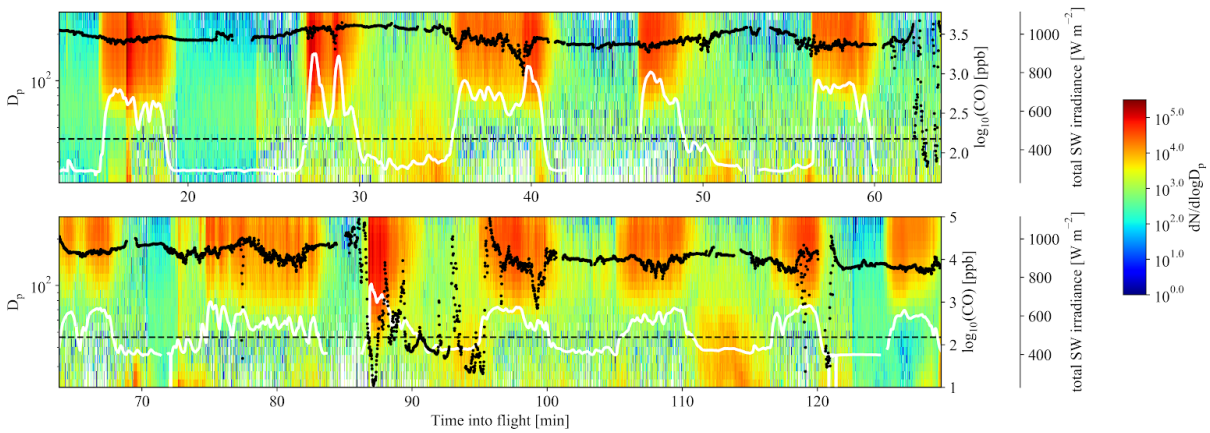

Figure S7. Number size distribution data, $dN/dlogD_p$, from the FIMS; CO (white solid line); and total short wave (SW) irradiance (black dots) data for the '726a' flight. The bottom panel is a continuation in time from the top panel. The dotted dashed line indicates CO=150 ppb, our cutoff for in-plume/out-of-plume. The second set of Lagrangian transects for this flight start at the plume at approximately 86 minutes into the flight.

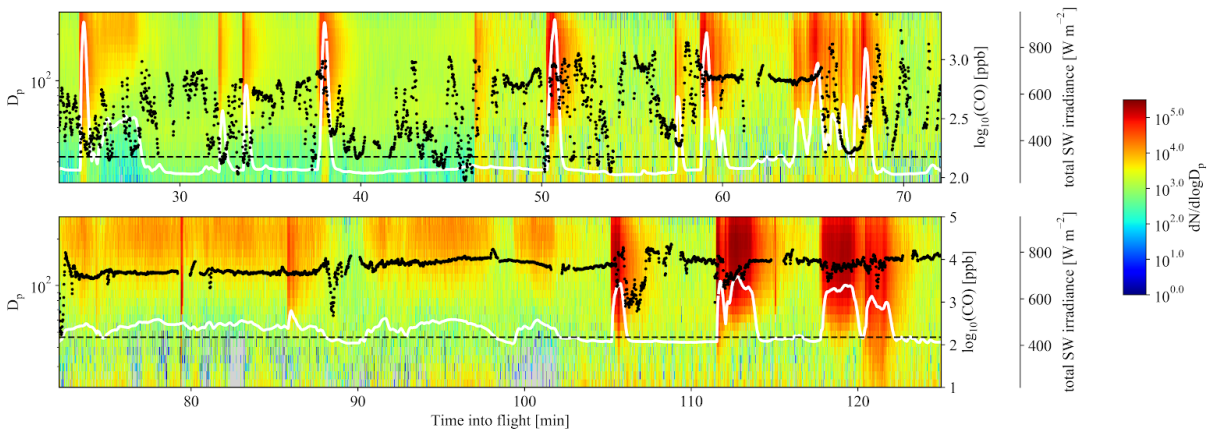

Figure S8. Number size distribution data, $dN/dlogD_p$, from the FIMS; CO (white solid line); and total short wave (SW) irradiance (black dots) data for the '730a' flight. The bottom panel is a continuation in time from the top panel. The dotted dashed line indicates CO=150 ppb, our cutoff for in-plume/out-of-plume.

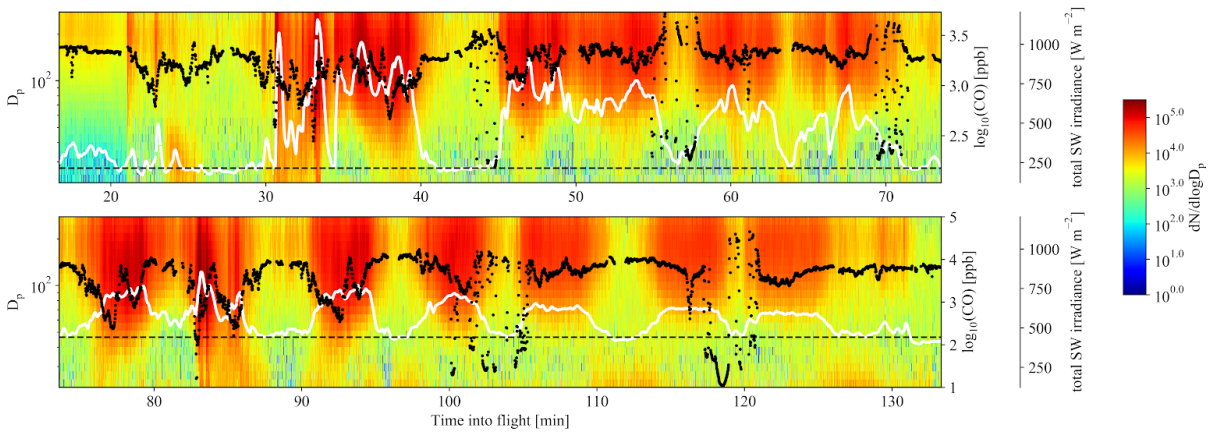

Figure S9. Number size distribution data, $dN/dlogD_p$, from the FIMS; CO (white solid line); and total short wave (SW) irradiance (black dots) data for the '730b' flight. The bottom panel is a continuation in time from the top panel. The dotted dashed line indicates CO=150 ppb, our cutoff for in-plume/out-of-plume. For this figure, the top panel contains all of the first Lagrangian set of flight transects, and the bottom panel contains all of the second Lagrangian set of flight transects.

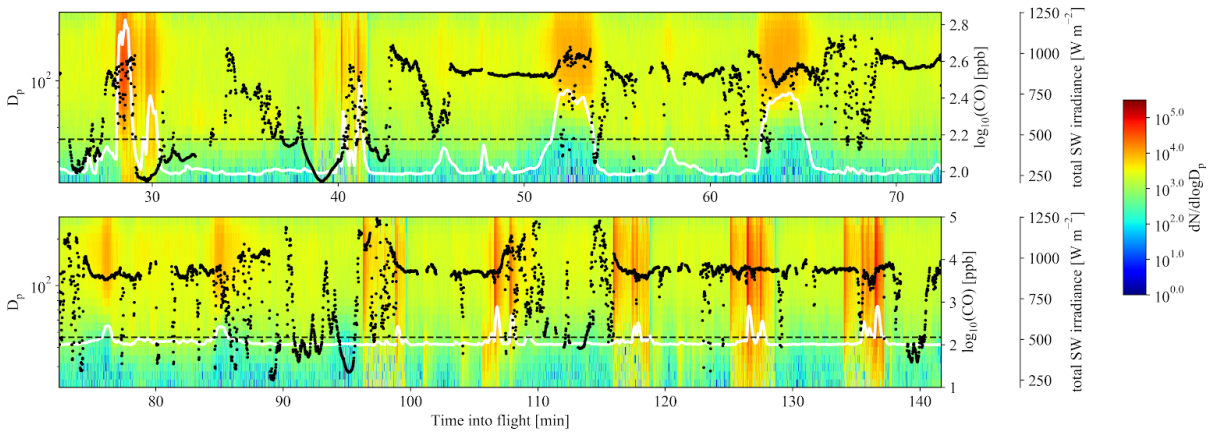

Figure S10. Number size distribution data, $dN/dlogD_p$, from the FIMS; CO (white solid line); and total short wave (SW) irradiance (black dots) data for the '809a' flight. The bottom panel is a continuation in time from the top panel. The dotted dashed line indicates CO=150 ppb, our cutoff for in-plume/out-of-plume.

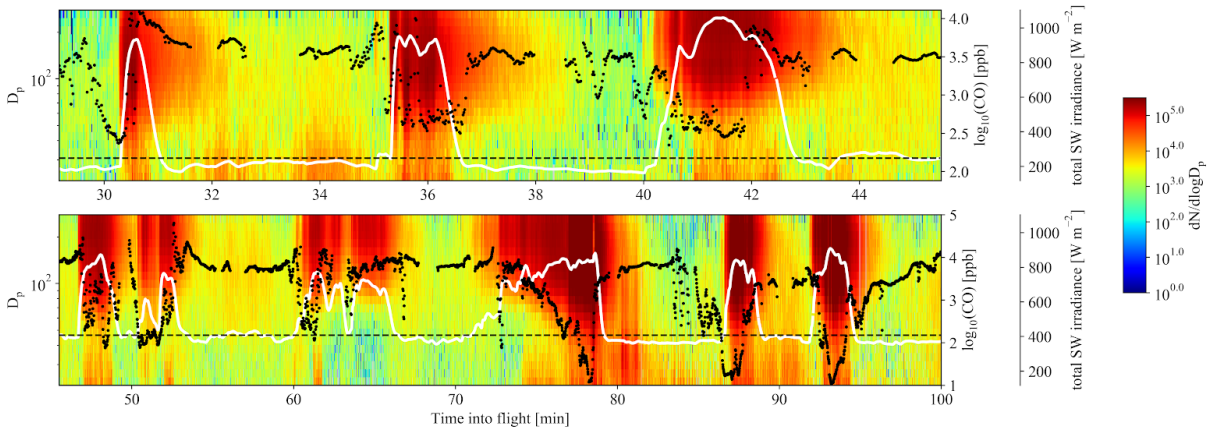

Figure S11. Number size distribution data, dN/dlogD_p, from the FIMS; CO (white solid line); and total short wave (SW) irradiance (black dots) data for the '821b' flight. The bottom panel is a continuation in time from the top panel. The dotted dashed line indicates CO=150 ppb, our cutoff for in-plume/out-of-plume.

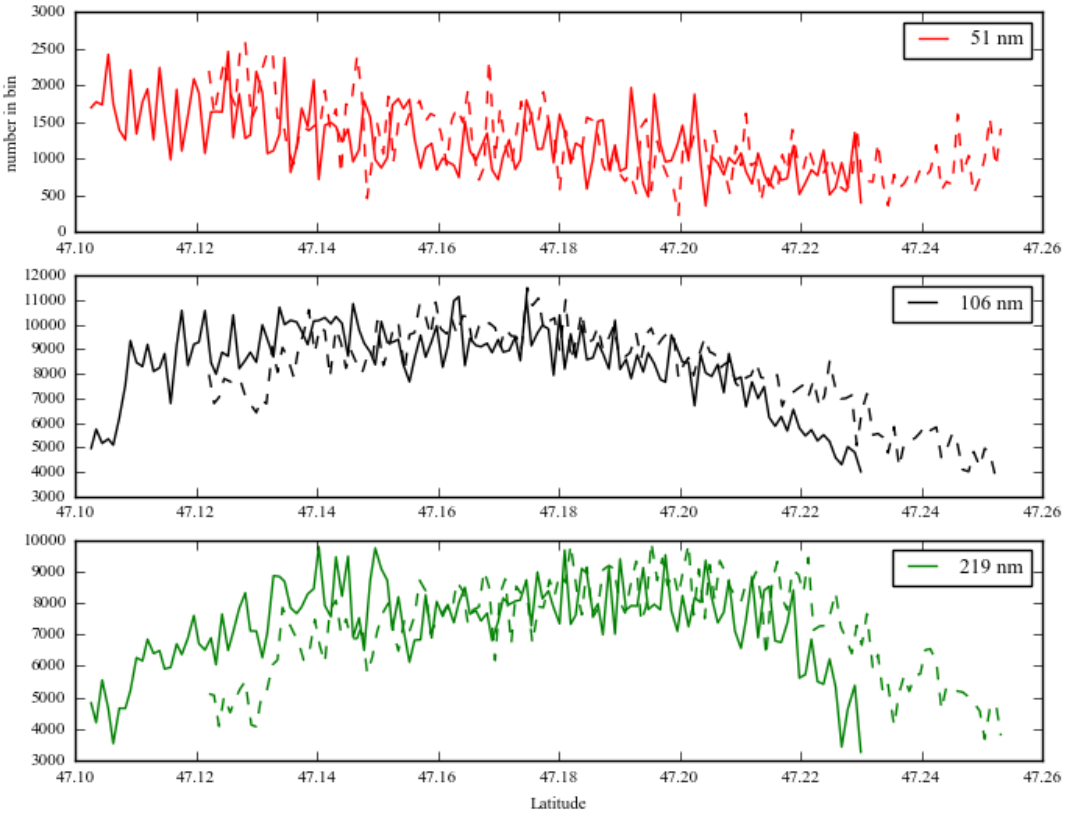

Figure S12. FIMS data for '809a' for the two legs that ~overlap (Figure S5) for the 51, 106, and 219 nm size bins. The solid line is from the plane flying north to south (right to left in this figure) and the dashed line is from the plane flying south to north (left to right in this figure). In the absence of FIMS measurement artifacts, we expect these two lines to roughly match each other. Each y axis is in units of number in bin.

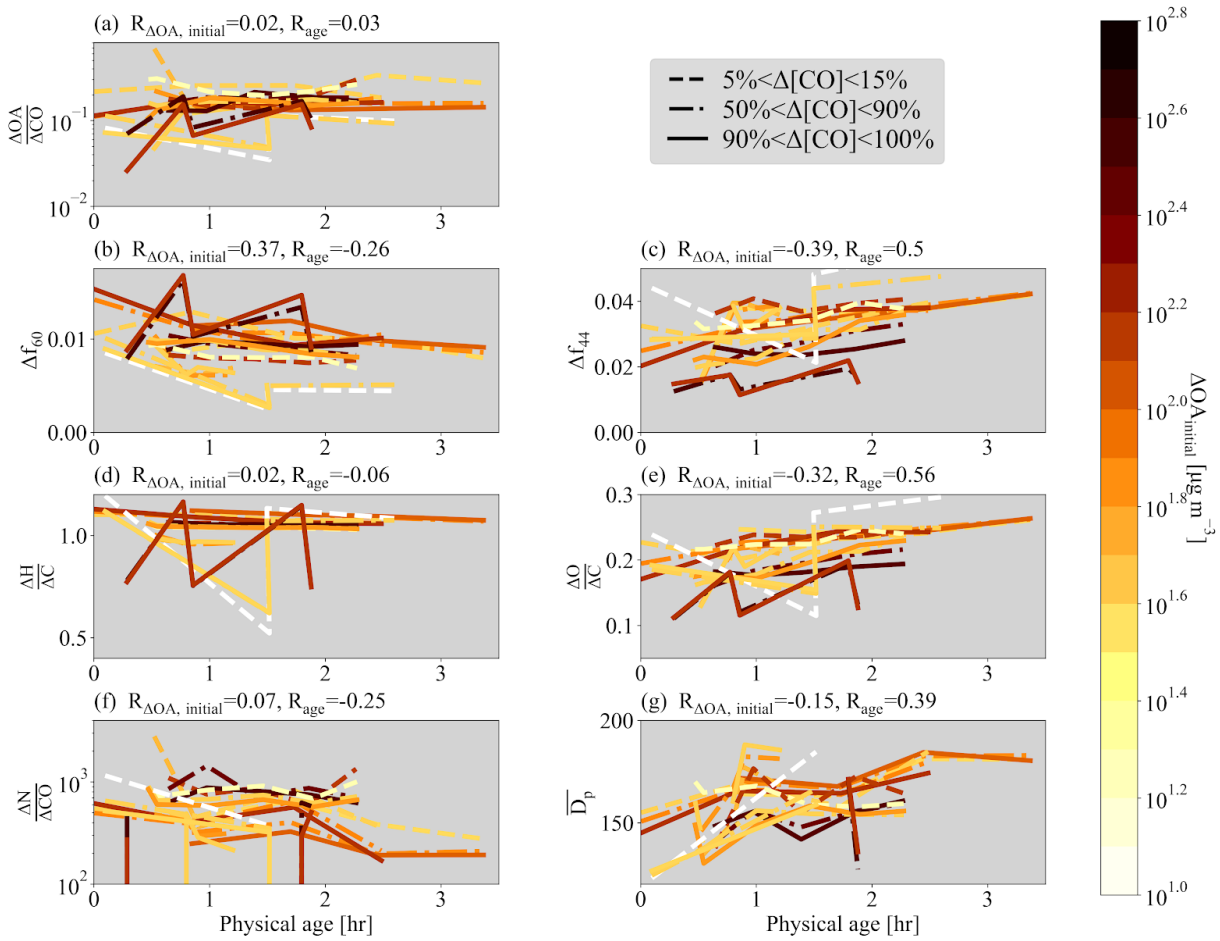

Figure S13. Same as Figure 2 but using only the first 50% of data for each leg of the FIMS and CO data for panels f-g.

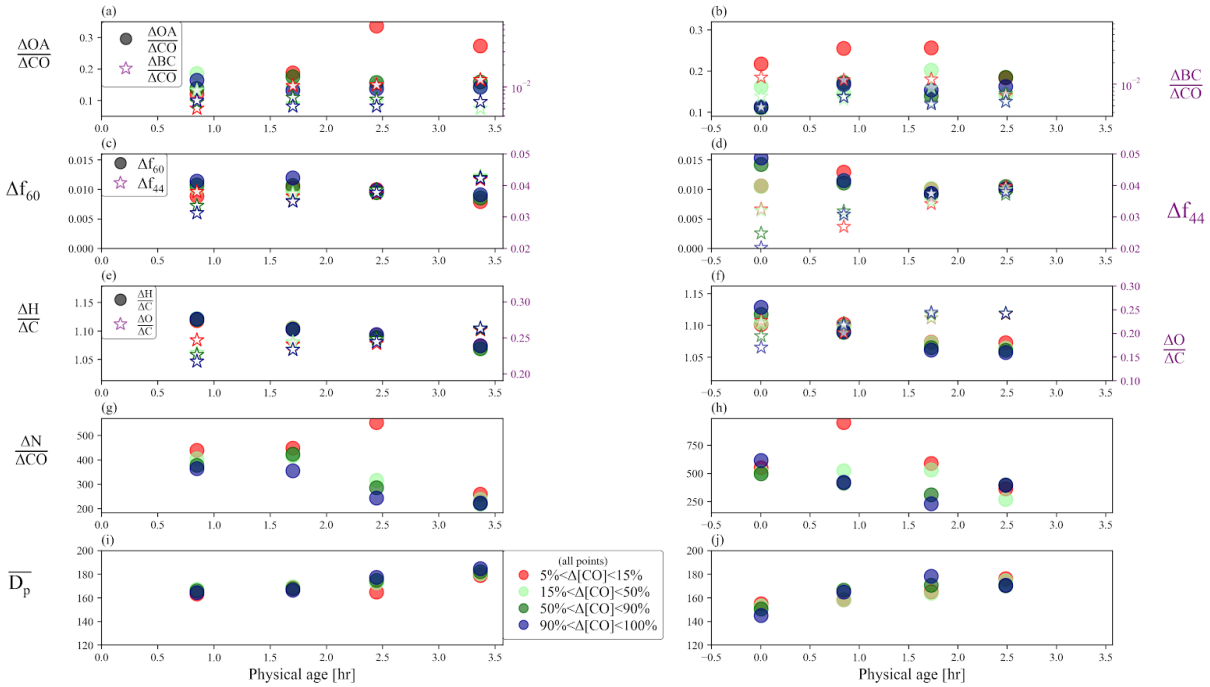

Figure S14. Aerosol properties for the first set (left-hand column) and second set (right-hand column) of pseudo-Lagrangian transects from flight '726a' (a-b) ΔOA/ΔCO (right y-axis) and ΔBC/ΔCO (left y-axis), (c-d) Δf_{60} (right y-axis) and Δf_{44} (left y-axis), (e-f) ΔH/ΔC (right y-axis) and ΔO/ΔC (left y-axis), (g-h) ΔN/ΔCO, and (i-j) $\overline{D_p}$ against physical age. For each transect, the data is divided into edge (the lowest 5-15% of ΔCO data; red points), core (90-100% of ΔCO data; blue points), and intermediate regions (15-50% and 50-90% of ΔCO data; light green and dark green points). ΔBC/ΔCO is shown in log scale and the x-axis for the right-hand column has been shifted backwards to improve clarity. Note that the left-hand and right-hand columns do not always have the same y-axis limits.

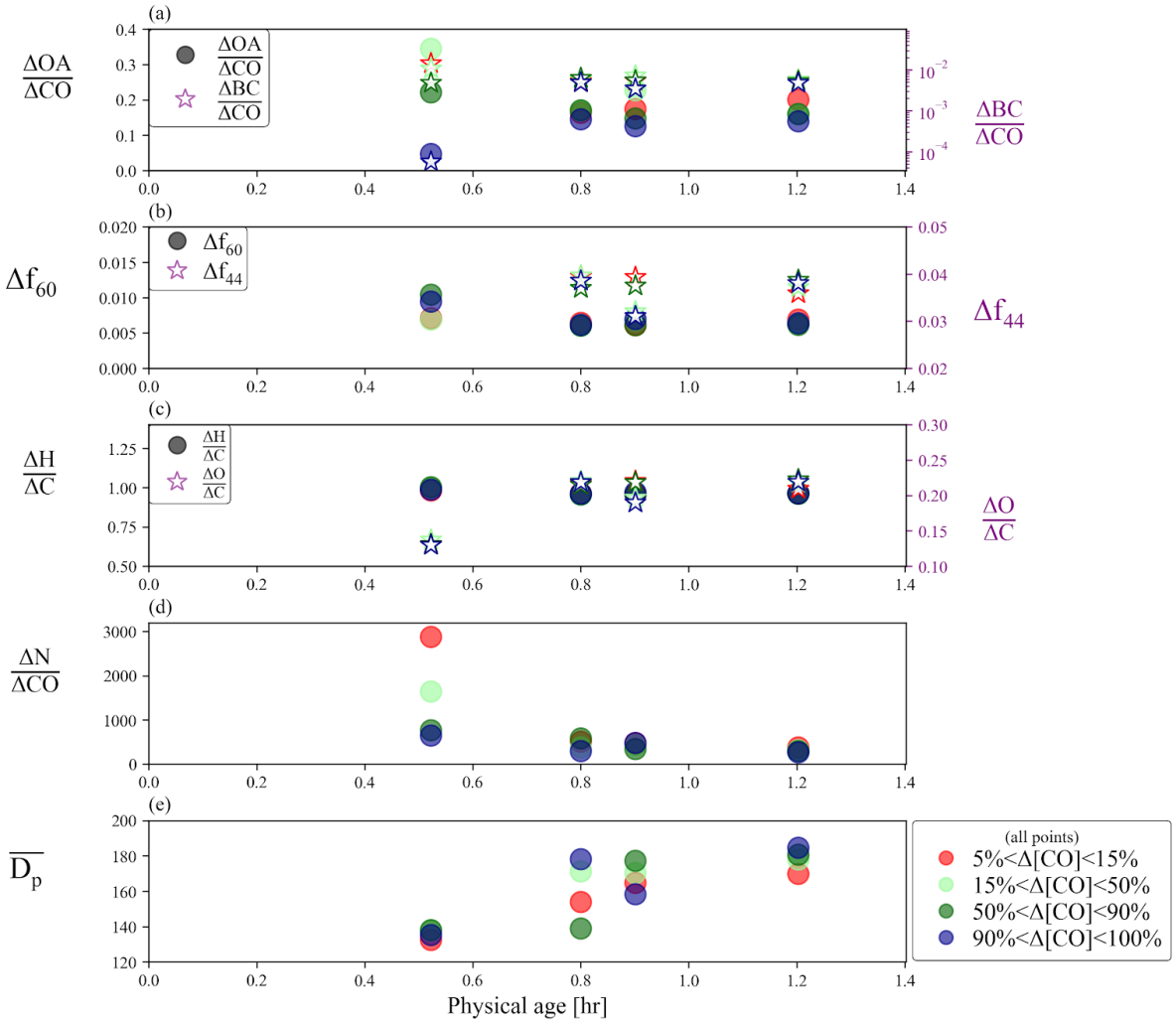

Figure S15. Aerosol properties for the set of pseudo-Lagrangian transects from flight '730a' (a) ΔOA/ΔCO (right y-axis) and ΔBC/ΔCO (left y-axis), (b) Δf_{60} (right y-axis) and Δf_{44} (left y-axis), (c) ΔH/ΔC (right y-axis) and ΔO/ΔC (left y-axis), (d) ΔN/ΔCO, and (e) $\overline{D_p}$ against physical age. For each transect, the data is divided into edge (the lowest 5-15% of ΔCO data; red points), core (90-100% of ΔCO data; blue points), and intermediate regions (15-50% and 50-90% of ΔCO data; light green and dark green points). ΔBC/ΔCO is shown in log scale to improve clarity.

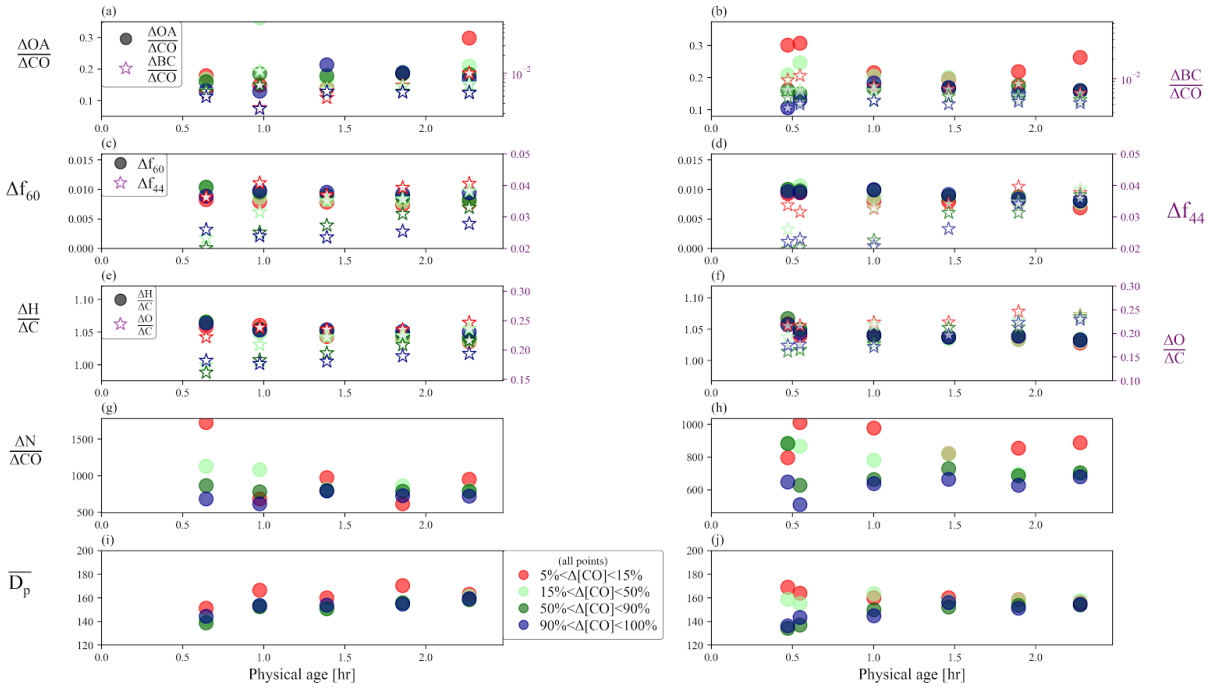

Figure S16. Aerosol properties for the first set (left-hand column) and second set (right-hand column) of pseudo-Lagrangian transects from flight '730b' (a-b) ΔOA/ΔCO (right y-axis) and ΔBC/ΔCO (left y-axis), (c-d) Δf_{60} (right y-axis) and Δf_{44} (left y-axis), (e-f) ΔH/ΔC (right y-axis) and ΔO/ΔC (left y-axis), (g-h) ΔN/ΔCO, and (i-j) $\overline{D_p}$ against physical age. For each transect, the data is divided into edge (the lowest 5-15% of ΔCO data; red points), core (90-100% of ΔCO data; blue points), and intermediate regions (15-50% and 50-90% of ΔCO data; light green and dark green points). ΔBC/ΔCO is shown in log scale to improve clarity. Note that the left-hand and right-hand columns do not always have the same y-axis limits.

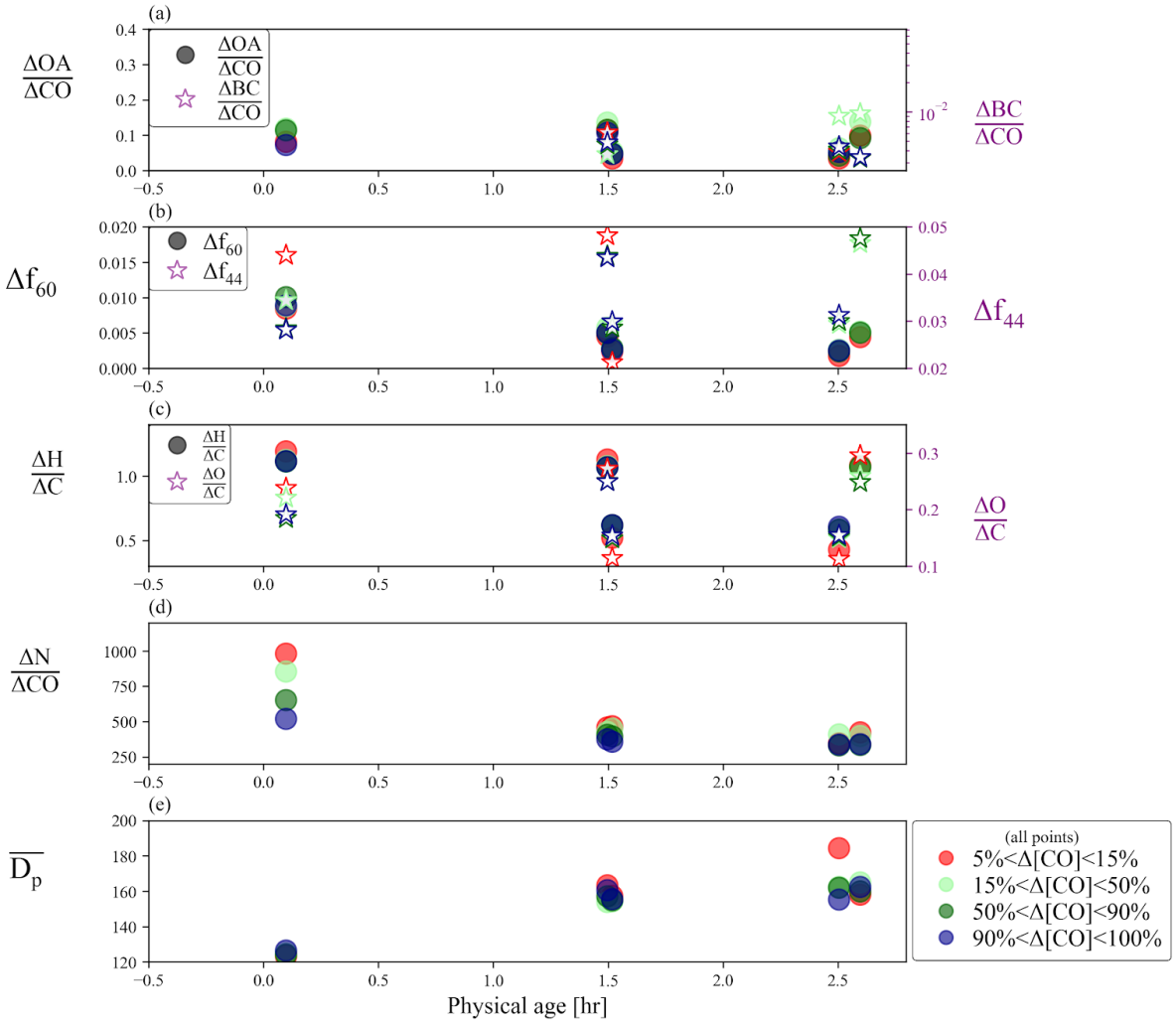

Figure S17. Aerosol properties for the set of pseudo-Lagrangian transects from flight '809a' (a) ΔOA/ΔCO (right y-axis) and ΔBC/ΔCO (left y-axis), (b) Δf_{60} (right y-axis) and Δf_{44} (left y-axis), (c) ΔH/ΔC (right y-axis) and ΔO/ΔC (left y-axis), (d) ΔN/ΔCO, and (e) $\overline{D_p}$ against physical age. For each transect, the data is divided into edge (the lowest 5-15% of ΔCO data; red points), core (90-100% of ΔCO data; blue points), and intermediate regions (15-50% and 50-90% of ΔCO data; light green and dark green points). ΔBC/ΔCO is shown in log scale and the x-axis for the right-hand column has been shifted backwards to improve clarity.

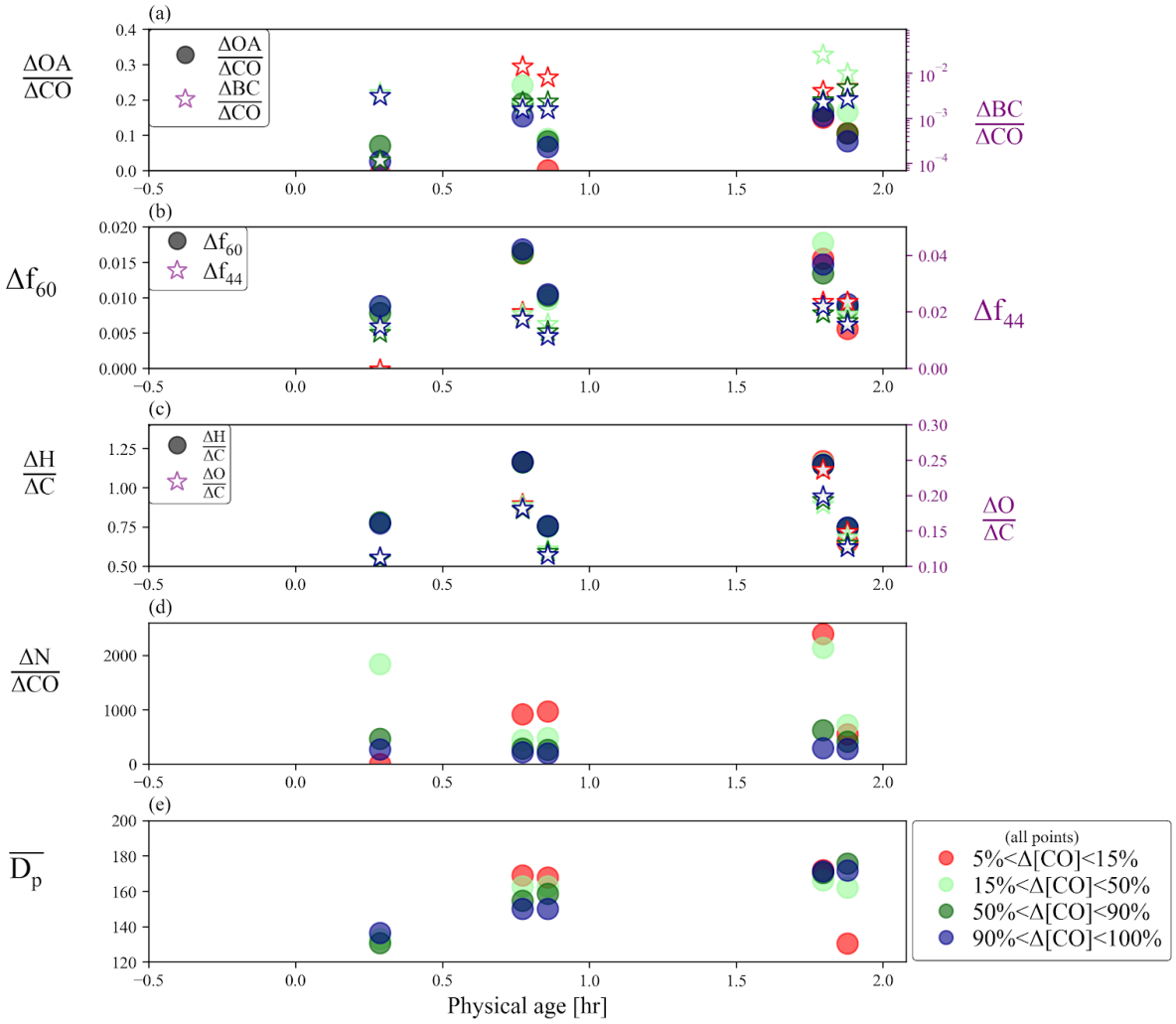

Figure S18. Aerosol properties for the set of pseudo-Lagrangian transects from flight '821b' (a) ΔOA/ΔCO (right y-axis) and ΔBC/ΔCO (left y-axis), (b) Δf_{60} (right y-axis) and Δf_{44} (left y-axis), (c) ΔH/ΔC (right y-axis) and ΔO/ΔC (left y-axis), (d) ΔN/ΔCO, and (e) $\overline{D_p}$ against physical age. For each transect, the data is divided into edge (the lowest 5-15% of ΔCO data; red points), core (90-100% of ΔCO data; blue points), and intermediate regions (15-50% and 50-90% of ΔCO data; light green and dark green points). ΔBC/ΔCO is shown in log scale and the x-axis for the right-hand column has been shifted backwards to improve clarity.

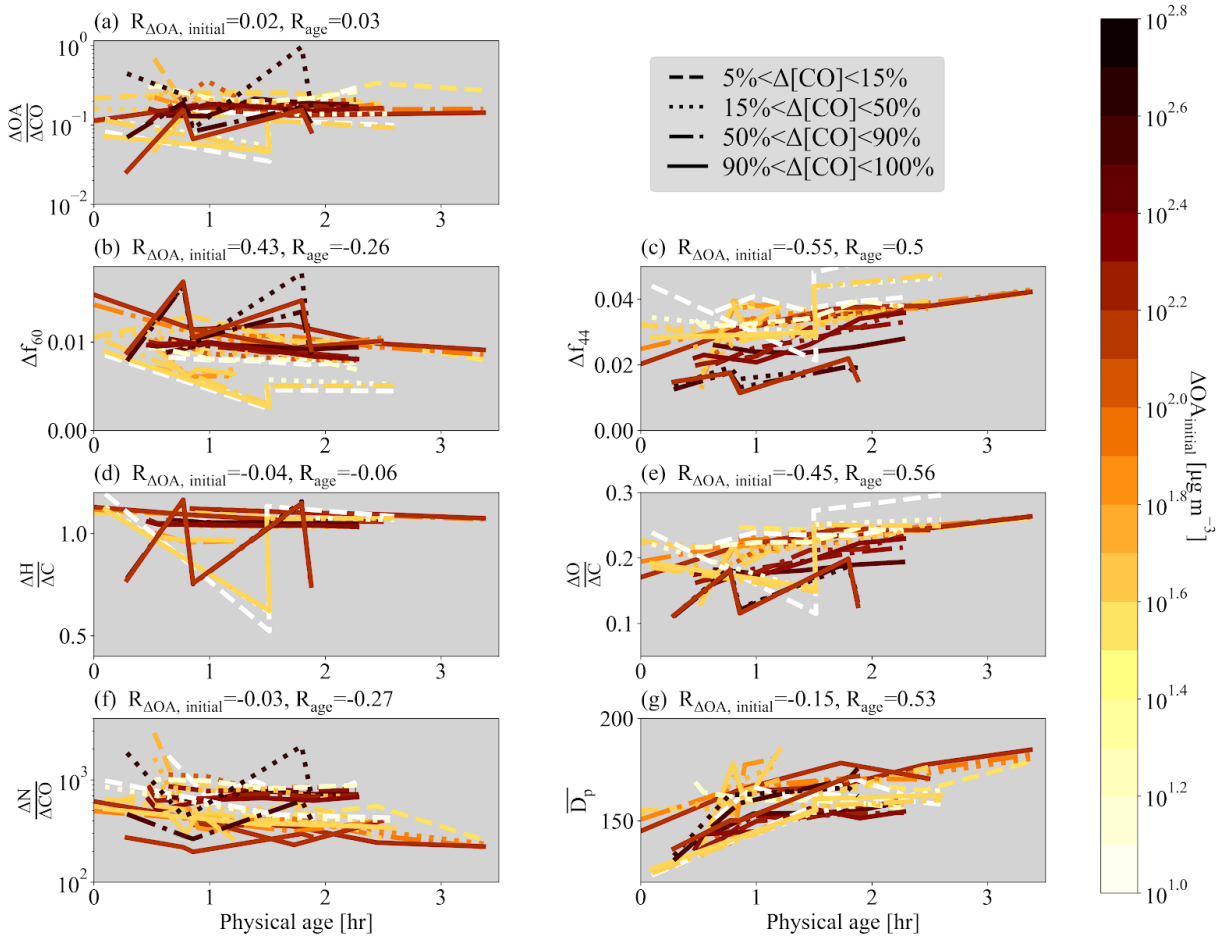

Figure S19. Various normalized parameters as a function of age for the 7 sets of pseudo-Lagrangian transects. Separate lines are shown for the edges (lowest 5-15% of ΔCO; dashed lines) cores (highest 90-100% of ΔCO; solid lines), and intermediate regions (15-50% and 50-90%; dotted and dashed-dot lines). (a) ΔOA/ΔCO, (b) Δf_{60}, (c) Δf_{44}, (d) ΔH/ΔC, (e) ΔO/ΔC, (f) $\Delta N_{40\text{-}262\ nm}/\Delta CO$, and (g) $\overline{D_p}$ between 40-262 nm against physical age for all flights, colored by $\Delta OA_{initial}$. Some flights have missing data. Also provided is the Spearman correlation coefficient, R, between each variable and $\Delta OA_{initial}$ and physical age for each variable. Note that panels (a) and (f) have a log y-axis. ~~Note that panels (a), (d), and (g) have a log y-axis.~~

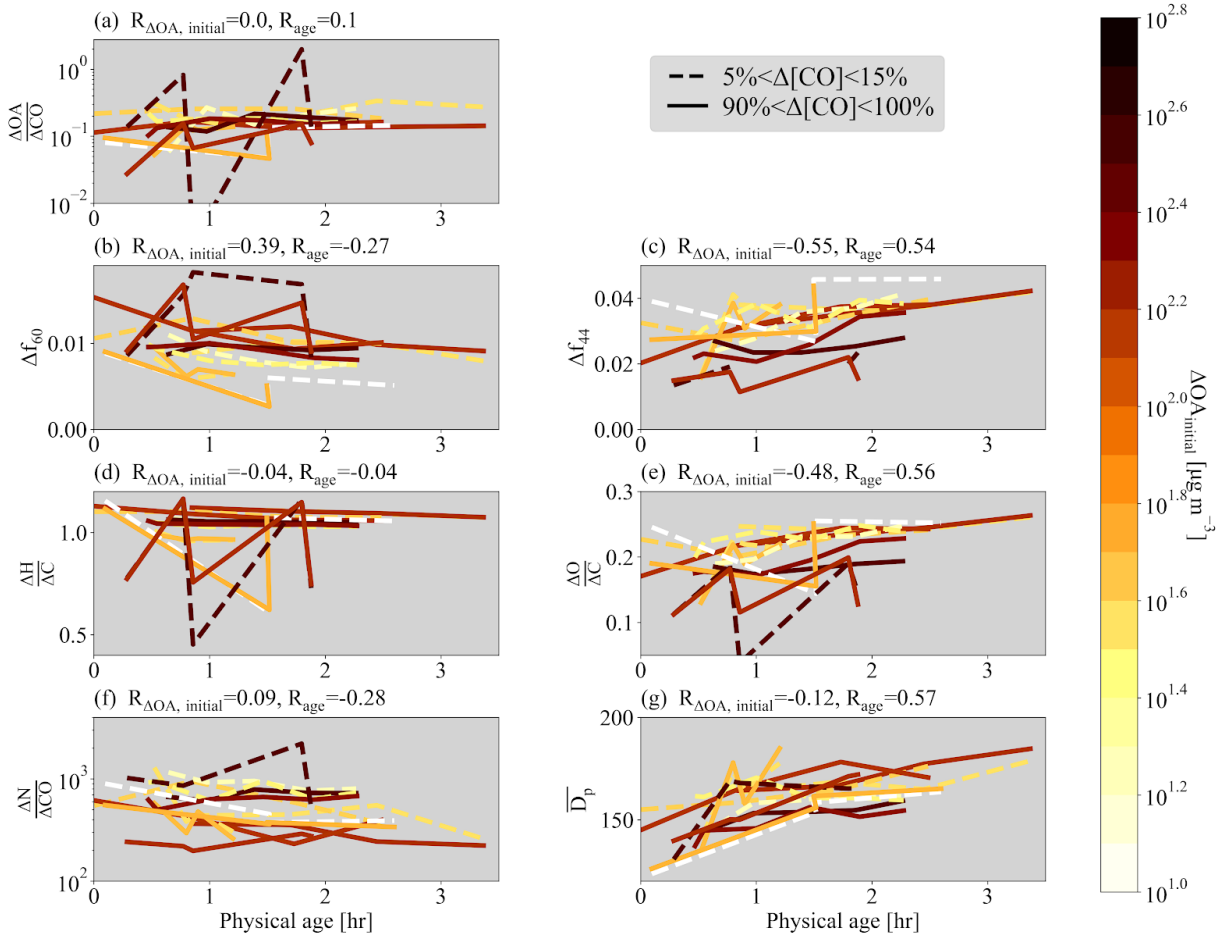

Figure S20. Various normalized parameters as a function of age for the 7 sets of pseudo-Lagrangian transects. Separate lines are shown for the edges (lowest 5-15% of ΔCO; dashed lines) and cores (highest 90-100% of ΔCO; solid lines). (a) ΔOA/ΔCO, (b) Δf_{60}, (c) Δf_{44}, (d) ΔH/ΔC, (e) ΔO/ΔC, (f) $\Delta N_{40\text{-}262\ nm}/\Delta CO$, and (g) $\overline{D_p}$ between 40-262 nm against physical age for all flights, colored by $\Delta OA_{initial}$. Some flights have missing data. Also provided is the Spearman correlation coefficient, R, between each variable and $\Delta OA_{initial}$ and physical age for each variable. Note that panels (a) and (f) have a log y-axis. ~~Note that panels (a), (d), and (g) have a log y-axis.~~ This figure is identical to Figure 2 but uses an in-plume CO cutoff of 200 ppb.

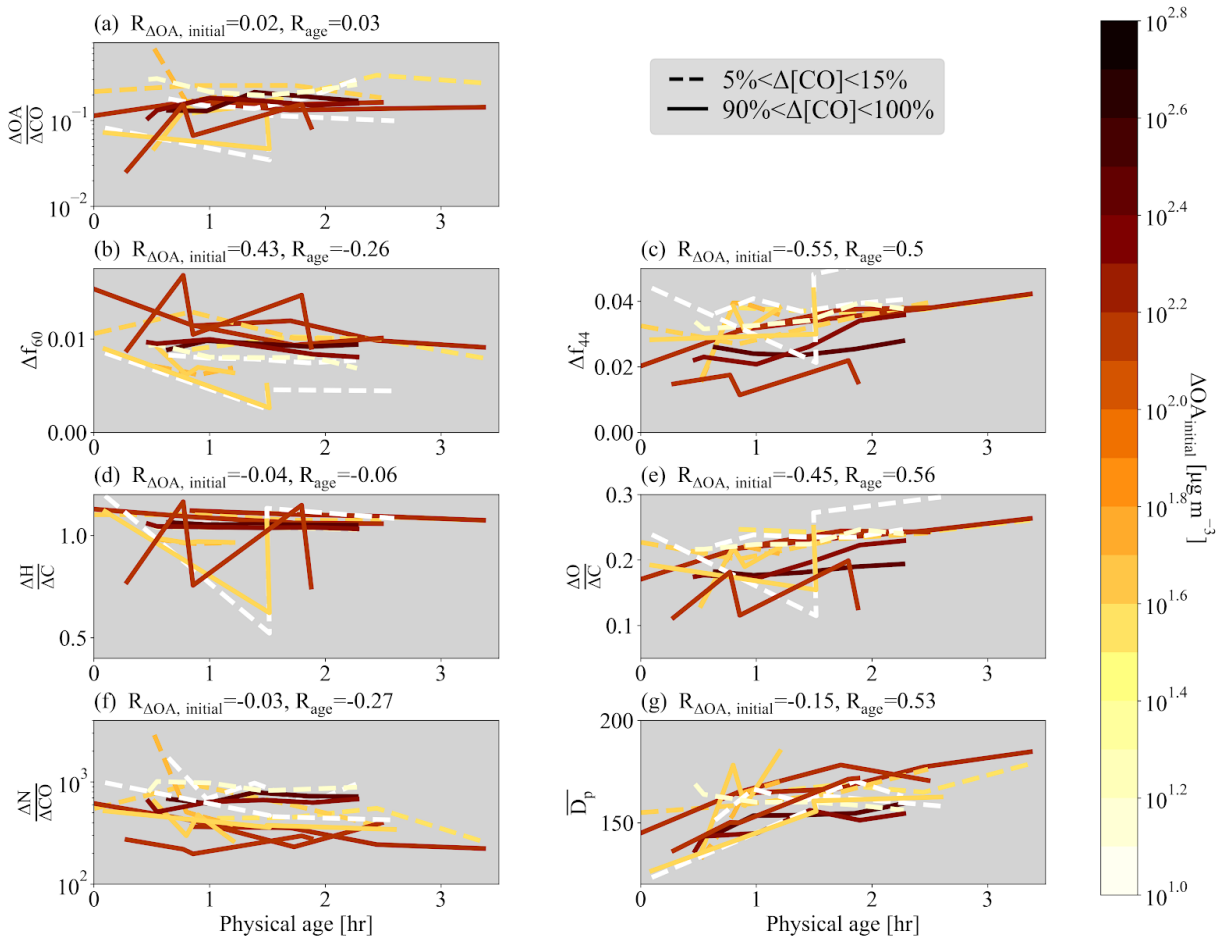

Figure S21. Various normalized parameters as a function of age for the 7 sets of pseudo-Lagrangian transects. Separate lines are shown for the edges (lowest 5-25% of ΔCO; dashed lines) and cores (highest 75-100% of ΔCO; solid lines). (a) ΔOA/ΔCO, (b) Δf_{60}, (c) Δf_{44}, (d) ΔH/ΔC, (e) ΔO/ΔC, (f) $\Delta N_{40\text{-}262\ nm}/\Delta CO$, and (g) $\overline{D_p}$ between 40-262 nm against physical age for all flights, colored by $\Delta OA_{initial}$. Some flights have missing data. Also provided is the Spearman correlation coefficient, R, between each variable and $\Delta OA_{initial}$ and physical age for each variable. Note that panels (a) and (f) have a log y-axis. ~~Note that panels (a), (d), and (g) have a log y-axis.~~ This figure is identical to Figure 2 but uses different ΔCO percentile widths.

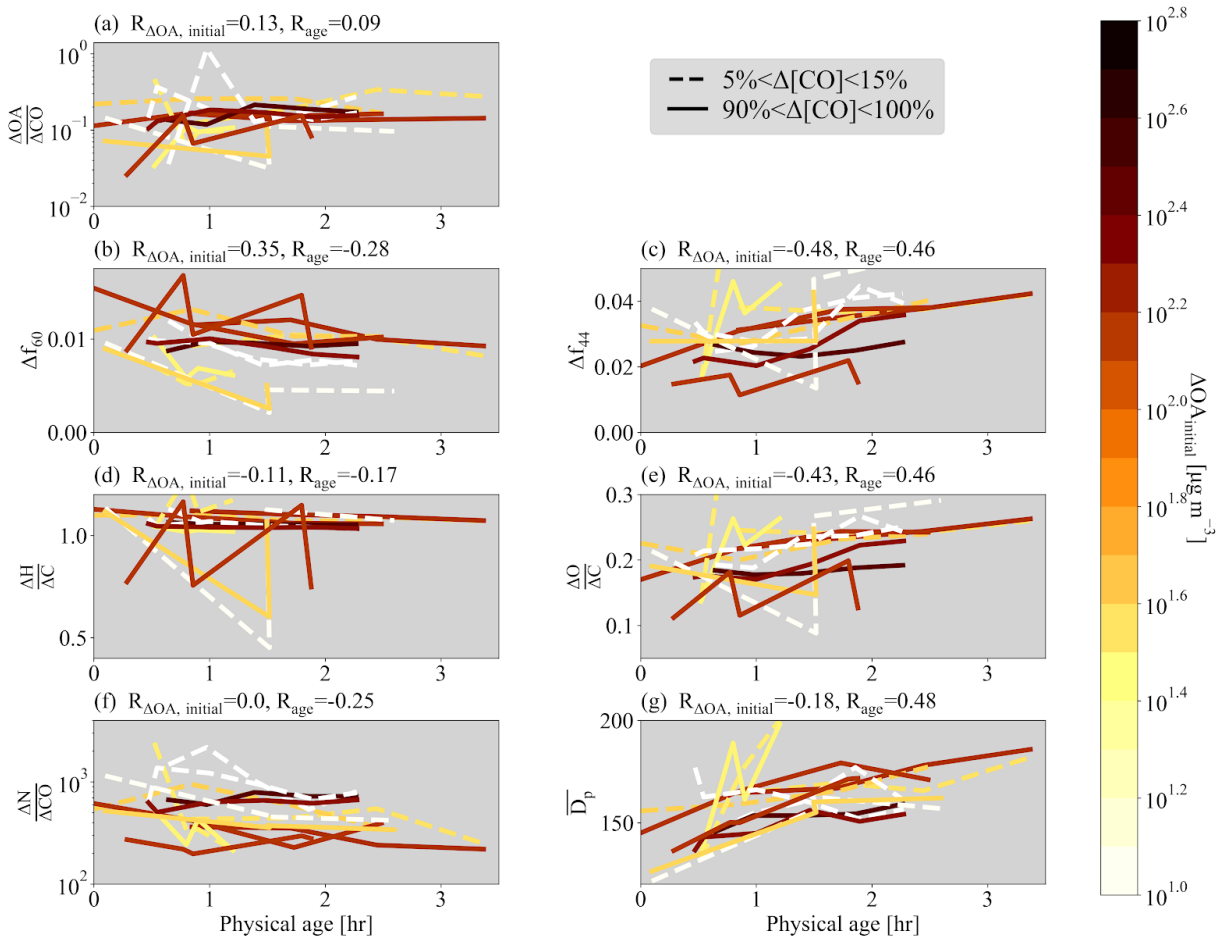

Figure S22. Various normalized parameters as a function of age for the 7 sets of pseudo-Lagrangian transects. Separate lines are shown for the edges (lowest 5-15% of ΔCO; dashed lines) and cores (highest 90-100% of ΔCO; solid lines). (a) ΔOA/ΔCO, (b) Δf_{60}, (c) Δf_{44}, (d) ΔH/ΔC, (e) ΔO/ΔC, (f) $\Delta N_{40\text{-}262\ nm}/\Delta CO$, and (g) $\overline{D_p}$ between 40-262 nm against physical age for all flights, colored by $\Delta OA_{initial}$. Some flights have missing data. Also provided is the Spearman correlation coefficient, R, between each variable and $\Delta OA_{initial}$ and physical age for each variable. Note that panels (a) and (f) have a log y-axis. ~~Note that panels (a), (d), and (g) have a log y-axis.~~ This figure is identical to Figure 2 except that it uses the location of the lowest 25% of CO data to determine the background concentrations of each species.

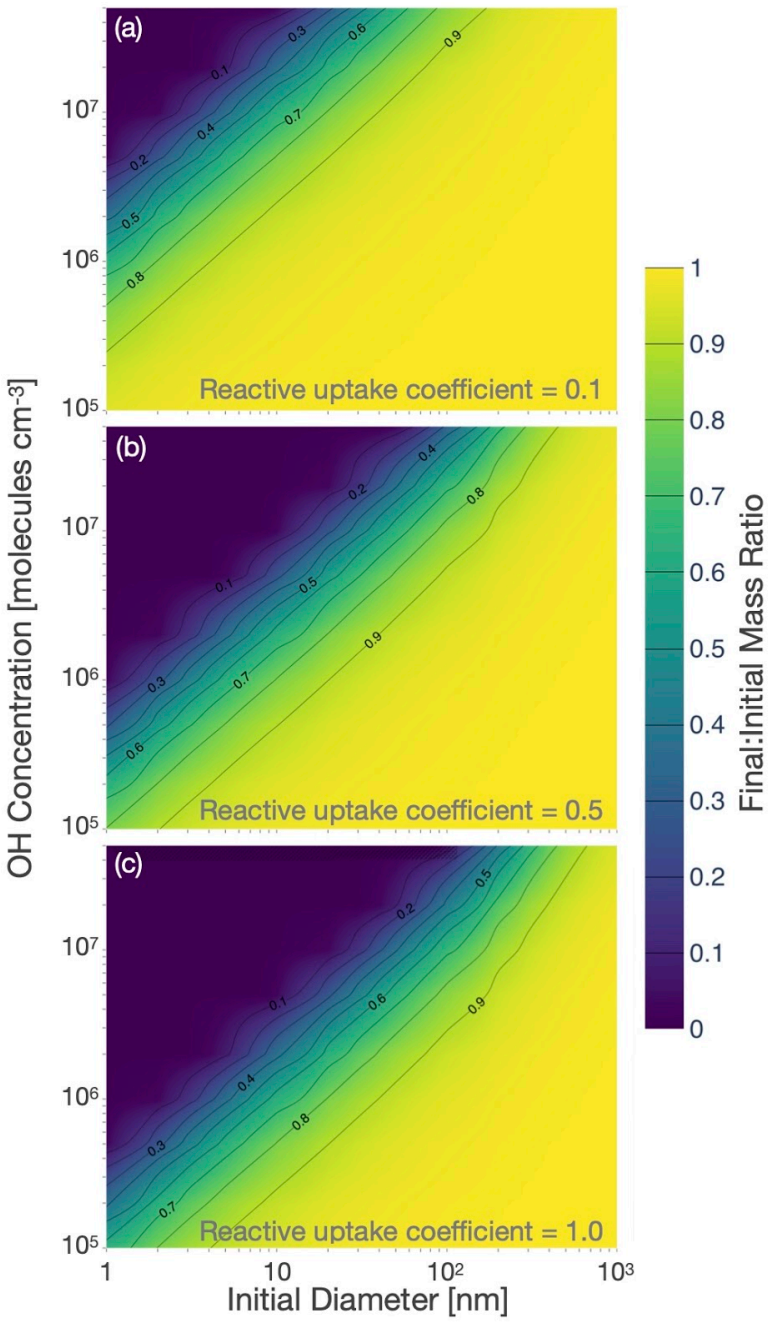

Figure S23. Calculated (final aerosol mass):(initial aerosol mass) ratios for mass loss through heterogeneous chemistry over a range of aerosol diameters and OH concentrations over 3 hours. As an upper-bound case, (a) it is assumed that for each OH collision, 200 amu of mass is lost. As a middle-bound, (b) it is assumed that 50% of OH collisions result in a 200 amu mass loss. As a more-realistic loss rate, (c) assumes that 10% of all OH collisions result in an 200 amu mass loss. See SI text S2 for more details.

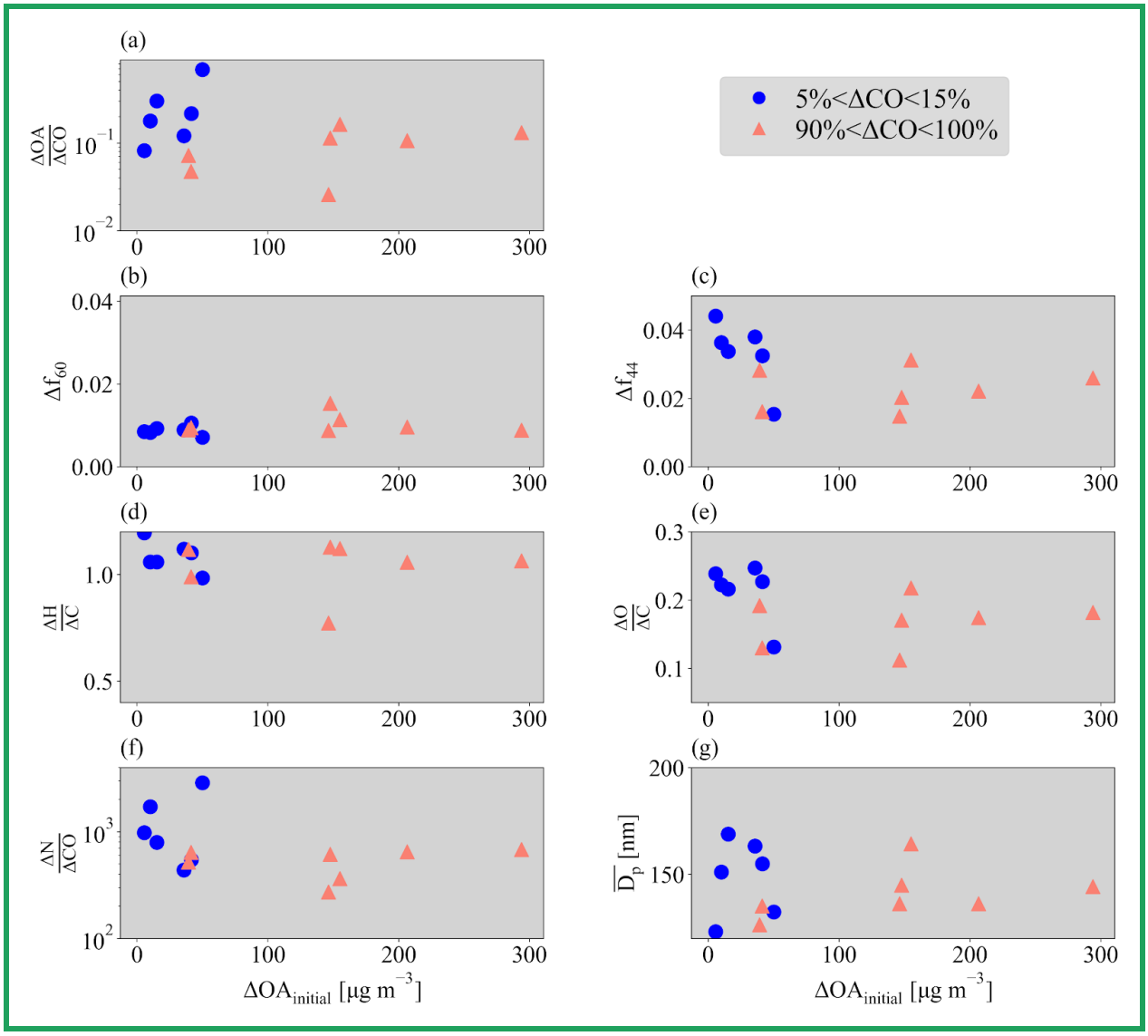

Figure S24. Scatter plot of each parameter of Figure 1 against $\Delta OA_{initial}$.

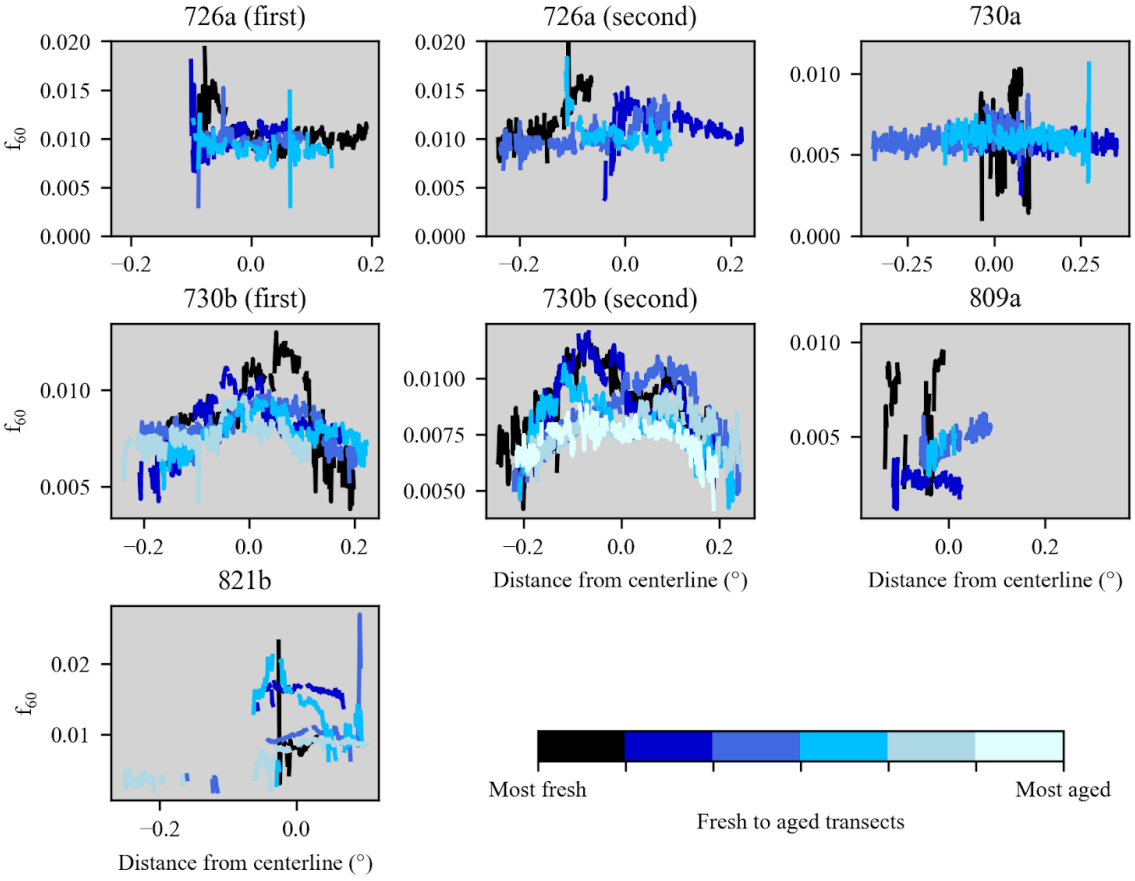

Figure S254. Raw f_{60} data for each flight along each transect included in this study. The titles indicate the flight. The black color indicates the earliest transect, with increasingly lighter colors indicating increasingly downwind transects. The centerline was estimated from the number size distribution and the estimated center of the fire (Figures S1-S6).

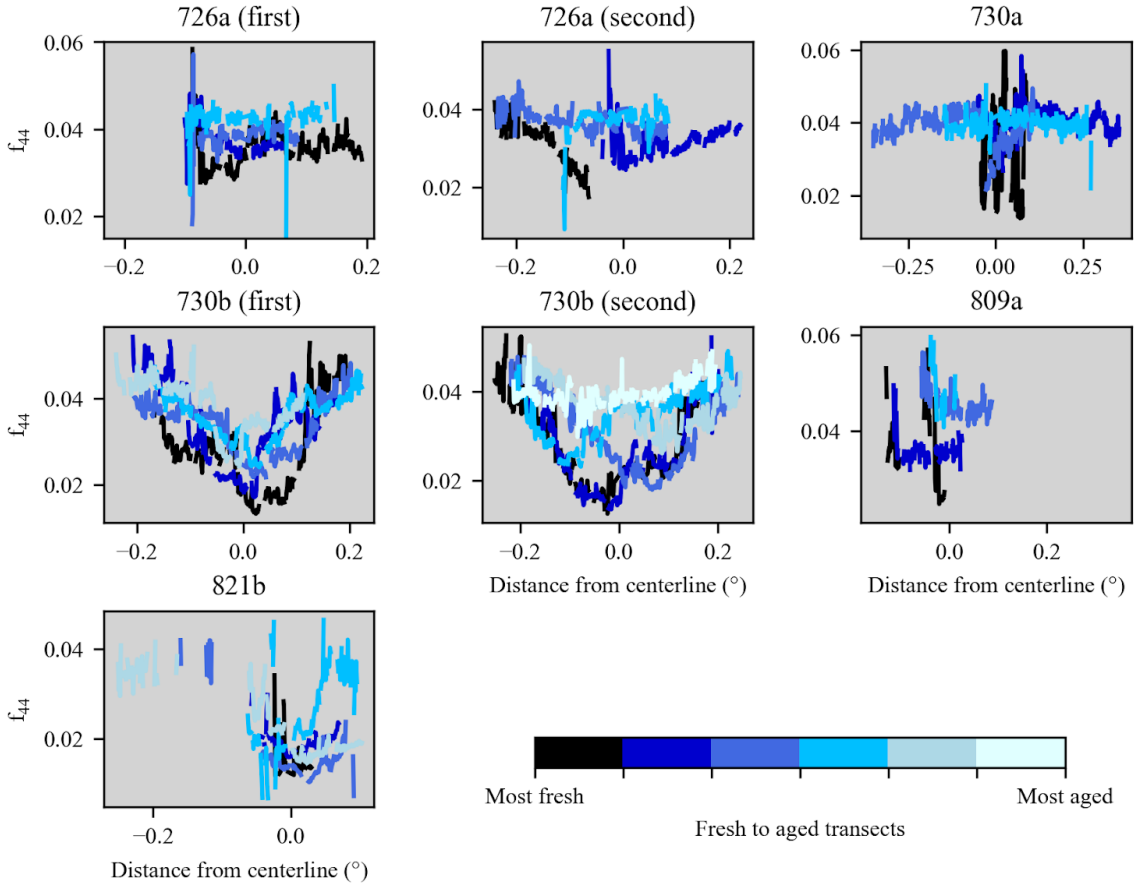

Figure S265. Raw f_{44} data for each flight along each transect included in this study. The titles indicate the flight. The black color indicates the earliest transect, with increasingly lighter colors indicating increasingly downwind transects. The centerline was estimated from the number size distribution and the estimated center of the fire (Figures S1-S6).

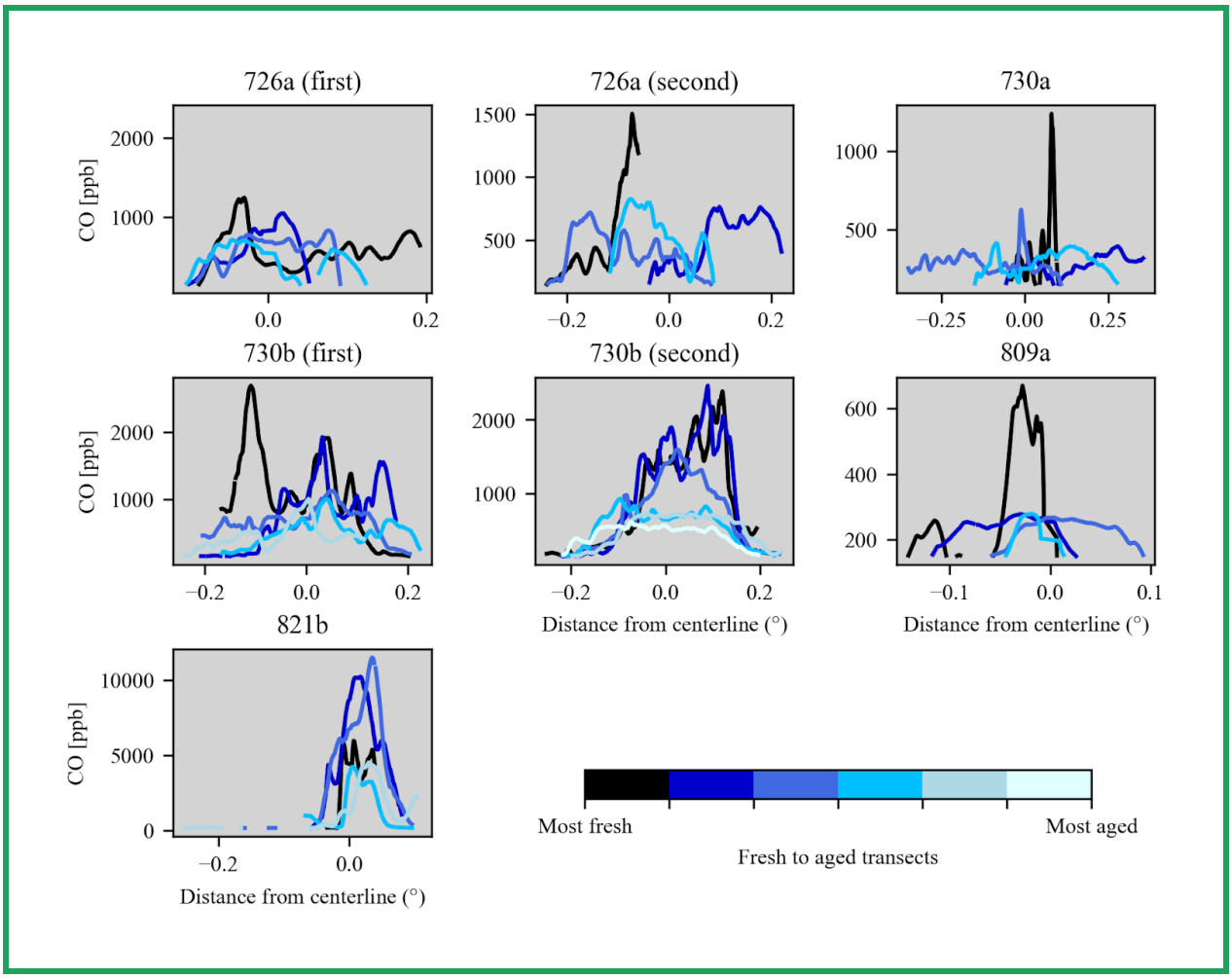

Figure S27. Total in-plume CO (ppbv) irradiance for each flight along each transect included in this study. The titles indicate the flight. The black color indicates the earliest transect, with increasingly lighter colors indicating increasingly downwind transects. The centerline was estimated from the number size distribution and the estimated center of the fire (Figures S1-S6).

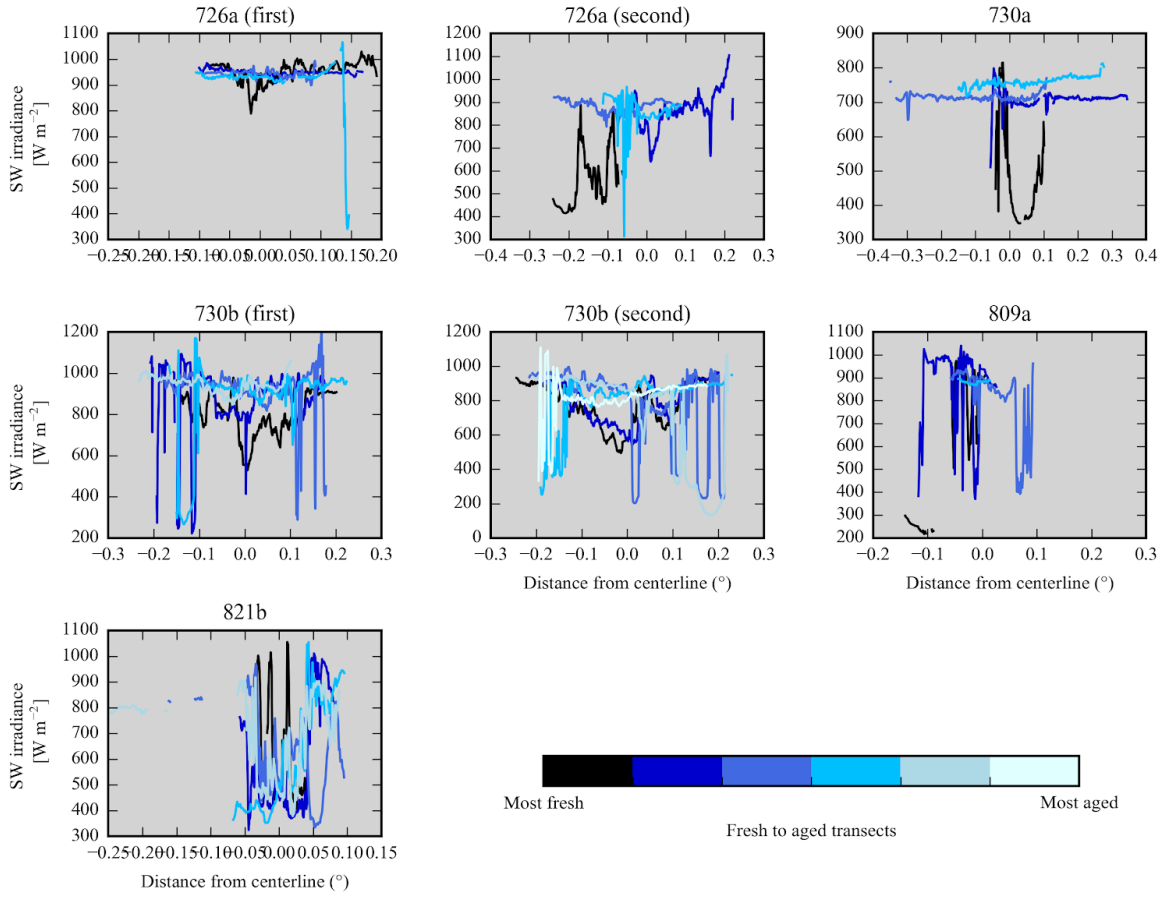

Figure S2~~8~~6. Total in-plume shortwave (SW) irradiance for each flight along each transect included in this study. The titles indicate the flight. The black color indicates the earliest transect, with increasingly lighter colors indicating increasingly downwind transects. The centerline was estimated from the number size distribution and the estimated center of the fire (Figures S1-S6).

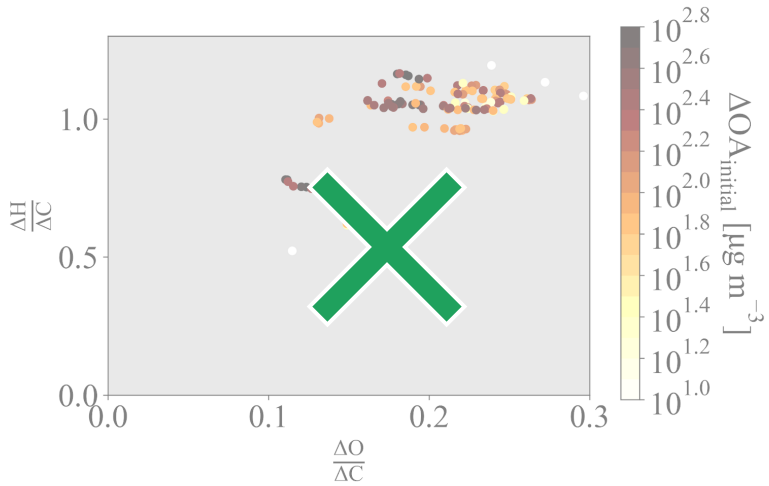

¶

~~Figure S27. The Van Krevelen diagram of ΔH/ΔC versus ΔO/ΔC for all points in the 7 sets of pseudo-Lagrangian transects, colored by $\Delta OA_{initial}$.~~ ¶

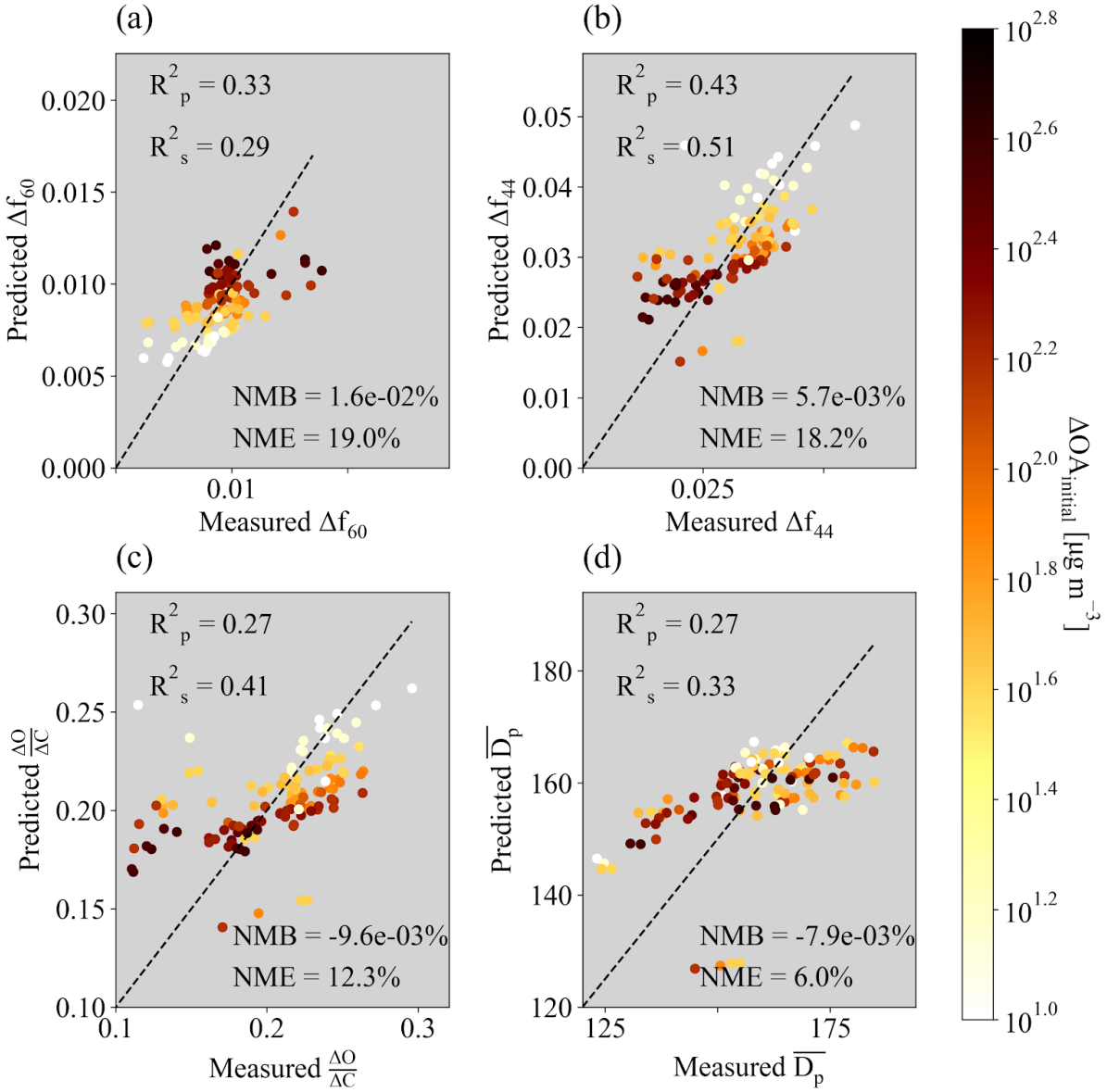

Figure S298. Measured versus predicted (a) Δf_{60}, (b) Δf_{44}, and (c) $\overline{D_p}$ between 40-262 nm, using the equation $ln(X) = a\ ln(\Delta OA_{initial}) + b\ ln(Physical\ age) + c$ (Eq. 5)where X=Δf_{60}, Δf_{44}, or $\overline{D_p}$. The values of a, b, and c are provided in Table S4. The Pearson and Spearman coefficients of determination (R^2_p and R^2_s, respectively) are provided in each panel, along with the normalized mean bias (NMB) and normalized mean error (NME). Included in the fit and figure are all four regions within the plume (the 5-15%, 15-50%, 50-90%, and 90-100% of ΔCO), all colored by the mean $\Delta OA_{initial}$ of each ΔCO percentile range.

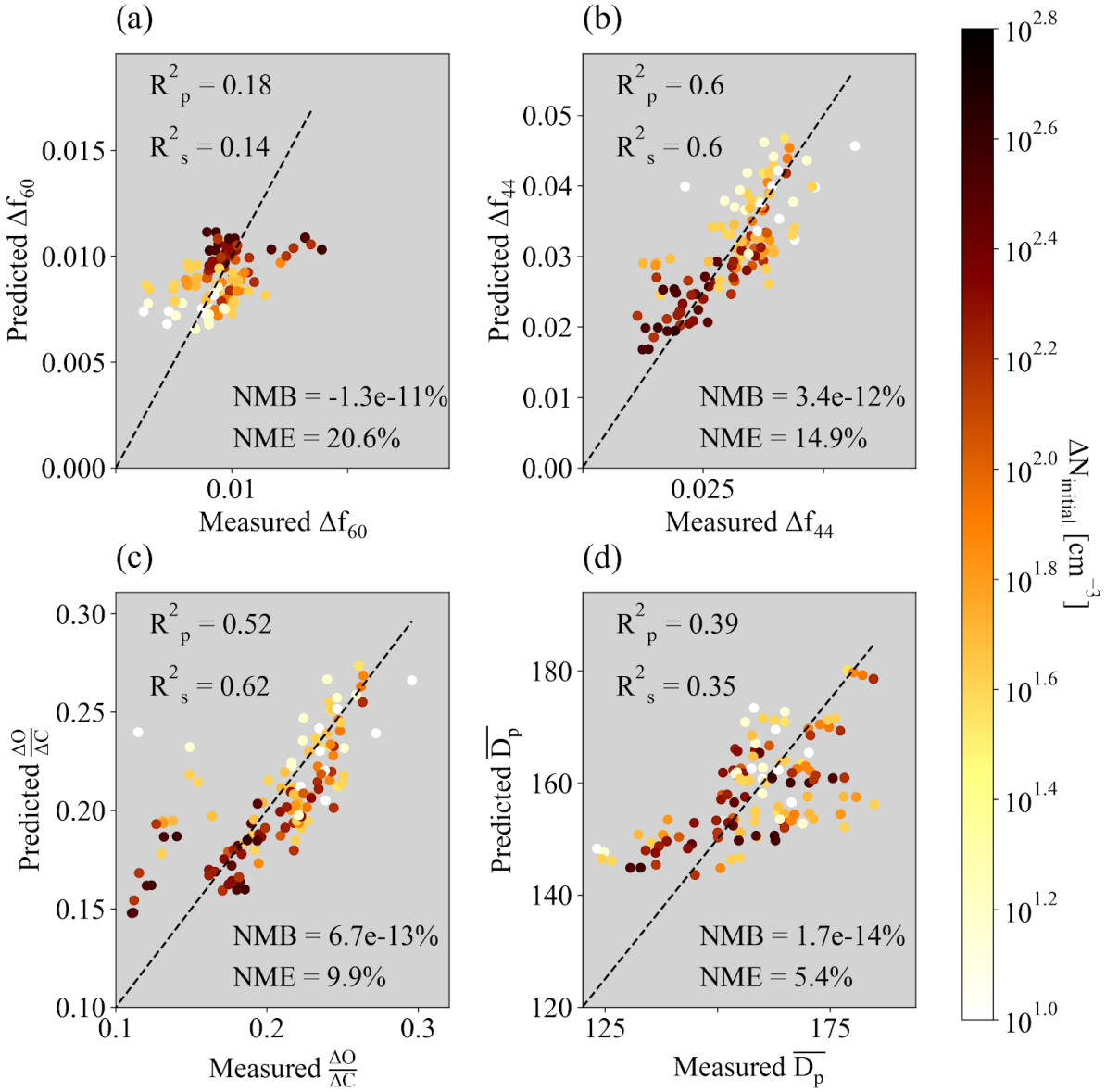

Figure S30~~29~~. Measured versus predicted (a) Δf_{60}, (b) Δf_{44}, and (c) $\overline{D_p}$ between 40-300 nm, using the equation $X = a\ log_{10}(\Delta N_{initial}) + b\ (Physical\ age) + c$ where X=Δf_{60}, Δf_{44}, or $\overline{D_p}$ where X=Δf_{60}, Δf_{44}, or $\overline{D_p}$. Note that the fit here is the same as that in Eq. 2 except that $\Delta N_{initial}$ replaces $\Delta OA_{initial}$. The values of a, b, and c are provided in Table S5. The Pearson and Spearman coefficients of determination (R^2_p and R^2_s, respectively) are provided in each panel, along with the normalized mean bias (NMB) and normalized mean error (NME). Included in the fit and figure are all four regions within the plume (the 5-15%, 15-50%, 50-90%, and 90-100% of ΔCO), all colored by the mean $\Delta OA_{initial}$ of each ΔCO percentile range.

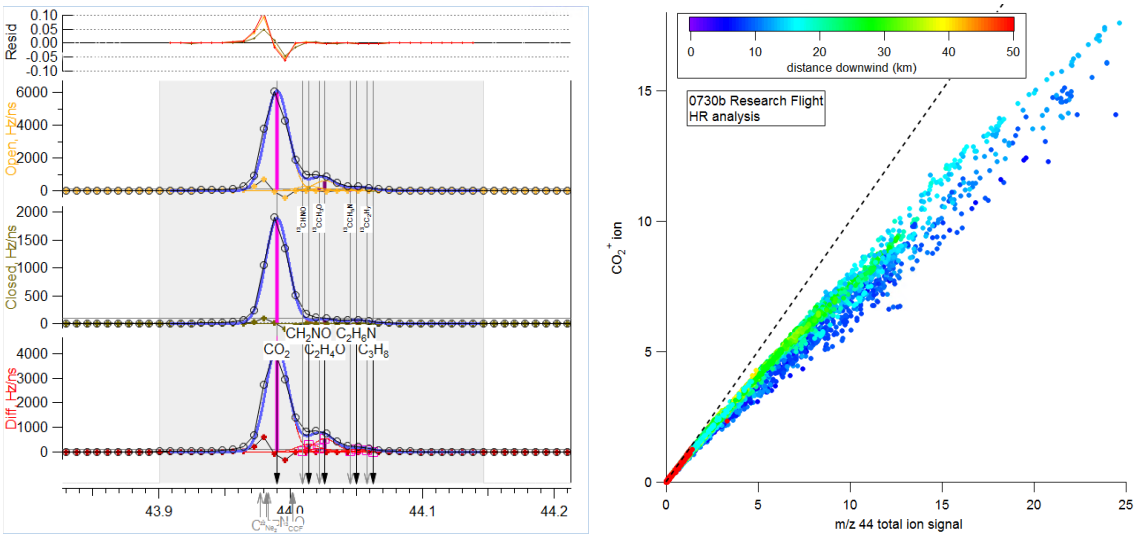

Figure S31. (a) High resolution fits at m/z 44 for a biomass burning plume during 0730b research flight with laser ON. (b) Correlation of HR CO_2^+ ion and HR total ion signal at m/z 44, colored by distance downwind (km) from fire.

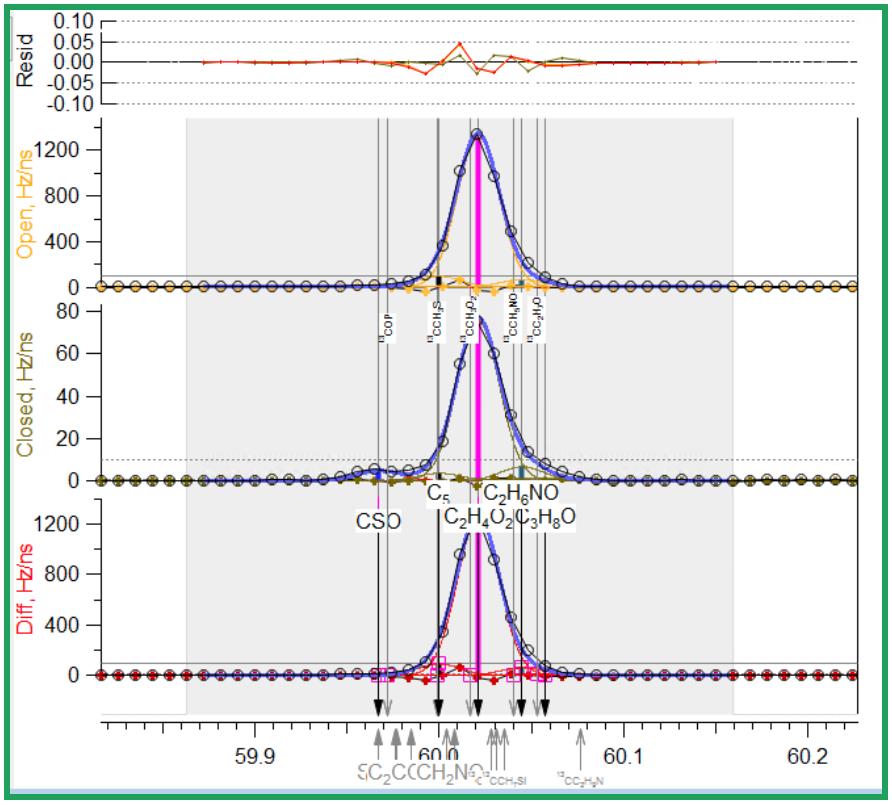

Figure S32. High resolution fits at m/z 60 for a biomass burning plume during 0730b research flight with laser ON.

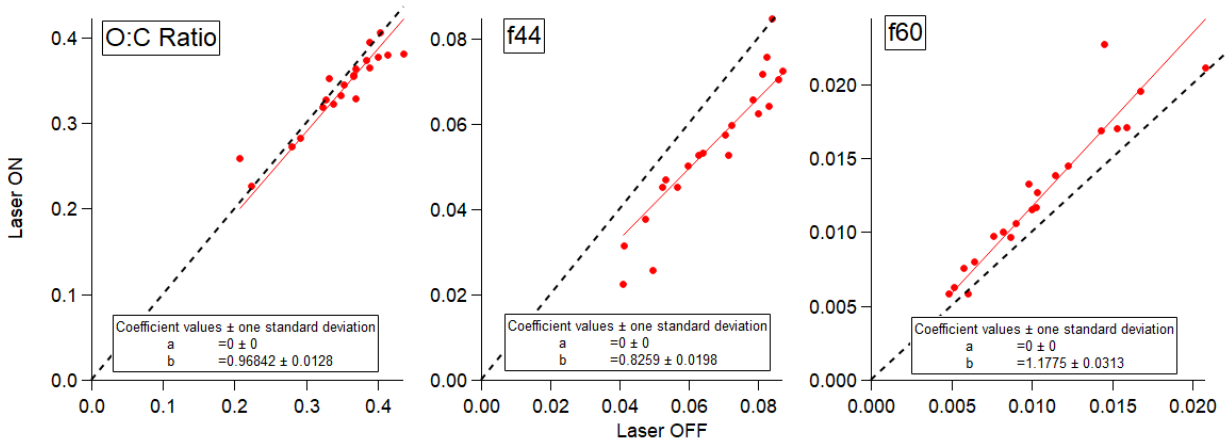

Figure S33. Laser ON versus laser OFF SP-AMS HR O:C, UMR f44, and UMR f60 ratios.

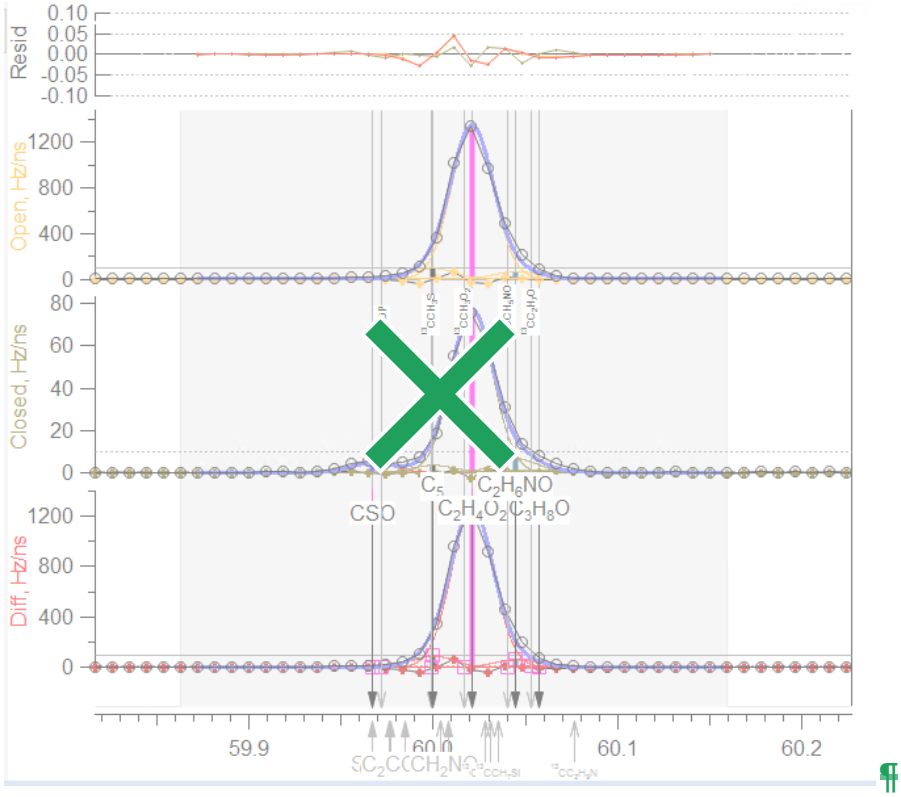

~~Figure S31. High resolution fits at m/z 60 for a biomass burning plume during 0730b research flight with laser ON.~~